B-cell receptor and Toll-like receptor signaling in Chronic Lymphocytic Leukemia (CLL) proliferation

Trieste, Italy

Claudio Martines

Supervisor: Dr. Dimitar Efremov

Molecular Hematology Group

TABLE OF CONTENTS

List of Abbreviations

APRIL Proliferation-inducing ligand
BAFF B-cell activating factor
BCR B-cell receptor
BM Bone marrow
BMSCs Bone marrow stromal cells
BTK Bruton's tyrosine kinase
CDK Cyclin-dependent kinase
CDRs Complementarity-determining regions
CLL Chronic Lymphocytic Leukemia
DLBCL Diffuse Large B-cell lymphoma
ERK Extracellular regulated kinase
FISH Fluorescence in situ hybridization
FRs Framework regions
HL Hodgkin lymphoma
HSCs Hematopoietic stem cells
Ig Immunoglobulin
IGHV immunoglobulin heavy variable
IL-15 Interleukin-15
IL-21 Interleukin-21
IL-4 Interleukin-4
IRAK4 Interleukin-1 receptor associated kinase 4
ITAM Immunoreceptor Tyrosine-based Activation Motif
MAPK Mitogen Activated Protein Kinase
MCL Mantle cell lymphoma
M-CLL mutated CLL
MDR minimal deleted region
NF-kB Nuclear Factor kappa B
NGS Next generation sequencing
NLCs Nurse-like cells
ORR Overall response rate
OS Overall survival
PB Peripheral Blood
PC Peritoneal Cavity
PDX Patient-derived xenograft
PFS Progression free survival
PI3K Phosphoinositide 3-kinase
RAG1 Recombination Activating 1
RS Richter syndrome
SC Subcutaneous
sIg surface immunoglobulin
SPL Spleen
SYK Spleen Tyrosine Kinase
TCR T-cell receptor
TdT Terminal deoxynucleotidyl transferase
PAMPs Pathogen Associated Molecular Patterns
DAMPs Damage Associated Molecular Patterns
TLR Toll-like receptor
TLS Tumor lysis syndrome
U-CLL unmutated CLL
VLA-4 very late antigen 4

Abstract

The B-cell receptor (BCR) pathway plays a key role in the pathogenesis of Chronic Lymphocytic Leukemia (CLL) and has emerged as a major therapeutic target in this disease. However, BCR stimulation is not sufficient to induce CLL cell proliferation *in vitro* suggesting that additional signals from the microenvironment are required to drive the expansion of the malignant cells. Numerous microenvironmental signals have been identified that can increase the survival and/or induce CLL cell proliferation *in vitro*. These signals typically represent various secreted or cell surface ligands that are expressed by different cell types present in the lymph node tumor microenvironment, such as T cells, macrophages and stromal cells, or molecules that would be expected to be released by apoptotic cells, such as apoptosis associated autoantigens or CpG-unmethylated mitochondrial DNA. Currently, there is considerable evidence that activated CD4 T cells play an important role in regulating CLL cell proliferation, as such cells are often seen in direct contact with CLL cells in lymph node proliferation centers and are required for the expansion of xenografted human CLL cells in immunodeficient NSG mice. Regarding other microenvironmental signals, the extent to which they contribute to the growth and survival of the leukemic cells *in vivo* has still not been fully established. The goal of this study was to investigate the relevance of some of these microenvironmental signals in regulating the growth and proliferation of the malignant B cells *in vivo,* with particular focus on BCR- and TLR-derived signals. This question was addressed using two mouse models of CLL and genetic disruption of the BCR- and TLR- signaling pathway by CRISPR/Cas9. The data presented in this thesis show that BCR signals are directly involved in driving CLL cell proliferation and cooperate with genetic lesions in negative cell cycle regulators during Richter transformation. In contrast, we show that cells with knockout of the TLR-signaling molecules IRAK4 or MyD88 are not negatively selected *in vivo*, arguing against an essential role for TLR-signals in driving leukemia cell proliferation. Finally, we provide evidence for a major role for macrophages in supporting the growth and survival of Richter Syndrome cells.

The novel CRISPR/Cas9 genome editing approach that was developed and described in this thesis also represents an important tool to investigate the relative relevance of additional microenvironmental signals for the growth of the malignant cells *in vivo*, because it allows for rapid disruption of signaling pathways implicated in the proliferation and survival of the leukemia cells.

1. INTRODUCTION

1.1 Definition

Chronic lymphocytic leukemia (CLL) is the most common adult leukemia in the Western countries and accounts for approximately 30% of all adult leukemias. It is primarily a disease of the elderly, with a median age at diagnosis of 70 years. The incidence of CLL changes based on geographical regions and the risk of developing CLL is higher for men than women (*Campo E et al. 2011; Chiorazzi et al. 2005*). Clinically, CLL is a heterogeneous disease with approximately one third of CLL patients having a rather indolent disease and normal life expectancy, and one third a rapidly progressive disease and reduced survival.

1.2 Diagnosis and staging

CLL is a chronic lymphoproliferative disorder characterized by progressive accumulation of mature, monoclonal B lymphocytes in peripheral blood, bone marrow and secondary lymphoid tissues. The immunophenotype of leukemic B-lymphocytes is characterized by immunoglobulin (Ig) light chain restriction (monoclonality), co-expression of CD5, CD19, and CD23 and low expression of surface immunoglobulins (sIg), CD79b and CD20. The diagnosis of CLL requires the presence in the peripheral blood of $5x10^9$/L monoclonal B lymphocytes for at least 3 months and most often is established in asymptomatic individuals, following a blood cell count performed during routine testing. When present, typical symptoms are lymphadenopathy, splenomegaly, anemia and thrombocytopenia *(Hallek M et al. 2008*). In addition, CLL patients have frequent infections and have an increased risk of developing secondary cancers as a consequence of impairment of the immune system. Another serious complication which affects around 5-10% of CLL patients is Richter transformation or Richter syndrome (RS), which represents the transformation of CLL in a more aggressive lymphoma, most commonly diffuse-large B-cell lymphoma (DLBCL). RS is associated with very rapid disease progression, limited therapeutic options and generally poor survival (*Sameer A et al. 2014*).

There are two clinical staging systems for CLL: modified Rai and Binet. The modified Rai system defines three risk categories, Rai stage low, intermediate- and high-risk, based on the presence of enlarged lymph nodes, splenomegaly and marrow involvement (*Rai KR et al. 1975*). The Binet

staging system employs similar parameters, but it also considers the number of involved anatomical lymph node areas (*Binet JL et al. 1981*).

1.3 Prognosis

Although the Rai and Binet staging systems provide powerful tools for establishing prognosis and for the selection of patients for treatment, these are not sufficient to identify subset of patients which may have, or may have not, benefits from particular treatments. In addition, these staging systems have a limited prognostic value in the early stages of the disease. Therefore, it is crucial to identify biomarkers that can predict CLL progression in patients at an early stage of the disease.

The most important prognostic factor is the **mutational status of the immunoglobulin heavy chain variable (IGHV) genes**, which encode the immunoglobulin portion of the B cell receptor (BCR) and can be considered a 'gold standard' for assessing prognosis of CLL patients at presentation. Based on this, CLL patients can be divided in two main subset with a very different disease behaviour and outcome: patients whose CLL cells express mutated IGHV genes, defined as >2% difference from the corresponding germ-line gene, are defined as mutated-CLL (M-CLL) patients, whereas CLL patients carrying less than 98% of homology with the closest germ-line gene are defined as unmutated CLL (U-CLL) patients. These two subsets show a very different clinical course: U-CLL patients show a progressive disease and a poorer prognosis than M-CLL patients (*Hamblin TJ et al. 1999; Damle RN et al. 1999*). In around 30-40% of CLL patients, the BCRs are encoded by unmutated IGHV genes, whereas in the remaining cases the genes are mutated. The IGHV mutational status in CLL patients remains constant over the course of the disease.

CD49d is one of the strongest independent negative prognostic factors of overall survival in CLL. It is the α4 subunit of the integrin heterodimer α4β1 (CD49d/CD29), named also very late antigen-4 (VLA-4), and is a surface molecule involved in the microenvironmental interactions of the CLL cells. VLA-4 is expressed on B and T cells and has two main ligands, VCAM-1, expressed by endothelial cells and bone marrow cells, and the extracellular matrix molecule fibronectin. VLA-4 is present on the cell surface in a resting conformation and can be activated by different stimuli including BCR-

stimulation, thus becoming capable of interacting with its ligands with high-affinity/avidity *(Tissino E et al. 2018*).

In CLL, VLA-4 mediates cell-cell and cell-matrix interactions which induce survival signals and protect CLL cells from drug induced apoptosis. CLL patients with >30% CD49d-positive leukemia cells displayed significantly shorter treatment-free and overall survival than patients with <30% CD49d positivity (*Bulian P et al. 2014; Dal Bo M et al. 2014; Dal Bo M et al. 2016; Tissino E et al. 2020*).

ZAP70 is a cytoplasmatic tyrosine kinase protein and is a key mediator of T-cell receptor (TCR) signaling. In CLL it is an important negative prognostic factor and among the most differentially expressed genes between M-CLL and U-CLL cases. ZAP70 is preferential expressed in U-CLL cases and predicts IGHV mutational status in more than 90% of patients (*Wiestner A et al. 2003*). ZAP70 expression in CLL-B cells enhances BCR signaling, which can contribute to the more aggressive disease in patients expressing ZAP70 (*Chen L et al. 2002*). However, the increased BCR signaling in CLL cells seems to be not dependent ZAP70's activity, but may be due to its adaptor protein activity (*Gobessi S et al. 2007; Chen L et al. 2008*). In addition, the overexpression of ZAP70 has been associated with greater migration capacity of CLL cells and increased expression of CCR7 and responsiveness to its ligands CCL19 and CCL21. This may facilitate the access of the leukemic cells into the proliferating centers in the secondary lymphoid tissues, where CLL cells proliferate, explaining the more progressive disease in ZAP70+ CLL patients (*Richardson SJ et al. 2006*).

Certain **genetic alterations** are also associated with poor prognosis and will be discussed in the next session.

1.4 CLL pathogenesis

1.4.1 Chromosomal Alterations

CLL exhibits marked genetic heterogeneity and a number of cytogenetic abnormalities with prognostic significance have been identified by fluorescent in situ hybridization (FISH) in more than 80% of CLL cases.

The most common chromosomal alteration is the **deletion 13q14** that occurs in around 50-60% of CLL cases and is generally monoallelic (*Dohner H et al. 2000*). The minimal deleted region (MDR) contains genes which encode for non-coding transcripts and for two micro-RNA genes (MIR15A, MIR16-1). In normal B cells these micro-RNAs inhibit the expression of key regulator genes of apoptosis and cell cycle, including B-cell lymphoma 2 (BCL-2), the cyclins CCND2 and CCND3 and cyclin-dependent kinases 4 and 6 (CDK4 and CDK6). Deletion of miR15A and miR16-1 abrogates this inhibitory effect favouring the constitutive survival and cycling of tumor B cells (*Cimmino A et al. 2005; Lovat F et al. 2015*).

Trisomy 12 is the second most frequent genetic abnormality detected by FISH in CLL patients. It occurs in ~20% of CLL cases and often patients with that abnormality show an atypical cellular morphology (*Autore F et al. 2018*). In addition, CLL cells with Trisomy 12 show an upregulation of integrin signaling and increased expression of adhesion molecules (*Riches JC et al. 2014*).

Deletion 11q22-q23 is present in ~20% of CLL cases and results in inactivation of tumor suppressor genes such as ATM, which is a regulator of TP53 and is involved in DNA repair processes. In CLL, ATM can be inactivated by deletion or mutation. In general, del11q is monoallelic with mutation of ATM gene in the other allele (*Austen B et al. 2000*). Inactivating lesions of ATM are associated with genomic instability. In about 80% of cases, the deletion also involves the BIRC3 gene, a negative regulator of the NF-kB pathway.

The 17p13 deletion involves the entire short arm of the chromosome 17 with disruption of the tumor suppressor gene TP53. The frequency of this genetic abnormality changes based on the clinical stage of the disease. In most cases of CLL, 17p13 deletion is accompanied by mutation of TP53 in the second allele (*Zenz T et al. 2010; Malcikova J et al. 2009*). TP53 alteration due to deletion of 17p13 or/and mutation in TP53 gene is correlated with increase genomic instability and is a predictor of chemorefractoriness and reduced survival. Now day, TP53 mutational status is the main discriminant in the CLL treatment and is one of the most important prognostic markers (*Gonzalez D*

et al. 2011; Dicker F et al. 2009). The study of Döhner H et al. was the first to show the prognostic impact of the different chromosomal alterations. 17p and 11q deletions were associated with more advanced and aggressive disease with median survival times of 32 and 79 months, respectively. The survival of patients with a normal karyotype or trisomy 12 or with 13q deletion in this study was 114, 111 and 133 months, respectively (Figure 1).

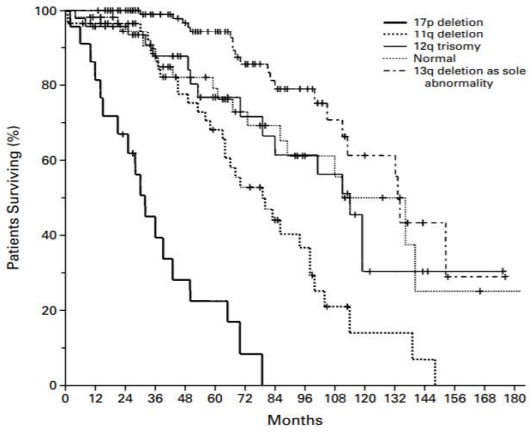

Figure 1. Probability of survival of CLL patients with particular genetic defects. Median survival time of patients with 17p deletion, 11q deletion, 12q trisomy, normal karyotype and 13q deletion (Döhner H et al. 2000).

1.4.2 Mutations

Next-generation sequencing (NGS) revealed additional recurrent genetic lesions in patients with CLL. These genetic lesions are heterogeneous and include copy number alterations and point mutations in over 200 putative CLL driver genes that cluster into one of several distinct biological pathways, including cell cycle, DNA damage response, RNA processing, chromatin modification, and BCR, WNT, MAPK, MYC, NOTCH and NF-kB signaling (*Knisbacher BA et al. 2022*) (Figure 2).

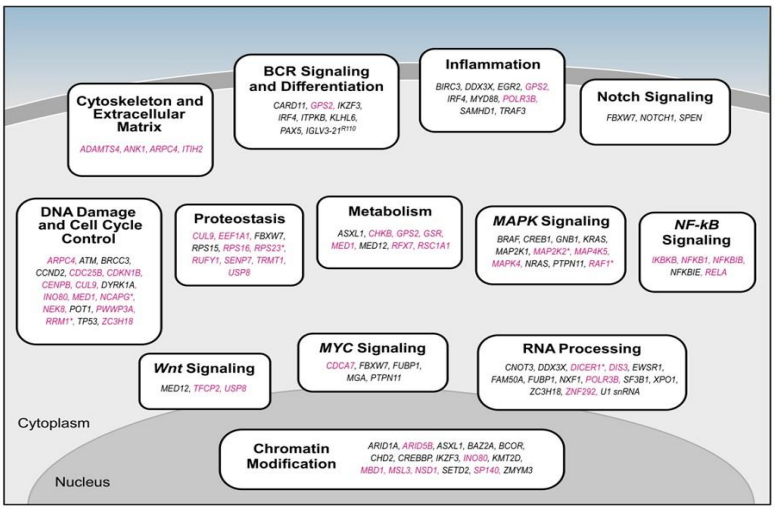

Figure 2. CLL biological pathways affected by candidate driver genes from Knisbacher BA et al. (2022).

The most frequently mutated gene in CLL is **NOTCH1.** This gene is found mutated in 10-20% of cases at the time of diagnosis with increasing frequencies in advanced disease stages and chemorefractory disease *(Fabbri G et al. 2011; Rossi D et al. 2012*). The NOTCH1 gene encodes for a transmembrane protein which, upon binding to its ligand, is proteolytically processed generating an active transcription factor that regulates genes involved in proliferation, metabolism and survival. Most mutations occur in the C-terminal PEST domain, which contains a degradation signal that increases the turnover of the NOTCH1 protein. Mutations in the PEST domain cause accumulation of active NOTCH1 isoform and increase the intensity and duration of NOTCH1 signaling. Mutated NOTCH1 has been associated with unmutated IGHV and trisomy 12 (*Balatti V et al. 2012; Rossi D et al. 2012; Rosati E et al. 2009*).

The Splicing Factor 3b Subunit 1 (**SF3B1**) is a key component of the spliceosome, a complex of ribonucleoproteins involved in the splicing of pre-mRNA and in the formation of mature mRNA removing introns in protein-encoding genes. SF3B1 mutations show a frequency of 5-10% in CLL at the time of the diagnosis and appear to increase over time with a frequency up to 20% in relapsed/refractory CLL patients. Mutations in this gene are also associated with more aggressive disease and a reduced survival. The consequence of SF3B1 mutations in CLL include deregulated mRNA splicing of genes involved in cell cycle progression and apoptosis (*Quesada V et al. 2011; Wang L et al 2011*).

In CLL genetic lesions involve also the activation of the NF-kB pathway. In particular, the **Myeloid differentiation antigen MyD88**, an adaptor protein downstream the Toll-like receptor (TLR) pathway, is mutated in ~3% of CLL cases. The most recurrent MYD88 mutation in CLL is the L265P mutation, which leads to constitutive activation of the NF-kB pathway (*Puente XS et al. 2011*). The same mutation is also found in ~90% of Waldenström macroglobulinaemia cases and in ~30% activated B cell (ABC)-type DLBCL (*Xinfang Yu et al. 2018*).

Another recurrent genetic lesion that activates the NF-κB signalling pathway is the **BIRC3** (Baculoviral IAP Repeat Containing 3 gene) gene inactivation. BIRC3 is frequently disrupted in CLL by mutations, deletions or a combination of both. BIRC3 is a negative regulator of MAP3K14, which is an activator of the non-canonical NF-κB pathway, and CLL cells with BIRC3 disruption show constitutive activation of NF-kB signaling. Approximately 4% of the CLL patients display mutated

BIRC3 at diagnosis and this genetic defect is associated with unfavorable clinical course and poor outcome independently of other risk factors (*Rossi D et al. 2012*).

In addition to BIRC3 mutation which leads to activation of the NF-kB pathway, truncating mutations in the **NFKBIE** gene which encodes IkBε, a negative regulator of NF-kB in B cells, have been reported as frequent in advanced stage CLL (*Damm F et al. 2014*). It has been observed that patients carrying this mutation showed lower IkBε expression and increased phosphorylation and nuclear translocation of the NF-kB transcription factor p65 (*Mansouri L et al. 2015*).

1.5 CLL treatment

At the time of diagnosis the majority of the patients does not require therapy and they should be monitored and subjected to "watch and wait". When they display symptomatic disease and signs of rapid progression of disease, the treatment should be initiated according to their levels of fitness. Current indications for initiating treatment are defined in the IWCLL guidelines (*Hallek M et al. 2018*).

Until very recently, relatively few therapeutic options were available for patients with CLL. These included chemotherapy and combination of chemotherapy and immunotherapy (chemoimmunotherapy). For many years cytostatic agents were the only drugs available for treatment of CLL patients (Figure 3). The alkylating agent chlorambucil was the standard first line treatment for CLL until phase 3 studies demonstrated an improved overall response rate (ORR) and prolonged progression-free survival (PFS) in patients treated with the purine analogue fludarabine (*Rai KR et al. 2000*). Subsequent studies showed that the ORR and PFS can be further improved by combining fludarabine with cyclophosphamide (*O'Brien SM et al. 2001*). A major step forward was the addition of the monoclonal anti-CD20 antibody rituximab to the fludarabine/cyclophosphamide combination, resulting in an even more effective regimen. This FCR regimen was the first to show an improvement in overall survival (OS) and has since become standard first line therapy for CLL (*Hallek M et al. 2010*). However, the FCR regimen is associated with significant myelosuppression and a high rate of early and late infections, which is why it is unsuitable for most elderly patients and patients with comorbidities (*Tam CS et al. 2008*).

Within the past years the therapy for CLL has undergone profound changes when treatment options with targeted agents emerged (Figure 3). The identification of the BCR as a major driver in various B cell malignancies resulted in the clinical testing and approval of multiple drugs that selectively target and inhibit molecules involved in propagating the BCR signal. Three main classes of drugs have demonstrated efficacy and some of these drugs have been approved for CLL treatment in recent years; these drug classes are Bruton's tyrosine kinase (BTK) inhibitors, phosphoinositide 3-kinase (PI3K) inhibitors and spleen tyrosine kinase (SYK) inhibitors *(Burger and Wiestner. 2018; Efremov D et al. 2020*).

The first inhibitor of the BCR pathway that has been tested was the inhibitor of the kinase SYK, which is constitutively activated in several B-cell malignancies including CLL (*Gobessi S et al. 2009*). These drugs showed moderate toxicity in unstimulated cells and inhibited the increase in CLL cell survival induced by BCR stimulation. Furthermore, *in vivo* experiments using the Eμ-TCL1 transgenic mouse model of CLL showed that treatment with the SYK inhibitor fostamatinib results in reduction in proliferation and survival of the leukemic B cells and prolonged survival of the treated animals (*Suljagic M et al. 2010*). Fostamatinib was the first BCR inhibitor that was tested in a clinical trial in patients with B cell malignancies (*Friedberg JW et al. 2010*), demonstrating a high response rate in CLL and mantle-cell lymphoma (MCL). However, this drug did not undergo further clinical development in CLL, although it was recently approved for the treatment of immune thrombocytopenic purpura.

Ibrutinib is an orally available inhibitor of the BTK enzyme which was approved for the treatment of patients with CLL in 2014. This drug irreversibly inhibits BTK by covalently binding to C481 residue in the ATP-binding pocket resulting in a blockade of BCR signalling pathway. In addition, ibrutinib also inhibits the signalling of other cell surface receptors, including chemokine receptors and adhesion molecules, which regulate the homing of CLL cells into the tissues in response to chemotactic factors such as CXCL12 and their adhesion to extracellular matrix and cell surface adhesion proteins. The consequence of this is a CLL cell redistribution into the blood with rapid resolution of lymphadenopathy (*Cheng S et al. 2014; Ponader S et al. 2012; Chen SS et al. 2016*).

Idelalisib is an orally available reversible inhibitor of PI3K with 30–400 times greater selectivity for PI3Kδ compared to PI3Kα, PI3Kβ, and PI3Kγ. Treatment of CLL cells with the selective PIK3δ inhibitor idelalisib displays reduced phosphorylation of several downstream molecules, such as AKT, and inhibits the survival and the proliferation of the leukemic cells (*Lannutti BJ et al. 2011*). It has been tested in combination with rituximab because the combination of the 2 drugs significantly prolonged

survival compared to rituximab alone in relapsed CLL (*Furman RR et al. 2014*). Idelalisib was approved for CLL treatment in 2014 also as first-line treatment in patients with TP53 disruption who cannot be treated with any other therapy.

Venetoclax is an oral selective inhibitor of the anti-apoptotic protein BCL2, which is overexpressed in CLL. Apoptosis is regulated by a complex of anti- and pro-apoptotic proteins which interact and they are triggered by external stimuli. The BCL-2 family proteins share the conserved BCL-2 homology (BH) domains and are classified into anti- and pro-apoptotic members which are divided into multidomain proteins with 4 different BH domains (BH1 to BH4) and the "BH3-only" proteins contain only the BH3 domain. One of the most important effectors of apoptosis are the pro-apoptotic proteins BAX and BAK, which when activated induce apoptosis. Whereas the anti-apoptotic multidomain members BCL-2, BCL-XL and MCL-1 inhibit the apoptosis by directly binding BAX and BAK. Accordingly, the overexpression of BCL-2 oncogene in CLL cells is associated with evasion of apoptosis, leading to resistance to chemotherapy. Venetoclax induces apoptosis in CLL cells by diminishing the capacity of BCL-2 to sequester the pro-apoptotic protein BIM (*Del Gaizo Moore et al. 2007*), which then activates BAX and BAK. This drug has shown a very high efficacy in CLL patients and the most important adverse event reported in a phase 1 trial was tumor lysis syndrome (TLS). Venetoclax was approved in 2016 for the treatment of CLL patients carrying TP53 aberrations (del17p and/or TP53 gene mutations) (*Roberts AW et al. 2016*) and subsequently for all adults with CLL/SLL disregarding prior treatment or mutation status.

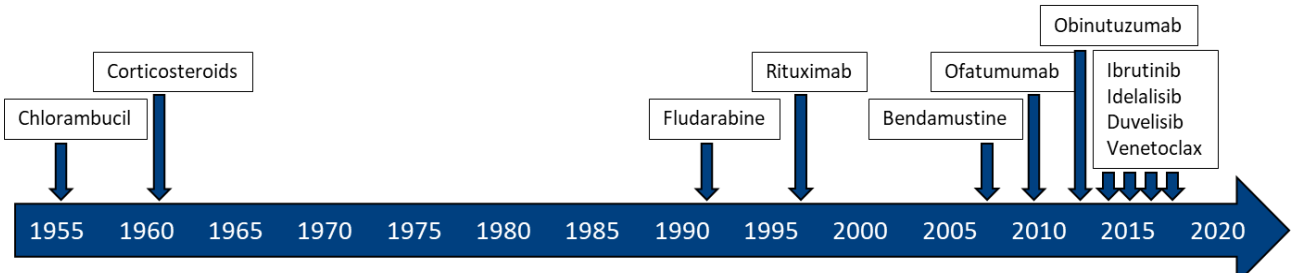

Figure 3. Timeline of regulatory approval of major drugs for CLL.

1.6 Richter's transformation

Richter syndrome occurs in 5-10% of CLL patients and is defined as the transformation of CLL into a more aggressive lymphoma with 2 variants: DLBCL variant in 90% of the cases or Hodgkin lymphoma (HL) variant, which accounts for the remaining cases. The genetic lesions that have been associated with RS mainly affect cellular processes such as DNA damage response, modulation of the cell cycle and proliferation. The most frequent mutations in RS are: TP53 disruption (50%-60%), which can be either present or acquired at the time of the RS diagnosis, NOTCH1 activation (30%), MYC abnormalities (20%) and deletion of the cell cycle inhibitors CDKN2A and CDKN2B (33%), which typically occurs at the time of transformation. The latter genetic defects are frequently associated with TP53 disruption and co-occur in ~25% of RS cases (*Fabbri G et al. 2013; Rossi D et al. 2011, Chigrinova E et al. 2013*). The median time from CLL diagnosis to RS is 1.8-5 years and therefore RS is not always a late event. Among DLBCL, 2 subgroups have been identified, those clonally related to CLL, which are ~80%, and those clonally unrelated to the underlying CLL (20%). The median overall survival differs significantly between these groups and clonally unrelated RS patients representing de novo DLBCL have a better prognosis with a median survival of 5 years than the clonally related RS, which show a median survival of approximately 1 year (*Parikh SA et al. 2014*).

1.7 B-cell development and CLL origin

B cells derive from haematopoietic stem cells (HSCs) in the bone marrow. These cells circulate in the blood and lymph, form specialised lymphoid organs, and infiltrate virtually every tissue in the body. B cell development is a highly regulated process that allows the generation of immunocompetent B lymphocytes from a committed B-cell progenitor. It can be divided into two stages: an antigen-independent stage which occurs in fetal liver and adult marrow and an antigen-dependent stage which occurs primarily in secondary lymphoid tissue, such as the spleen and lymph nodes. The generation of B lymphocytes initiates in fetal liver and later on it continues in the bone marrow through entire life.

B-cells are characterized by the expression of immunoglobulins, which are formed by two identical heavy and two identical light chains, each with a constant (C) and a variable (V) region. The V region is the part of the molecule that binds to the antigen, whereas the C region has effector functions (Figure 4).

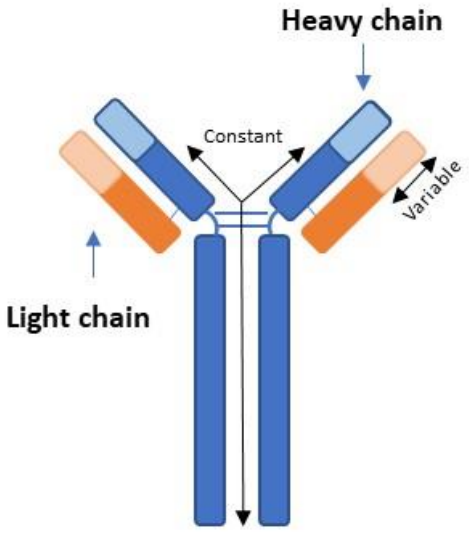

Figure 4. Structure of the B-cell receptor. The BCR is composed of two identical heavy chains and two identical light chains which are connected by disulfide bonds. Each heavy and light chain contains a constant region and a variable region, which bind the antigen.

Each V region contains four areas of relatively limited diversity, known as the framework regions (FRs), and three areas with considerable sequence diversity, known as complementarity determining regions (CDRs). The CDRs contain the amino acid residues that directly contact the antigen and thus confer the specificity of the Ig molecule.

A key event in the commitment to the B lineage from HSCs is the immunoglobulin gene rearrangement between diversity (D) and joining (J) gene segments in CD34+/CD10+/CD19− progenitor (pro-B) cells. Once the D to J rearrangements on both alleles occur, pro-B cells then undergo further differentiation by completing variable (V) to DJ rearrangements at heavy chain locus and expressing CD19, a B-lineage specific cell surface molecule. V(D)J recombination is mediated by different enzymes such as Recombination activating gene1/2 (RAG1/2) and Terminal deoxynucleotidyl Transferase (TdT). CD34+/CD10+/CD19+ surface phenotype defines precursor (pre-B) cells and at this stage the B lymphocytes express on the membrane the μ chain in association with the surrogate light chain (SLC) and the CD79a (Igα) and CD79b (Igβ) signalling molecules, forming a pre-BCR. Subsequently, recombination of VJ at the light chain locus occurs through similar DNA recombination events. Once this process has been completed, a BCR composed of surface IgM, CD79a and CD79b is expressed on the cellular membrane, highlighting the transition from pre-B cells to immature B cells (Figure 5).

In the bone marrow, the immature B lymphocytes which recognize self antigens are eliminated or inactivated, in order to maintain self tolerance with a process defined as negative selection. Thus, only the B lymphocytes incapable to recognize self antigens will migrate in peripheral blood as mature B cells (Cambier JC et al. 2007).

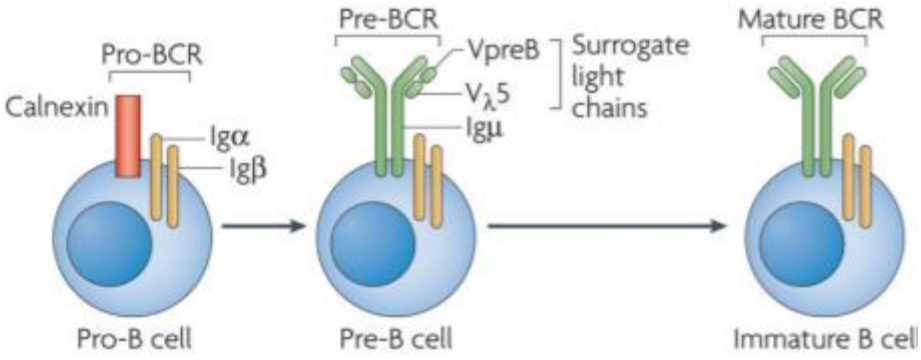

Figure 5. Stages of B-cell development. B cell development in the bone marrow (Cambier JC et al. 2007).

The differentiation in mature B lymphocytes is characterized by the co-expression of surface IgM and IgD and they are called "naïve B lymphocytes" because all the previous differentiation stages are antigen-independent.

When the mature B lymphocytes move out from the bone marrow to the blood, they can encounter various antigens against which they set up effective mechanisms to eliminate them in collaboration with other cells types. After antigen binding, B cells migrate in the secondary follicles of the lymph nodes, which are characterized by two regions: dark zone and light. In the dark zone, the B cells undergo clonal expansion and somatic hypermutation (SHM). The SHM is a process induced by the Activation-Induced Cytidine Deaminase (AID), an enzyme which introduces point mutations in the IGHV and IGHL genes, promoting an increase of antigen affinity. Because the SHM is a random process, relatively few cells will have an increased affinity and only these cells are positively selected and leave the germinal center (GC).

In the light zone the Ig constant region is involved in a process called class-switch recombination, which generates different subclasses of antibodies (for example, IgG or IgA) with different effector functions. These lymphocytes then exit the germinal centers and follow a differentiation process that culminates in the production of memory B cells and plasma cells for antibody secretion. Production of B lymphocytes continues for the whole life, but gradually it diminishes with age.

Certain B cells subsets can differentiate into antibody secreting cells without passing through the germinal centre reaction. These include marginal zone B cells, which produce primarily antibodies against T independent antigens, and B1 B cells, which typically produce low-affinity polyreactive autoantibodies.

The observation that CLL cells uniformly express the surface marker CD5 led to the hypothesis that CLL is derived from B1 lineage B cells. Subsequently, the discovery that two subgroups of patients with CLL can be distinguished on the basis of the presence or absence of mutations in the IGHV genes, indicated that the IGHV- mutated CLLs are derived from antigen-experienced B cells that have transited through the germinal centres, whereas the IGHV- unmutated CLLs are derived from

naïve B cells. However, comparative gene expression profiling of CLL specimens and subsets of non-transformed human B cells showed that both IGHV- mutated and IGHV- unmutated subtypes are similar to CD27+ memory B cells, suggesting that both CLL subtypes originate from antigen-experienced B cells, with the M-CLL and U-CLL subtypes having been derived from post- GC and GC-independent cells, respectively (*Klein U et al. 2001; Seiffert M et al. 2012*). A 2012 study comparing the epigenetic profiles of patients with CLL showed that the degree of genome methylation in CLL cells is generally similar to that in memory B cells, although CLL- associated differences might reflect the existence of a currently unknown non-malignant B cell subpopulation (*Kulis M et al. 2012*). Overall, the distinction between IGHV-mutated CLL putatively derived from GC- experienced B cells and IGHV-unmutated CLL arising from GC-independent memory B cells is currently the most valid model (Figure 6).

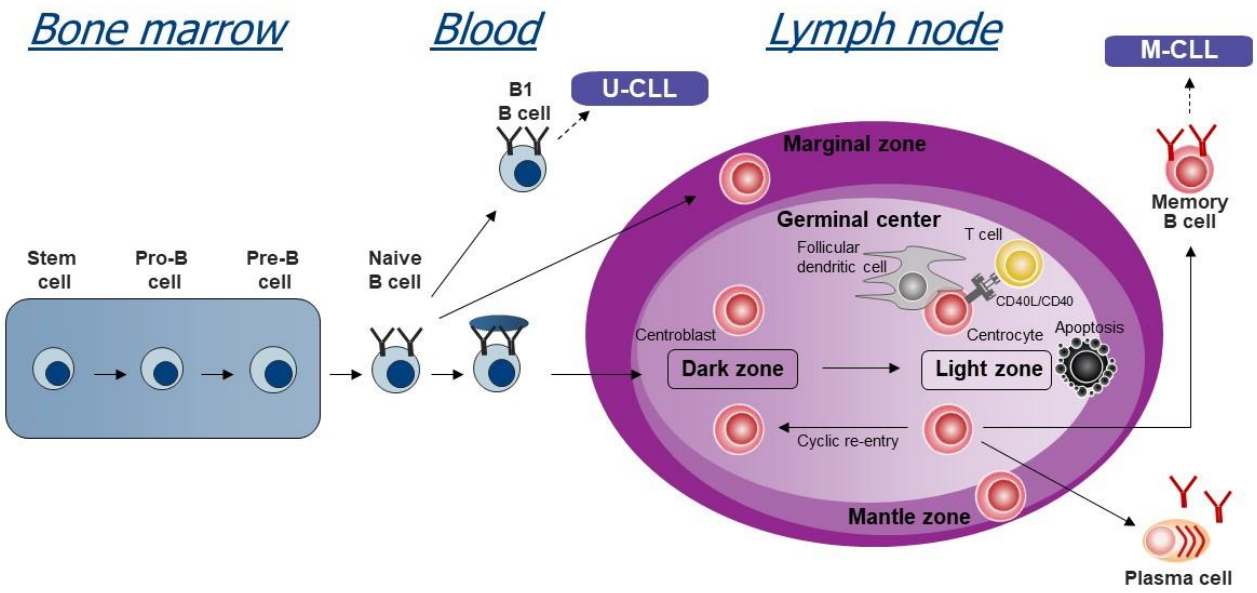

Figure 6. B cell development and cell of origin of unmutated and mutated CLL cells

1.8 Regulation of CLL cell proliferation and survival

CLL is a prototype of a disease strongly dependent on signals from the microenvironment. The CLL microenvironment is composed of various cell-types such as T-cells, monocyte-derived nurse-like cells, mesenchymal stromal cells, extracellular matrix components and soluble factors that can promote the growth of the malignant cells. Recent works have demonstrated that the trafficking, survival and growth of CLL cells is tightly dependent on the support of these surrounding microenvironmental cells.

Several lines of evidences indicate that CLL cell survival and proliferation extremely depends on signals generated in the lymphoid tissue: CLL cells isolated from peripheral blood (PB) of patients usually undergo spontaneous apoptosis when cultured *in vitro* but this may be prevented by adding soluble molecules or co-culturing with other cell types which are present in the tumor microenvironment, suggesting that *in vivo* there are signals that support the survival and growth of CLL cells. These signals can be recapitulated *in vitro* by stimulating CLL cells with various cytokines and chemokines, such as interleukin-4 (IL-4), interleukin-15 (IL-15), interleukein-21 (IL-21) and CXCL12, or by molecules expressed on cells in the microenvironment, such as CD40L, Jagged, BAFF, VCAM-1 (Figure 7) (*Ghia P et al. 2008*).

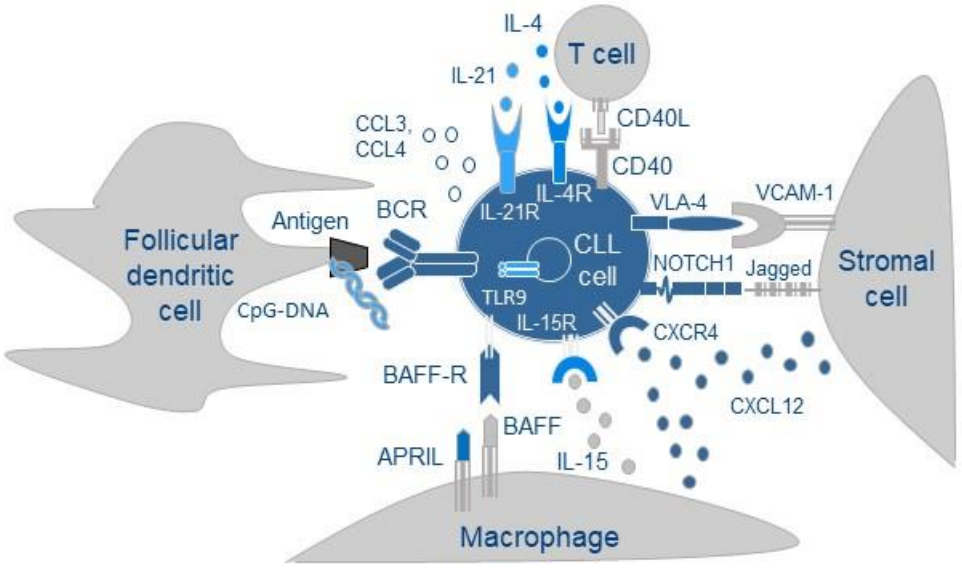

Figure 7. Crosstalk between malignant B cells and microenvironmental cells. Mesenchymal stromal cells express above all CXCL12, whereas NLCs express CXCL12 and CXCL13 and both cells attract CLL cells through CXCR4 and CXCR5, expressed on CLL cell surface. The integrin VLA-4 is involved in establishing cell-cell adhesion with the stromal cells. CLL cells can recruit T cells in the proliferating centers, which then secrete various cytokines and stimulate CD40 on the CLL cell surface. These interactions promote CLL survival and induce proliferation.

T-cells are key components in the CLL lymph node microenvironment and T cells/T-cell factors provide signals that support CLL cell survival and proliferation. CLL cells attract T cells into the proliferating centers by producing the chemokines CCL22, CCL3 and CCL4 and are in close contact with activated CD4+ T cells (Figure 8). *In vitro* stimulation through the T-cell factor CD40L has shown to reduce the spontaneous apoptosis of the CLL leukemia cells (*Scielzo C et al. 2011*). In addition to CD40L, two T-cell derived cytokines implicated in CLL proliferation and survival are IL-21 and IL-4. *In vitro* IL-4 supports CLL cell survival without inducing cell division. A recent Gene Set Enrichment Analysis (GSEA) has been shown that IL-4 target genes are enriched in lymph node derived CLL cells compared with peripheral blood CLL cells, suggesting that CLL cells are stimulated by IL-4 in the lymphoid tissues (*Dancescu M et al. 1992*). IL-21, produced mainly by follicular T helper cells, strongly potentiates the effects of CD40L/IL4 stimulation and induces also CLL-cell proliferation (*Pascutti MF et al. 2013*). In addition, the relevance of T cell signals *in vivo* has been demonstrated by Bagnara et al. which have shown that activated CD4+ T-cells are required to induce CLL cell proliferation in a xenograft murine model of CLL (*Bagnara D et al. 2011*).

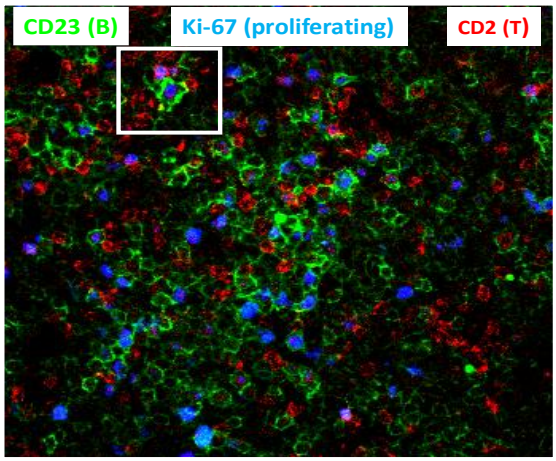

Figure 8. Immunofluorescent analysis of CLL cells in proliferating centers. T cells were stained with CD23 and CLL B-cells were stained with CD23 and ki67, proliferation marker.

Mesenchymal stromal cells such as bone marrow stromal cells (BMSCs) are another important cellular element in the tissue compartment. Stromal cells are composed of a heterogenous population which provide structural and functional support to CLL cells by producing chemokines, cytokines, pro-angiogenetic factors and through direct cell-cell contact (*Panayiotidis P et al. 1996*).

Nurse like cells (NLCs) derive from monocytes and protect CLL cells from spontaneous and drug-induced apoptosis. NCLs secrete chemokines such as CXCL12 (SDF-1α) and CXCL13 which attract CLL cells expressing the corresponding receptors CXCR4 and CXCR5 into the protective tissue niches. CXCR4 is highly expressed on CLL cell surface and binding of SDF-1α to CXCR4 induces the activation of the MAP kinase/AKT pathway, which is crucial for CLL cell survival, and regulates leukemia cell adhesion. In particular, hyperactivation of CXCR4 signalling in the Eμ-TCL1 mouse model has been associated with accelerated development of leukemia and transformation of CLL into aggressive lymphoma (*Lewis R et al. 2021*). In addition, NLCs produce and release TNF superfamily members: the B-cell activating factor (BAFF) and a proliferation-inducing ligand (APRIL), which support the survival and the proliferation of the malignant clones (*Audrito V et al. 2015; Burger JA et al. 2000; Nishio M et al. 2005; Endo T et al. 2007*).

A crosstalk between NLC and CLL cells may occur in the tumor microenvironment, where CLL cells can induce NLC differentiation through different factors: CLL cells express high levels of the enzyme nicotinamide phosphoribosyl-transferase, which induces polarization of monocytes into macrophages. The high mobility group protein B1 (HMGB1) is a nuclear protein which is released by damaged or dying cells and its levels are found high in plasma of CLL patients. HMGB1, released by the CLL cells, induces the differentiation of NLCs through the TLR-9/RAGE pathway and that differentiation can be inhibited by blocking the HMGB1/TLR-9/RAGE pathway (*Jia L et al. 2014*).

1.9 B-cell receptor signaling in CLL pathogenesis

B-cell receptor pathway and its associated protein tyrosine kinases play an essential role for development, survival and proliferation of normal B lymphocytes and expansion in B cell malignant clones (*Efremov D et al. 2020*).

Each B cell expresses a unique BCR in order to recognize one single epitope from foreign antigens and mount a specific antibody response. The BCR is a transmembrane protein and as described above is composed of a surface Ig molecule that is noncovalently associated with a heterodimer of CD79A (Igα) and CD79B (Igβ) on the plasma membrane. The surface Ig represents the antigen binding portion of the BCR, whereas the CD79A/CD79B heterodimer is the functional unit (Figure 9).

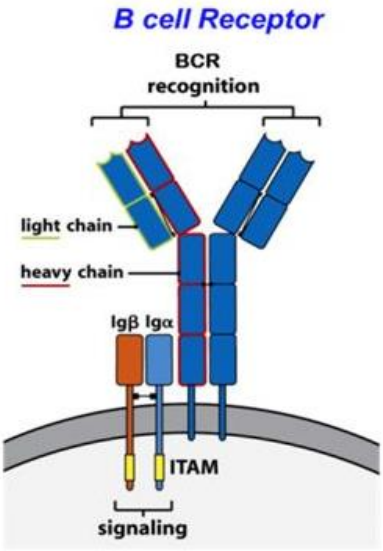

Figure 9. The B-cell receptor complex. Every BCR has a recognition portion that binds the antigen and it is associated with signalling molecules Igα and Igβ. The latters possess the ITAM motifs in their cytosolic tails and become phosphorylated when BCR binds an antigen (Janeway CA et al. 2001).

The uniqueness of every single BCR is due to gene rearrangements within the Ig loci that occur at the pro-B and pre-B cell stages of differentiation.

Binding of antigen to the BCR causes the formation of a “signalosome” that is composed of various protein kinases, phosphatases and scaffold-proteins, which propagate the signal inside the cells. The Igα and Igβ heterodimers have two conserved tyrosine residues, called immunoreceptor tyrosine-based activation motifs (ITAMs), which, after binding of the surface Ig to antigen, are phosphorylated by SRC kinase such as LYN (Lck/Yes-related novel protein tyrosine kinase) or SYK

(spleen tyrosine kinase). This event is the first step of the signal transduction from the cell surface to the nucleus (*Johnson SA et al. 1995*). The BCR signal is then propagated by SYK, which phosphorylates the downstream adaptor B-cell linker (BLNK), that in turn recruits BTK and phospholipase Cγ2 (PLCγ2). In parallel, activation of phosphatidylinositol-4,5-bisphosphate 3-kinase (PI3K) takes place leading to the generation of the second messenger phosphatidylinositol-3,4,5-triphospahte (PIP3), which then recruits the kinase AKT and other molecules involved in transducing the BCR signal. Activation of PLCγ2 leads to generation of the second messenger inositol1,4,5-triphosphate (IP3) and diacylglycerol (DAG), which induce the release of intracellular Ca2+ and activation of protein kinase C (PKC). The signaling proceeds with the activation of mitogen-activated protein kinases (MAPKs), including extracellular signal-regulated kinase (ERK), p38 kinase, c-Jun NH2-terminal kinase (JNK) and transcription factors, such as nuclear factor B (NF-kB) and nuclear factor of activated T-cells (NF-AT) (Figure 10) (*Stevenson FK et al. 2011; Niiro H et al. 2002*).

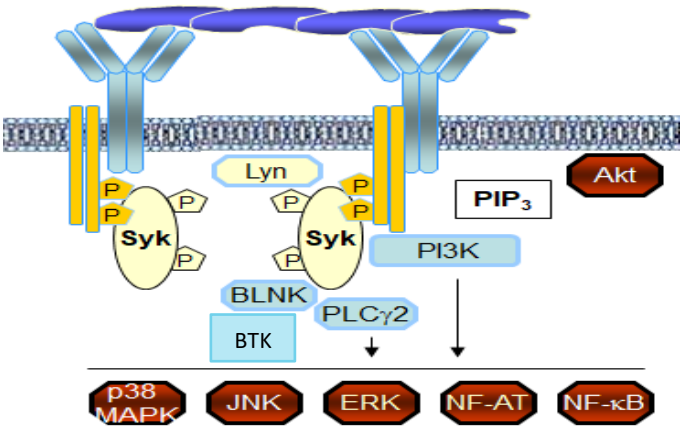

Figure 10. BCR signalling. Aggregation of the BCR with external antigen induces the phosphorylation of the ITAMs within the cytoplasmic tails of the Ig-α/Ig-β heterodimer. Phosphorylation of the ITAMs is mediated by LYN or other members of the SRC family kinases. SYK is subsequently recruited to the phosphorylated ITAMs and activated by a multistep process that involves phosphorylation by SRC family kinases and trans-autophosphorylation. SYK further propagates the BCR signal by phosphorylating and recruiting several signalling intermediates, such as BLNK, BCAP, VAV, SHC and PI3K. Recruitment of PI3K leads to the production of phosphatidylinositol- 3, 4, 5-triphosphate (PIP3) and subsequent BTK and AKT activation. SYK and BTK then activate PLCγ2, which produces the second messengers inositol-1, 4, 5-triphosphate (IP3) and diacylglycerol (DAG). These second messengers induce the release of intracellular Ca2+ and activate PKC, which then activate the transcription factors NFAT and NF-κB. Other molecules that are activated downstream of SYK are the mitogen-activated protein kinases ERK, JNK and p38MAPK. The cellular outcome in response to BCR engagement depends on the relative activity of the above described signalling molecules, and is influenced by the nature of the antigen, the availability of co-stimulatory signals and the stage of B cell differentiation.

The BCR pathway is constitutively activated in CLL and two mechanisms of BCR interaction have been proposed as responsible for this constitutive activation. The first one is the classical mechanism that is triggered by binding to external antigen (Figure 11A). CLL BCRs encoded by unmutated IGHV genes typically bind with low affinity to autoantigens generated during apoptosis or oxidation, such as non-muscle myosin heavy chain IIA (MYHIIA), vimentin, filamin B, cofilin-1, dsDNA, Sm, or oxidized lipoproteins (*Catera R et al. 2008; Lanemo MA et al. 2008*). Binding of these antigens to the leukemic BCRs induces an intermittent BCR signals, similar to the one induced by crosslinking the BCR with anti-IgM. The latter has been shown to induce the expression of anti-apoptotic and cell cycle regulatory proteins, such as Mcl-1, CCND2, and CDK4, which could support the development of the disease by increasing CLL cell survival and promoting CLL cell proliferation (*Petlickovski A et al. 2005; Deglesne PA et al. 2006; Guarini A et al. 2008*).

The second mechanism was identified as a unique feature of CLL BCRs and involves intermolecular interactions between the CDR3 of one BCR and internal immunoglobulin motives located in neighbouring BCRs expressed on the same cell, resulting in a continuous low intensity BCR signal that has been named cell-autonomous BCR signalling (*Dühren-von Minden M et al. 2012*). This signal appears to be responsible for the increase in the basal activity of several signalling molecules that are located immediately downstream of the BCR, such as the kinases LYN, SYK, PI3K, BTK, and PKC (Figure 11B) (*Gobessi S et al. 2009; Efremov D et al. 2014*).

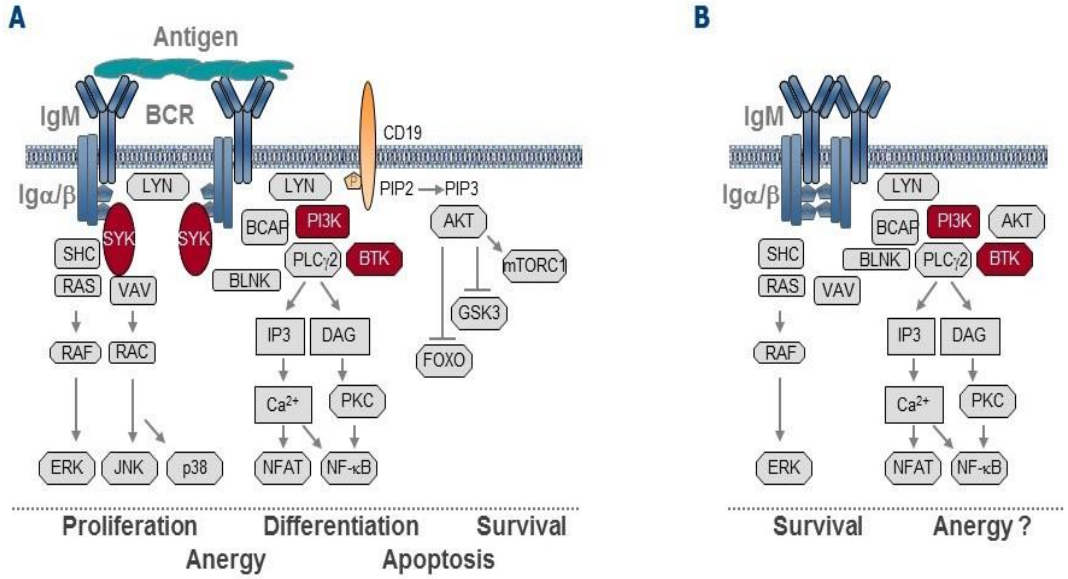

Figure 11. Two types of signals through BCR. BCR signals generated in CLL B cells. A) Antigen- dependent BCR signal generated by crosslinking of neighbouring BCRs by an external self- or foreign antigen or an antigen surrogate such as anti-IgM antibodies. B) Cell-autonomous BCR signal generated by an inter-molecular interaction between the HCDR3 and FR2 region of the same smIg (Efremov D et al. 2014).

Signals generated by both mechanisms display an important role in the pathogenesis of CLL and this has been elegantly demonstrated in the study of Iacovelli et al. which investigated the capacity of different antigen-BCR and BCR-BCR interactions to induce leukaemia in the well-established Eμ-TCL1 mouse model of CLL (*Iacovelli S et al. 2015*). The Eμ-TCL1 transgenic mice are characterized by the overexpression of the TCL1 oncogene in the B cell compartment and are predisposed to develop a CD5+/IgM+ CLL like leukemia in the adult age. TCL1 promotes oncogenic progression through binding and regulating factors which are implicated in cell-cycle, proliferation and survival such as AKT, a central member of BCR-pathway (*Laine J et al. 2000; Stachelscheid et al. 2022*). These mice were crossed with mice expressing various transgenic BCRs, including BCRs with cell-autonomous activity and BCRs specific for different foreign or self-antigens. B cells that expressed transgenic BCRs that become activated by low-affinity extrinsic autoantigens and/or cell-autonomous interactions entered into the leukemogenic process and became CLL cells, whereas leukemias did not develop from B cells expressing high-affinity BCRs regardless of antigen form. These data suggest that both types of BCR interactions, the antigen-dependent and cell-autonomous BCR interactions, cooperate in the pathogenesis of CLL.

Further evidences for the key role of the BCR in CLL pathogenesis and progression derive from the different clinical behaviour of patients carrying somatic mutations in the clonal IGHV genes (M-CLL) compared to patients with no mutations in the IGHV sequence (U-CLL). Patients with U-CLL show a more aggressive disease and shorter survival, whereas patients with M-CLL exhibit an indolent disease and a longer survival (*Damle R et al. 1999; Hamblin et al. 1999*). The differences in clinical behaviour are thought to result from the greater responsiveness to BCR stimulation in the U-CLL cases or the different antigen specificity of the U-CLL and M-CLL BCRs. U-CLL cells express polyreactive low-affinity BCRs which can recognize and bind multiple auto-antigens, resulting in chronic activation of the BCR pathway (*Burger at al. 2013*). The mechanism of BCR activation in M-CLL is less clear, as these BCRs typically do not display poly- or autoreactivity (*Herve M et al. 2005*). In this subset the BCR pathway may be primarily activated by cell-autonomous BCR interactions, resulting in generation of continuous low-amplitude signals that increase CLL cell survival but do not affect CLL proliferation (*Chiorazzi N and Efremov D. 2013*).

Evidence for the *in vivo* BCR pathway activation came from gene expression profiling studies performed by Herishanu and colleagues, which have observed that freshly isolated CLL B cells express high levels of genes that are induced by BCR engagement. BCR target genes were especially enriched in CLL cells isolated from lymph nodes, suggesting that *in vivo* CLL cells are continuously

exposed to antigen. In addition, higher levels of BCR target genes were found in U-CLL compared to M-CLL cells, further suggesting that U-CLL cells are more often exposed to antigenic stimuli *(Herishanu Y et al. 2011*).

Furthermore, approximately 30% of CLL cases express "quasi-identical" BCRs, called "stereotyped" BCRs, suggesting that there is selection of BCRs with particular antigen-binding capacities. This is an additional evidence that BCR-dependent mechanisms select and drive the expansion of the malignant clones in a substantial proportion of CLL cases (*Agathangelidis A et al. 2012*).

The most relevant evidence for the key role of the BCR pathway in CLL derives from the clinical activity of the BCR inhibitors (Figure 12).

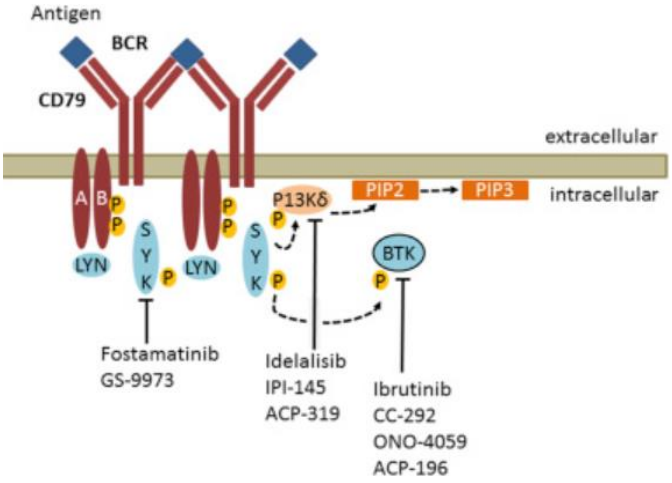

Figure 12. Inhibitors of BCR downstream signaling molecules. Fostamatinib inhibits the kinase SYK; Idelalisib is a PI3kδ inhibitor and Ibrutinib is the BTK inhibitor.

Although BCR pathway plays a pivotal role in CLL pathogenesis and progression, unlike normal B-cells, *in vitro* stimulation of BCR is not sufficient to induce CLL cell proliferation suggesting that additional signals, which *in vitro* are missing, may drive the proliferation of the CLL cells and affect the progression of the disease.

1.10 Toll-like receptor signaling in CLL pathogenesis

Toll-like receptors (TLRs) play a crucial role in innate immune system activation by recognizing pathogen associated molecular patterns (PAMPs), which are conserved structural components of viruses, bacteria and fungi, and damage associated molecular patterns (DAMPs), which are derived from damaged or injured tissues. TLRs activate the innate immune system and also determine the development of the adaptive immune response. The TLR family consists of ten members (TLR1-TLR10) belonging to the family of interleukin-1 receptors (IL-1R). TLR family members have a different subcellular distribution being expressed either on the plasma membrane or in the endosomal compartments. The TLRs that bind to bacterial components are on the cell surface and include TLR1, 2, 4, 5 and 6. The others TLRs, i.e. 3, 7, 8 and 9, are localized in endosomes and recognize virus/bacteria-associated nucleic acids (dsDNA, ssDNA and RNA) (Figure 13).

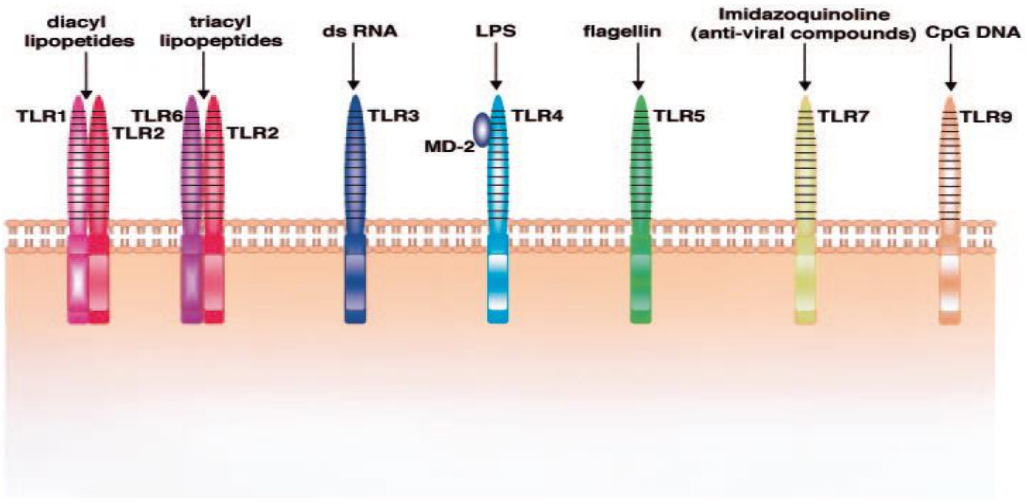

Figure 13. Types of ligand recognized by TLRs: Different ligands are recognized by different TLRs in different cellular compartments.

TLRs are transmembrane receptors and their structure includes an N-terminal leucin-rich-repeat (LRR) domain for the ligands and a cytosolic domain, intracellular Toll/interleukine-1 receptor domain (TIR), for the signaling inside the cells (Figure 14).

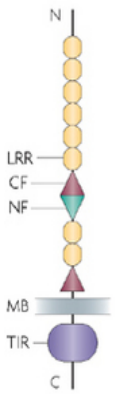

Figure 14. TLR Structure. TLR is characterized by extracellular and intracellular domains.

Following TLR ligation with appropriate ligand, TLRs recruit adaptor proteins to the TIR domain, such as MyD88, which is required by all TLRs, except TLR3 (Figure 10). Others adaptor proteins that are recruited are TIR domain containing adaptor protein inducing IFN-β (TRIF), TRIF related adaptor molecule (TRAM) and TIR domain containing adaptor protein (TIRAP). The adaptor proteins work as scaffolds for the recruitment of downstream components which include IL-1 receptor associated kinases (IRAKs). IRAK 1, 2, 3 (also known as IRAKM) and 4 are serine/threonine kinases that activate NF-kB. Upon stimulation, MyD88 recruits IRAK4 and IRAK1, which is activated through phosphorylation by IRAK4.

Phosphorylated IRAK1 recruits TRAF6, an E3 ubiquitin ligase that activates the Ik-B kinase complex (IKK), leading to degradation of the NF-kB inhibitor IkB and translocation of NF-kB to the nucleus. In addition, activation of TAK1 induces also the activation of MAP-kinases, such c-Jun-NH2 terminal kinase (JNK). NF-kB, translocated to the nucleus, induces the transcription of downstream genes involved in the inflammatory response, such as IL-2 and IL-6, and genes that regulate cell proliferation and survival, such as cyclin-D1, cyclin-D2 and c-Myc (Figure 15) (*Correa JMI et al. 2014*).

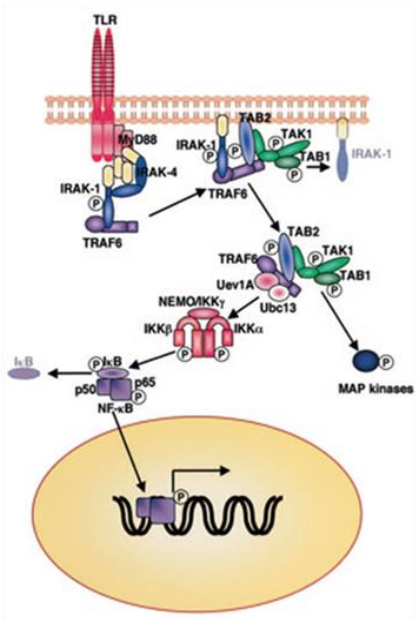

Figure 15. IL-1R/TLR pathway. For the activation of TLR pathway is required the recruitment of adaptor and kinase proteins with final activation of NF-kB which translocate to nucleus.

TLRs are expressed at low levels in naïve human B-cells, whereas memory and activated B cells express greater levels of TLR 1, 6, 7, 9, 10. Following activation of BCR and CD40 stimulation, there is an increase of expression of TLRs, above all TLR9. Exposure of human B cells to TLR ligands is sufficient to induce proliferation, class switch recombination and antibody secretion (*Browne EP. 2012*).

In certain B-cell malignancies, such as Waldenstrom macroglobulinemia, diffuse Large B-cell lymphoma and less frequently CLL, the TLR pathway can be constitutively activated by the L265P mutation in the MyD88 adaptor protein, which results in recruitment of IRAK4 with activation of several downstream effector pathways, including NF-kB, PI3K/AKT, ERK, JNK and p38MAPK. Inhibition of IRAK4 with selective kinase inhibitors induces apoptosis in MyD88 mutated DLBCL and Waldenstrom macroglobulinemia cell lines, further suggesting that the TLR pathway could play a role in the pathogenesis of certain B cell malignancies, including CLL (*Ngo VN et al. 2011*).

In CLL ~3% of patients carry the MyD88 L265P mutation, which is found in IGHV-mutated patients and is associated with younger age at diagnosis (*Improgo MR et al. 2019*). CLL cells express higher level of TLR9 than normal B cells, although a considerable variability exist (*Grandjenette C et al. 2007*). TLR9 is a nucleotide-sensing TLR which is activated by unmethylated CpG oligonucleotides (CpG-ODNs). B cells can acquire DNA after BCR-mediated internalization. In particular CLL BCRs from patients with aggressive disease, IGHV unmutated patients, frequently bind to autoantigens on apoptotic cells, which are typically associated with DNA molecules. Such BCRs could allow CLL cells to internalize DNA-containing immune-complexes with activation of TLR9 molecules which are located at the endosomal compartment (*Catera R et al. 2008; Lanemo MA et al. 2008*) (Figure 16).

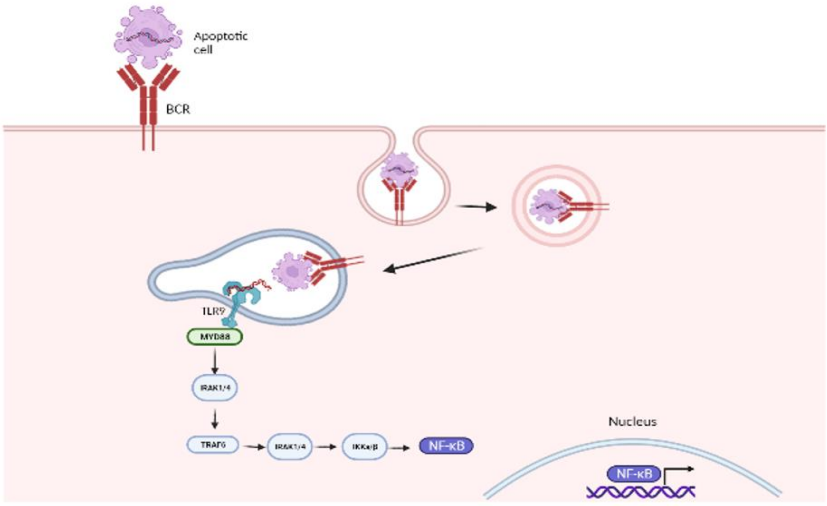

Figure 16. TLR9 activation by interaction with the BCR: BCRs bind and internalize immune-complexes containing TLR9 ligand which are shuttled to the endosomes leading activation of TLR9 pathway with translocation of the active form of the transcription factor NF-kB into the nucleus (Created with Biorender).

In CLL, heterogenous responses have been observed in different patients when leukemic cells were exposed to the synthetic TLR9 ligand, CpG-ODNs. Studies performed some years ago revealed that U-CLL cells respond to TLR9 triggering by activating downstream signaling pathways which induce proliferation of the malignant cells. In proliferating cells, CpG-ODN stimulation induced degradation of the NF-kB inhibitor IkB and prolonged phosphorylation of the AKT, ERK, JNK and MAP-kinases. In contrast, CpG-ODN stimulation in M-CLL cells resulted in only weak activation of downstream TLR-signaling pathways, which was associated with a G_1/S phase cell cycle arrest and induction of apoptosis (*Longo PC et al. 2007*).

IL-15 has been reported to prevent CpG-ODN induced apoptosis of M-CLL cells and increase the proliferation of CpG-ODN stimulated U-CLL cells (*Mongini P et al. 2015*). IL-15 is an inflammatory cytokine found in stromal cells of bone marrow, lymph nodes and spleen, which are the sites where CLL cells proliferate. These tissue compartments also contain apoptotic cells, which could provide a source of CpG-DNA to CLL cells. Stimulation of M-CLL cells with IL-15 enhances phosphorylation of ERK1/2 and AKT, indicating that IL-15 could compensate the apoptotic effect of CpG-ODN by facilitating the activation of these kinases. Moreover IL-15 induces upregulation of pro-survival proteins, such as BCL-2, BCL-X_L and MCL-1.

Together, these data raise the possibility that *in vivo* both CLL subsets may potentially receive growth-promoting signals through the TLR pathway, which could represent a novel therapeutic target in CLL. Additional evidences supporting a potential involvement of the TLR-pathway in CLL *in vivo* include the upregulation of TLR9 target genes in lymph-node isolated CLL cells compared to peripheral blood CLL cells (*Dadashian EL et al. 2019*), as well as recent findings that CLL patients display high plasma levels of cell-free DNA which correlate with a more aggressive clinical course (*Kennedy E et al. 2021*). Moreover, a recent study reported that pharmacological inhibition of the TLR-pathway using an inhibitor of the kinase IRAK4 delays the expansion of the leukemia cells in the Eμ-TCL1 adoptive transfer model (*Gimenez N et al. 2020*). All together these data suggest that the TLR-pathway can be activated *in vivo* and may affect CLL disease progression.

2. AIMS OF THE PROJECT

The main objectives of this thesis are:

1. A comprehensive investigation of the role of BCR-signals in driving CLL cell proliferation.

2. Investigating the role and the contribution of TLR-signals in driving CLL cells proliferation in murine models of the disease.

3. Materials and methods

Patient samples

Blood samples were collected from patients who satisfied standard morphologic and immunophenotypic criteria for B-cell CLL. Informed consent was obtained from all patients according to the Declaration of Helsinki, and approval for the study was obtained from the institutional human research committee at the Catholic University Hospital 'A Gemelli'. Peripheral blood mononuclear cells were separated by Ficoll gradient centrifugation, and CLL B cells were purified by negative selection with anti-CD3, anti-CD14 and anti-CD16 mouse monoclonal antibodies and Dynabeads coated with anti-mouse IgG (Dynal Biotech, Oslo, Norway). The purity of the selected B-cell populations was evaluated by staining with anti-CD5 and anti-CD19, followed by flow cytometric analysis on a FACS Celesta flow cytometer (BD Biosciences). In all cases, the purity of the CLL B-cell samples exceeded 98%.

Real-time PCR analysis (RQ-PCR)

Total cellular RNA was isolated from CLL B cells using the Trizol reagent (Thermo Fisher Scientific). cDNAs were generated from 250-500 ng of total RNA using random hexamers, MuLV Reverse Transcriptase and RNAse inhibitor, according to the manufacturer's instruction (Thermo Fisher Scientific). qRT-PCR was performed on the CFX96 Touch Real-Time PCR Detection System (Bio-Rad) using Applied Biosystems TaqMan gene expression assays for Myc (human Hs00153408_m1, mouse Mm00487804_m1), CCND1 (human Hs00765553_m1), CDK4 (human Hs00364847_m1, mouse Mm_00726334_s1), CCND2 (human Hs00153380_M1, mouse Mm_00438070_m1), CDKN1A (human Hs00355782_m1, mouse Mm_00432448_m1), CDKN2A (human Hs00923894_m1, mouse Mm00494449_m1), CDKN2B (human Hs00793225_m1, mouse Mm00483241_m1) and Actin (human Hs99999903_m1, mouse Mm00607939_m1), according to the manufacturer's recommendations (Thermo Fisher Scientific). Samples were run in triplicate, and relative quantification was performed with the comparative Ct method.

CRISPR/Cas9-editing of murine CLL, RS-PDX cells and human CLL cell lines

CRISPR/Cas9-editing of murine Eμ-TCL1 leukemia cells was done as recently described (Chakraborty S. et al, Blood 2021). Briefly, cells were thawed and cultured in RPMI-1640 supplemented with 10% heat-inactivated FBS, 100U/mL penicillin, 0.1mg/mL streptomycin, 2mM L-glutamine, 1mM sodium pyruvate (Invitrogen) and 1μM CpG-1668 (InvivoGen) at a concentration of $1x10^7$ cells/ml for 20 hours prior to CRISPR/Cas9 editing with the Alt-R system (Integrated DNA Technologies). To generate the Cas9 ribonucleoprotein (RNP) complex that targets the MyD88 gene, a predesigned MyD88 cr-RNAs (1.5μM) was combined with 1.5μM ATTO 550-labeled tracr-RNA, 0.75μM recombinant Cas9 protein and 1.5μM Alt-R Cas9 electroporation enhancer in 5μL nuclease-free duplex buffer (all from Integrated DNA Technologies). The Cas9 RNP complex was then electroporated using the Amaxa Nucleofector II device and the Z-001 program into $6x10^6$ leukemic cells resuspended in 100μl Mouse B cell Nucleofector solution (Lonza).

For CRISPR/Cas9-editing of the human RS-patient-derived xenograft (PDX) tumors, cells were thawed, cultured in the same medium as above at a concentration of $5x10^6$ cells/ml and stimulated with 1μM CpG-2006 and 25ng/ml human IL-15 for 20 hours prior to transfection of the Cas9 RNPs using the NEPA21 Super Electroporator (Nepagene, Chiba, Japan) and the transfection conditions are described in Table 1. Control cells were transfected with Cas9 RNPs without cr-RNA. Following transfection, cells were cultured for 3 days with 3T3-msCD40L fibroblasts and 10 ng/ml human IL-4 prior to injection in NSG mice.

For CRISPR/Cas9-editing of the human CLL cell lines, $1.2x10^7$ were transfected with Cas9 RNPs using the NEPA21 Super Electroporator and the transfection conditions are described in Table 1. Then, edited-cells were cultured for 3 days prior injection in NSG mice.

Editing efficiency was evaluated by amplicon capillary electrophoresis on a 3500 Genetic Analyzer (Applied Biosystems) of PCR fragments spanning the region of genomic DNA around the targeted site, as described in more detail elsewhere (Chakraborty S et al. 2021). Cr-RNA sequences are provided in Table 2.

Table 1. Conditions for the NEPA21 Super Electroporator

No. of cells	Volume of electroporation medium*	Parameters	Poring pulse	Transfer pulse
$6x10^6$	100 µl	Voltage (V)	275	20
		Pulse length (ms)	1	50
		Pulse interval (ms)	50	50
		Number of pulses	4	5
		Decay rate (%)	10	40
		Polarity	+	+/-

*Opti-MEM Reduced Serum Medium was used as electroporation medium

Table 2. Nucleotide sequences of cr-RNAs used in this study.

Name of the Gene	cr-RNA sequences	PAM Sequence
TRP53 (Mus musculus)	CATAAGGTACCACCACGCTG	TGG
CDKN2A (Mus musculus)	GGAAGGCTTCCTGGACACGC	TGG
CDKN2B (Mus musculus)	GGAAGGCTTCCTGGACACGC	GGG
IGHM (Mus musculus)	AGGACCGTGGACAAGTCCAC	AGG
MYD88 (Mus musculus)_1st crRNA	TATATCCTCACGGTCTAACA	AGG
MYD88 (Mus musculus)_2nd crRNA	CCCACGTTAAGCGCGACCAA	GGG
IRAK4 (Homo sapiens)	GATGAACGACCCATTTCTGT	TGG
Immunoglobulin Heavy Constant Mu (Homo sapiens)_1st crRNA	CAGGACACCTGAATCTGCCG	GGG
Immunoglobulin Heavy Constant Mu (Homo sapiens)_2nd crRNA	GCCTTCCAAGGACGTCATGC	AGG

DNA extraction and PCR amplification of the CRISPR/Cas9 targeted region

DNA was extracted from cells derived from Eμ-TCL1 cells, purified with EasySep Mouse CD19 Positive Selection Kit (Stemcell Technologies), or human CLL and RS-PDX cells using the KAPA Express Extract (Sigmaaldrich) in 50 μl of reaction volume which included: 44 μl DNAase-free water, 5 μl of 10x Extraction buffer and 1 μl of Extraction enzyme. Samples were then incubated for 10 min at 75°C for lysis and for 5 min at 95° C to inactivate the enzyme. Samples were centrifuged briefly to pellet cellular debris. 2 μl DNA extract was used as PCR template.

A PCR master mix containing the appropriate volume of all reaction components was prepared based on the following table 3:

Table 3. PCR master mix:

	Volume (50 μl)
PCR buffer 10x	5 μl
MgCl2	3 μl
Forward primer	0.5 μl
Reverse primer	0.5 μl
Ampli Taq Gold polymerase	0.25 μl
DNA	2 μl
DNase free water	38.75 μl

PCR conditions used are the following: 95°C for 10 min, repeated cycles 95°C 15 sec/62°C 15 sec/72°C 20 sec for 40 times, and extension at 72° for 10 min

The sequences of the primers used for the amplification of the CRISPR/Cas9 targeted region are provided in Table 4.

Table 4. Sequences of primers used for evaluation of Cas9 editing activity by fragment length analysis.

Name of the Gene	(5'-3') Forward Primer	(5'-3') Reverse Primer
TRP53 (Mus musculus)	[FAM]GAGTATCTGGAAGACAGGCAGA	GCTGGAGTCAACTGTCTCTAAG
CDKN2A (Mus musculus)	[FAM]GTGCAGATTCGAACTGCGAGG	CATCGCGCACATCCAGCCGA
CDKN2B (Mus musculus)	[FAM]TCCACGGAGCAGAACCCAACT	CCCAGGCGTCACACACATCC
IGHM (Mus musculus)	[FAM]TGTGACAGAGGAGGAATGGAAC	ATCAGGGAGACATTGTACAGTGT
MYD88 (Mus musculus)_1st crRNA	[FAM]TGGCACAAAGCCAGGAAGCAC	TTTGTTGGATGCCTGGCAGGG
MYD88 (Mus musculus)_2nd crRNA	[FAM]TCCGCCAGCAAGGTCCAGT	TCCGGGTCCCTGGACTCCTT
IRAK4 (Homo sapiens)	[FAM]TGAATTGAAGAATGTCACAAATAAC	TTACTGCTGCAAGCTTCTTCACT
Immunoglobulin Heavy Constant Mu (Homo sapiens)_1st crRNA	[FAM]TGCACCTGGTCCGTGGTGAC	TCCCAAAGTGAGCGTCTTCGT
Immunoglobulin Heavy Constant Mu (Homo sapiens)_2nd crRNA	TACAAGAACAACTCTGACATCAG	[FAM]TCACCTGGAAGAGGCACGTTC

Agarose gel electrophoresis of DNA

Size fractionation of DNA samples was performed through electrophoresis in 2% (w/v) agarose gel (Invitrogen) prepared in TBE 1X (89 mM Tris; 89 mM Boric acid; 2 mM EDTA; pH 8.3), containing 1µl of SYBR safe/10 ml agarose gel (Thermo Scientific). PCR samples and DNA size markers were loaded onto the gel and run at 80 mA in TBE 1X buffer. PCR products were visualized by UV transilluminator machine and the image was captured with Gel Doc EZ imager (BioRad).

Isolation and culture of macrophages

For the in vitro co-culture experiments, peritoneal cavity (PC) macrophages were isolated from NSG mice by peritoneal cavity lavage, using PBS/3% FBS. After centrifugation, PC cells were resuspended in RPMI-1640 medium supplemented with 10% heat-inactivated FBS, 100U/mL penicillin, 0.1mg/mL streptomycin, 2mM L-glutamine and 1mM sodium pyruvate at a concentration of $1x10^4$ cells/ml and placed in culture to allow the macrophages to adhere to the plate for 5 hours at 37°C. Nonadherent cells were removed by gently washing two times with warm PBS. For the generation of bone-marrow derived macrophages, the cells were harvested from the femurs of NSG mice and cultured in RMPI-medium containing 10 ng/ml of macrophage colony–stimulating factor (M-CSF). After 4 days in culture, nonadherent cells were removed by gently washing two times with warm PBS and adherent cells were harvested and analyzed by flow cytometry to determine the percentage of CD11b+/F4-80+ cells. The harvested peritoneal cavity or bone marrow-derived macrophages were then cultured at a ratio 1:50 with Eμ-TCL1 cells or human RS-PDX cells. Viability analysis 5×10^5 cells/ml murine TCL1 leukemia or human RS-PDX cells were cultured in presence or absence of macrophages as indicated in the figures or figure legends. Afterwards, cells were pelleted by centrifugation and stained with Annexin V-FITC and PI (both from Tau Technologies B.V.). Data were acquired on a FACS Celesta and analysed using FlowJo software.

***In vitro* cell proliferation assays**

For in vitro BrdU proliferation analysis of murine Eμ-TCL1 cells, $1x10^6$ cells were stimulated with 1μM CpG-1668 or 5μg/ml LPS or co-cultured in presence of macrophages isolated from the PC of NSG mice for 28 hours prior to addition of 10μM BrdU. For *in vitro* BrdU proliferation analysis of human RS-PDX cells, $1x10^6$ cells were stimulated with 1μM CpG-2006 or were cultured in presence of macrophages isolated from the PC of NSG mice for 28 hours and then incubated with 10μM BrdU. The duration of BrdU incorporation prior to harvesting is indicated in the figure legends. After harvesting, cells were labelled with the fixable viability eFluor 780, fixed with 2% paraformaldehyde, permeabilized using 3 M HCl plus 2% Tween 20 solution, neutralized with 0.1M sodium borate buffer pH 9.0 and stained with anti-BrDU-V450 antibody (BD Horizon, cat. #563445).

Flow cytometry analysis

Single cell suspensions were prepared from spleens and subcutaneous tumors by grinding the tissue through 70 µm cell strainers (BD Biosciences). Erythrocytes were lysed using ACK-lysing buffer (Thermo Fisher). Cells from peritoneal cavity were obtained by lavage and were not treated further. Staining of cell surface proteins was performed in phosphate-buffered saline (PBS) with 1% fetal calf serum and 0.1% sodium azide for 30 min at 4 °C. The following antibodies were used:

- CD5-anti-mouse-PE (BD Pharmingen, cat. #553023)
- CD19-anti-mouse -BV421 (BD Pharmingen, cat. #562701)
- CD19-anti-mouse-APC (BD Pharmingen, cat. #561738)
- CD19-anti-human-APC (Miltenyi Biotec, cat. #130-113-642)
- Goat F(ab')2 anti-human IgM-PE (Thermo Fisher, cat. #H15104)
- anti-mouse IgM-APC (BD Pharmingen, cat. #550676)
- CD11b-anti-mouse-APC (Miltenyi, cat. #130-098-088)
- F4/80-anti-mouse-FITC (Biorad, cat. #MCA497FA)
- CD45.1-anti-mouse-PE (eBioscience, cat. #12-0453-83)
- CD45.2-anti-mouse-BV421 (BD Pharmingen, cat. #562895)

Data were acquired on a FACSCelesta (BD Biosciences) and analyzed using FlowJo software (FlowJo, Ashland, OR, USA).

Immunoblotting analysis

Cells were washed in ice-cold PBS, pelleted and lysed in RIPA lysis buffer (10mM Tris-HCl, pH 7.4, 5mM EDTA, 150 mM NaCl, 0.1% SDS, 0.1% sodium deoxycholate) containing protease and phosphatase inhibitors (Sigma-Aldrich). Total cell lysates were kept on ice for 30 minutes, mixing them every 10 minutes, and then centrifuged in a benchtop centrifuge (Eppendorf) at 16000xg for 20 minutes at 4°C. The protein concentration of each cell lysate was determined with the RC DC Protein Assay (Bio-Rad). 20-50 μg of protein lysates were denaturated by boiling at 95°C for 5 minutes, in the presence of 1X SDS loading buffer (200mM Tris-HCl pH 6.8, 400mM DTT, 8% SDS, 0.4% Bromophenol blue, 40% glycerol). SDS PAGE gels were prepared as Table 5.

Table 5: SDS gel preparation

Components	Resolving Gel 8% (10 ml)	Stacking Gel (5 ml)
30% Acrylamide mix	2.7 ml	830 μl
Tris-HCl pH 8.8	2.5 ml	-
Tris-HCl pH 6.8	-	630 μl
Ammonium persulphate	100 μl	50 μl
SDS 10%	100 μl	50 μl
TEMED	10 μl	5 μl
H2O	4.6 ml	3.4 ml

The protein samples were separated by SDS-PAGE and transferred on Immobilon-P polyvinylidene difluoride membranes (Millipore). Membranes were blotted at 4°C in the presence of 5% non fat dry milk with the following antibodies: c-MYC (cat. #5605, 1:1000), CCND2 (cat. #3741, 1:1000), IRAK4 (cat. #43635, 1:1000), phospho-p65 (cat. #3033, 1:3000), β-actin (cat. #3700, 1:10000) (all from Cell Signaling Technology), CDKN2A (cat. #PA5-20379,1:1000), CDKN2B (cat. #PA5-49749), CDKN1A (cat. #AHZ-0422), MyD88 (cat. #14622363, 1:1000) (all from Invitrogen), TP53 (Merck Millipore, cat. #PAb421), rabbit IgG-HRP-linked (cat. #111-035-046, 1:5000) and mouse IgG-HRP-linked (cat. #115-035-071, 1:5000) (both from Jackson Immunoresearch Laboratories). Immunodetection was done on an ALLIANCE LD2 chemiluminescence Imaging System (Cleaver Scientific Ltd., Warwickshire, UK), using ECL Plus enhanced-chemiluminescence detection reagents (GE Healthcare, Chicago, IL, USA).

Histology and immunohistochemistry

Formalin-fixed murine splenic tissue samples were embedded in paraffin and sliced at 4 μm. Sections were stained with H&E and antibodies against BrdU (AbCam, cat. #ab6326, 1:200) or phospho-histone H3 (Merck Millipore, cat. # MM_NF-06-570, 1:100). BrdU-positive and phospho-histone H3-positive cells were quantified using the Image J software.

***In vivo* experiments with murine models**

All animal procedures were performed under a protocol approved by the Italian Ministry of Health (no. 347/2017-PR). CRISPR/Cas9-edited Eμ-TCL1 leukemia cells were transferred by intraperitoneal injection of $3x10^7$ cells in 2-3 months old NSG or C57BL/6 mice. The human RS-PDX or CLL cell lines cells were inoculated intraperitoneally ($2x10^6$ cells) and subcutaneously in the right flank of NSG mice ($1.2x10^7$ cells in 0.2ml of a 50:50 mixture of cells and Matrigel Matrix). For the *in vivo* treatment experiments, C57BL/6 mice or NSG mice were fed with standard diet containing vehicle control or medicated chow containing 0.25g/kg R221 (kindly provided by Rigel Pharmaceuticals, Inc).

Statistical analysis

Data are expressed as means ±SD. Differences in leukemia cell numbers, % proliferating cells, % viable cells and mutant allele frequency were evaluated using the t test, Mann-Whitney rank sum test or oneway repeated measures ANOVA, as indicated in the figure legends. Survival curves and medians were calculated with the method of Kaplan-Meier. The log-rank test was used to compare differences between estimated survival curves. All statistical analyses were performed using the SigmaStat Version 3.1 program (Systat Software). P values are indicated in the figures

Chapter 4. RESULTS

4.1 BCR signals regulate CLL cell proliferation

(Chakraborty S, Martines C et al, Blood. 2021; 138:1053-1066)

4.1.1 BCR stimulation results in induction of cell-cycle regulatory genes

CLL cells do not proliferate following BCR stimulation, indicating that other signals from the microenvironment are required. In a work in collaboration with other colleagues of the Molecular Hematology lab, to further investigate the role of BCR pathway in CLL cell proliferation, we re-analyzed a previously generated gene-expression data set of unstimulated and immobilized anti-IgM (Imm-aIgM) stimulated CLL cells (*Dal Bo M et al. 2015*).

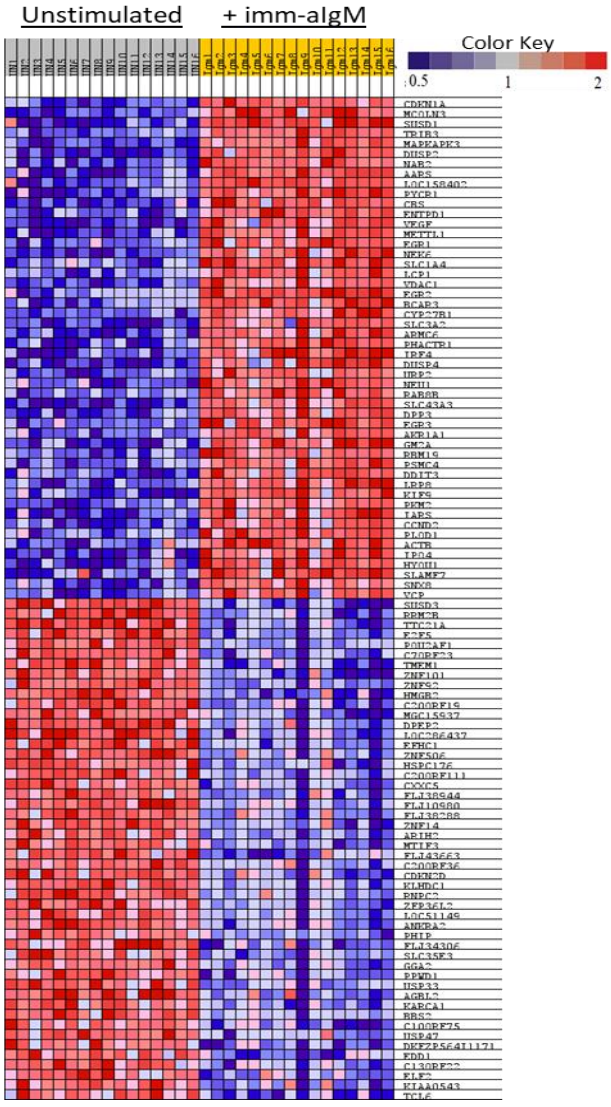

Figure 17. BIOCARTA pathway analysis of differentially expressed genes between unstimulated and BCR-stimulated human CLL cells. Differentially expressed genes unstimulated CLL cells and stimulated CLL cells (n=16) with immobilized anti-IgM for 20hrs and analysed on the Agilent Whole Human Genome Microarray 4x44K Platform (GEO accession number GSE52776). The top 50 upregulated and top 50 downregulated are shown.

The gene-expression data set was analysed by Pathway enrichment analysis using the BIOCARTA database, which, among the 735 differentially expressed genes (FC>2.0 and p<0.001), identified gene sets involved in the G1-phase cell cycle regulation as the most differentially expressed. The differentially expressed genes included MYC, CCND1, CCND2, and CDK4, which were all upregulated, and CDKN2D, which was downregulated in anti-IgM–stimulated CLL cells, consistent with entry of the leukemic cells into the G1 phase of the cell cycle. However, upregulation of the negative regulators CDKN1A and CDKN2B was also observed, with CDKN1A appearing as the most differentially expressed gene in this analysis (Figure 17).

The finding that BCR-stimulation induces the expression of positive and negative regulators of the cell-cycle was further validate by RQ-PCR experiments showing that the most differentially expressed genes MYC, CDK4, CCND1, CCND2, CDKN1A and CDKN2B were upregulated in CLL cells cultured with Imm-aIgM. The changes in the protein levels were also validated by immunoblotting analysis that showed increased expression of c-MYC, CCND2, CDKN1A and CDKN2B in CLL cells stimulated for 14 or 36 hrs with Imm-aIgM (Figure 18A and B).

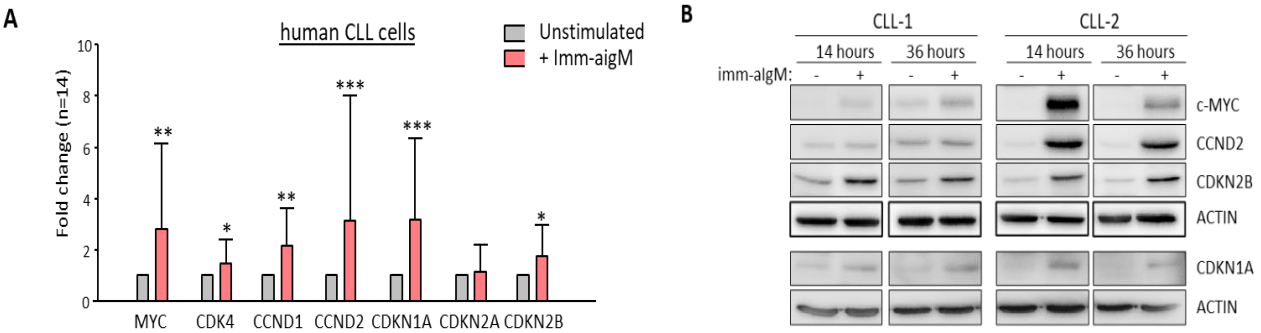

Figure 18. Positive and negative regulators of the cell cycle are induced by BCR-stimulation in CLL cells. A) Peripheral blood mononuclear cells (PBMCs) were isolated from CLL patients (n=14) whole blood by Ficoll density gradient and then cultured in presence or absence of Imm-aIgM for 20hrs prior to RNA extraction. Significant differences with respect to unstimulated CLL cells are indicated by asterisks: *P < .05, **P < .01, ***P < .001. B) CLL cells were stimulated for 14 or 36hrs with Imm-aIgM prior to protein extraction and analysis of protein levels by immunoblotting.

To investigate whether BCR engagement induces similar changes in murine CLL cells, we used Eμ-TCL1-derived leukemia cells reactive with the autoantigen phosphatidylcholine (PtC). PtC is a membrane phospholipid that is exposed by senescent or apoptotic cells on their surface and it is recognized by the CLL BCR in 30-40% of spontaneously generated Eμ-TCL1 leukemias (*Suljagic M et al. 2010; Chen SS et al. 2013*).

Stimulation of PtC-binding leukemia cells with PtC liposomes resulted in significant induction of CDKN1A and CDKN2B. In addition, the cell-cycle inhibitor CDKN2A, which lies adjacent to CDKN2B on chromosome 9p21, was also induced in these experiments (Figure 19).

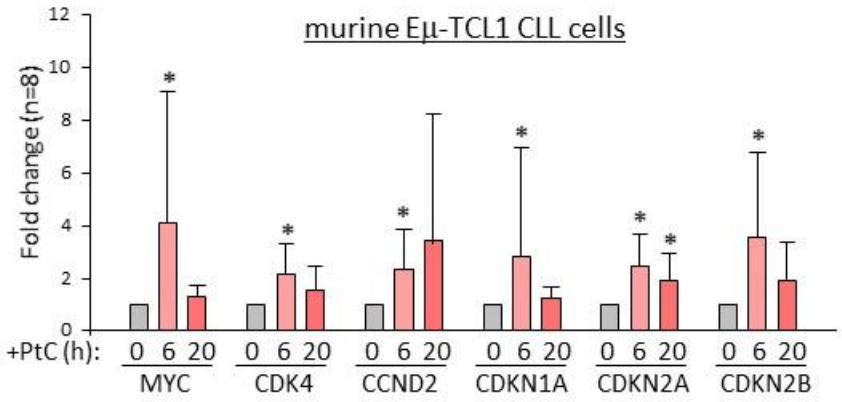

Figure 19. BCR-stimulation induces expression of cell-cycle regulatory genes in murine CLL cells. Eμ-TCL1 cells expressing an anti-PtC BCR were cultured for 6 or 20hrs in presence of PtC liposomes prior to RNA isolation.

4.1.2 Genetic disruption of CDKN2A, CDKN2B and TP53 results in accelerated tumor growth in murine CLL cells in vivo

The finding that the cell-cycle inhibitors CDKN1A, CDKN2A, and CDKN2B are induced upon BCR engagement suggested that upregulation of these proteins could represent a mechanism to prevent the proliferation of antigen-stimulated CLL cells in the absence of costimulatory signals. On the other hand, the fact that these genes are often directly or indirectly inactivated in RS because of deletions involving the CDKN2A/2B locus (30% of cases) and mutations or deletions the CDKN1A transcriptional activator TP53 (50% of cases) suggested that genetic defects in these genes may contribute to CLL progression by allowing for costimulatory signal-independent proliferation. To further explore this possibility, we simultaneously targeted CDKN2A, CDKN2B, and TP53 in 1 Eμ-TCL1-derived leukemia expressing an anti-PtC BCR (TCL1-355). Targeting of CDKN2A, CDKN2B, and TP53 was performed by nucleofection-mediated delivery of ribonucleoprotein (RNP) complex containing a recombinant Cas9 and a pool of guide RNAs (gRNAs) against the above mentioned genes. After transfection, the targeted and control cells were then expanded in immunodeficient NSG mice and were subsequently transferred in syngeneic recipients to evaluate the effects of TP53/CDKN2A/2B knockdown on leukemia growth and proliferation. After *in vivo* passages, the

proportion of mutant and wild-type (WT) alleles in the targeted cells was evaluated by amplicon capillary electrophoresis analysis of indels which showed that TP53/CDKN2A/2B-edited leukemic cells were positively selected (Figure 20A and B).

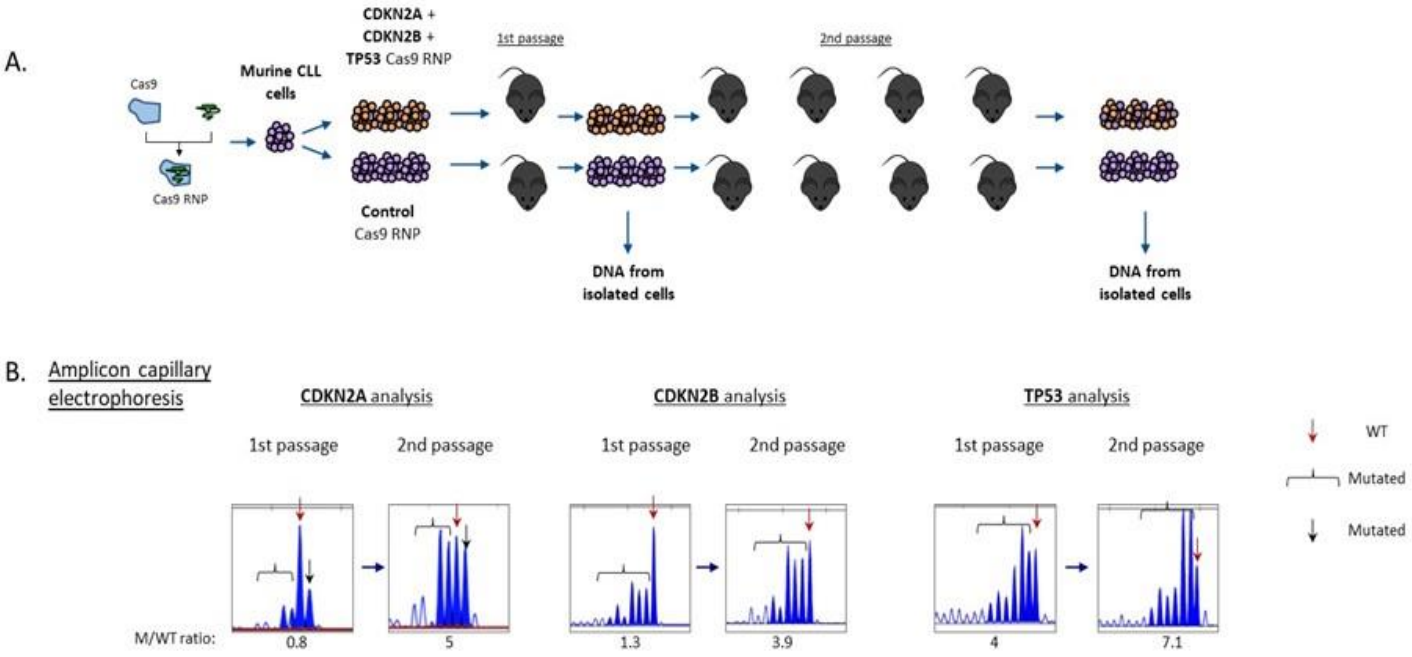

Figure 20. TP53/CDKN2A/2B-targeted leukemia cells are positively selected *in vivo*. A) Schematic representation of the CRISPR/Cas9 procedure to target the CDKN2A, CDKN2B and TP53 genes in primary murine CLL cells. B) Amplicon capillary electrophoresis of targeted cells: TP53/CDKN2A/2B-targeted leukemia cells isolated from spleens of mice after the 1st and 2nd passage. Wild type alleles are indicated by a red arrow, mutant alleles are indicated by a black arrow or brackets.

To investigate whether genetic lesions in those 3 genes affect the tumor growth *in vivo*, TP53/CDKN2A/2B-edited and control murine CLL cells were transferred in 2 different groups of syngeneic recipient mice. After 21 days, mice were sacrificed and we performed tumor burden analysis. Combined targeting of CDKN2A, CDKN2B, and TP53 resulted in accelerated leukemia growth, as evidenced by the significantly higher number of leukemic cells in the peritoneal cavity, peripheral blood, and spleen of mice that received Cas9-edited vs control TCL1-355 leukemia cells (Figure 21A). In addition, the spleens of mice with Cas9-edited cells showed morphological changes consistent with Richter transformation, including more diffuse infiltration, larger and more pleomorphic cells, a larger percentage of cells with macronucleoli and a significantly higher percentage of proliferating 5-bromo-29-deoxyuridine-positive (BrdU+) or phosphohistone H3+ cells,

further suggesting that cells with combined TP53/CDKN2A/2B deficiency have a growth advantage compared with wild-type CLL cells (Figure 21B).

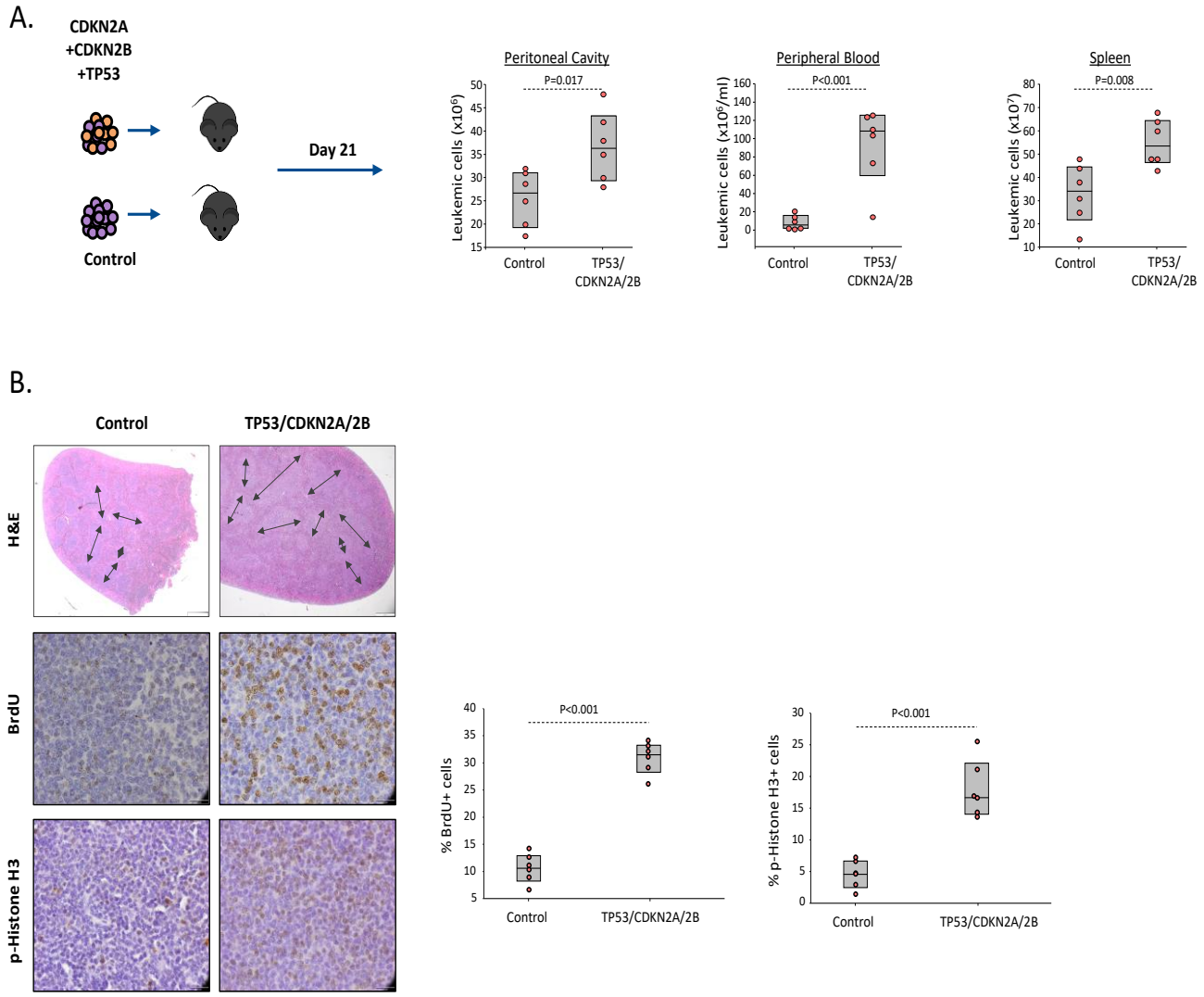

Figure 21. Combined CDKN2A, CDKN2B and TP53 disruption accelerates tumor growth in murine CLL cells. A) 3x10^7 control or CDKN2A/2B/TP53 targeted murine CLL cells were injected intraperitoneally in groups of 6 mice. Analysis of absolute numbers of CD5+/CD19+ leukemia cells in peritoneal cavity, peripheral blood and spleen of mice at 21 days after receiving TP53/CDKN2A/2B-targeted or control leukemia cells. B) Hematoxylin-and-eosin (H&E) staining (top panels) and immunohistochemistry analysis of proliferating BrdU+ or phospho-histone H3+ cells in spleens of mice 21 days after receiving TP53/CDKN2A/2B-targeted or control leukemia cells. Images were captured with an Olympus BX53 microscope using an Olympus UC90 camera and CellSens Entry software. Statistical analysis was performed using the Student t test.

4.1.3 TP53/CDKN2A/2B knockdown murine CLL cells proliferate spontaneously *in vitro*

Next, to investigate whether cells with combined TP53/CDKN2A/2B deficiency are capable of spontaneous proliferation in the absence of co-stimulatory signals, we analyzed *in vitro* the growth of control, CDKN2A/2B-, TP53- and TP53/CDKN2A/2B-targeted TCL1 #355 leukemia cells, each isolated from spleens of 3 different mice. The percentage of viable leukemic cells dropped by 70% to 95% within the first week of culture in each of the 4 genotypes, but a small percentage of leukemic cells remained viable during the subsequent 4 to 5 weeks. Starting from the 6th week of culture, the number of TP53/CDKN2A/2B-targeted cells started to increase and by this time all of the control, CDKN2A/2B- and TP53-targeted cells had died (Figure 22A). Importantly, amplicon capillary electrophoresis revealed complete disappearance of the wild-type CDKN2A, CDKN2B and TP53 alleles in these cells, suggesting that biallelic loss of all three genes is required for spontaneous growth *in vitro*. Consistent with this finding, immunoblotting analysis revealed no detectable expression of TP53, CDKN1A, CDKN2A and CDKN2B protein in the spontaneously proliferating cells (Figure 22B).

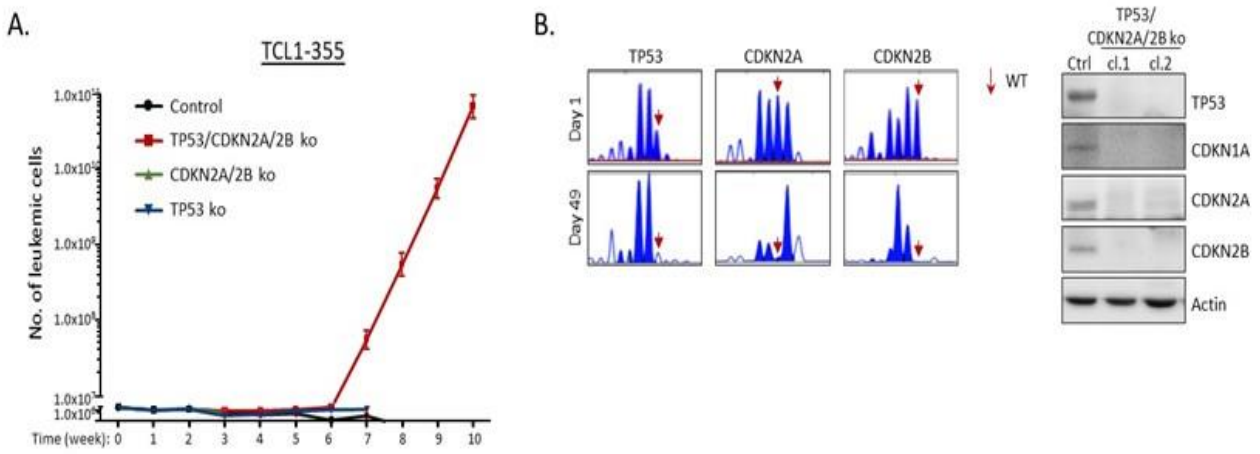

Figure 22. Murine CLL cells with biallelic loss of CDKN2A, CDKN2B and TP53 proliferate spontaneously *in vitro*. A) Absolute number of viable TP53/CDKN2A/2B-targeted, CDKN2A/2Btargeted, TP53-targeted or control TCL1-355 leukemia cells at different time points in culture. B) Indel analysis by amplicon capillary electrophoresis of TP53/CDKN2A/2B-targeted cells at day 1 and day 49 (the position of the wild type allele is indicated by a red arrow) and immunoblotting analysis of TP53, CDKN1A, CDKN2A and CDKN2B protein expression in two different clones of spontaneously proliferating murine leukemia cells with biallelic TP53/CDKN2A/2B disruption.

4.1.4 The spontaneous TP53/CDKN2A/2B knockdown murine CLL cells require signals from the BCR for their growth *in vitro* and *in vivo*

The previous experiments showed that biallelic loss of TP53/CDKN2A/2B overcomes the need for costimulatory signals in driving proliferation of murine CLL cells *in vitro*, but did not prove that this proliferation is still dependent on BCR signals. To further address this issue, we targeted the IgM constant region gene by CRISPR/Cas9 in the spontaneously proliferating murine leukemia cells with biallelic TP53/CDKN2A/2B deficiency. An editing efficiency of 60% was observed by indel analysis, consistent with the detection of a similar proportion of surface IgM negative cells by flow cytometry. The surface IgM negative cells became undetectable within 10 days of culture and were outgrown by cells with retained surface IgM expression. In parallel, a reduction in the ratio of IgM mutant vs wild-type alleles was observed. A small proportion of indels remained detectable even after prolonged culture, presumably reflecting the presence of cells with monoallelic IgM disruption and normal surface IgM expression, further suggesting that a functional BCR is required for the spontaneous proliferation of these cells. Transfer of these cells in NSG mice showed that cells with a disrupted IgM heavy chain gene are also negatively selected *in vivo* (Figure 23A). The finding that cells with combined TP53/CDKN2A/2B deficiency require BCR expression indicated that they should be sensitive to treatment with a BCR inhibitor. To further evaluate this possibility, TP53/CDKN2A/2B cells were treated *in vitro* with the BTK inhibitor ibrutinib, the phosphatidylinositol 3-kinase-d inhibitor idelalisib, or the SYK inhibitor R406 (active substance of the drug fostamatinib).

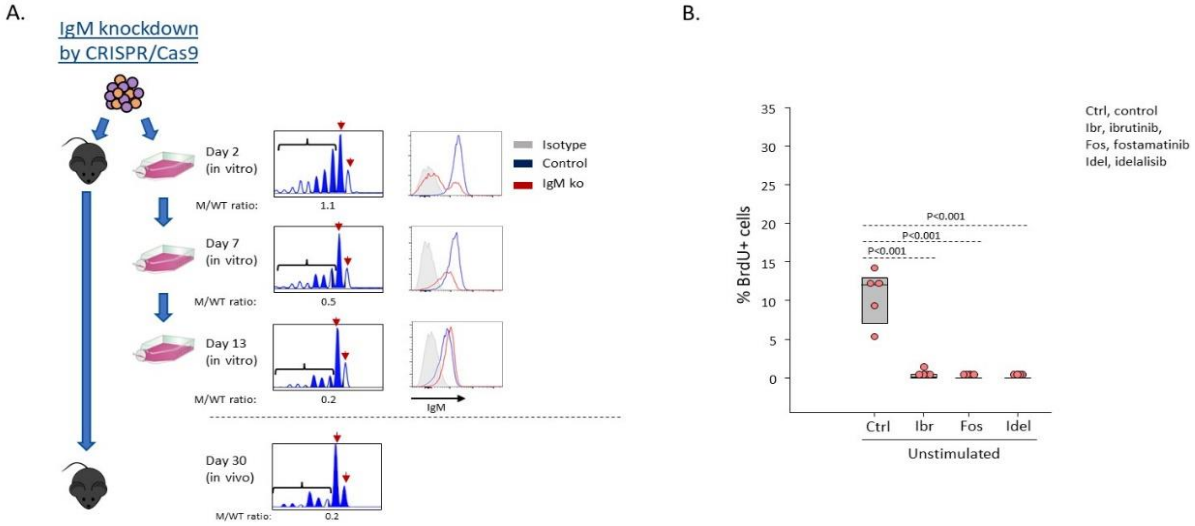

Figure 23. Murine leukemic TP53/CDKN2A/2B ko cells require BCR signals for proliferation and are still sensitive to the BCR inhibitors. A) Time course analysis of changes in IgM mutant vs wild type allele ratio *in vitro* and *in vivo* and surface IgM expression *in vitro*. B) BrdU incorporation analysis of the spontaneously proliferating cells treated with 1 μM Ibrutinib or Fostamatinib or Idelalisib for 20 hrs and incubated for 6 hrs with BrdU before harvesting for flow cytometry analysis.

BrdU incorporation experiments showed almost complete growth inhibition, further suggesting that proliferation of these cells is dependent on BCR signals (Figure 23B).

4.2 Toll-like receptors signals in CLL cell proliferation

(Martines C, Chakraborty S et al. Blood. 2022: blood.2022016272. Epub ahead of print. PMID: 36084319.)

4.2.1 Inhibition of TLR-signals delays leukemia progression in Eμ-TCL1 adoptive transfer model

The possible mechanism of TLR-pathway activation *in vivo* is through a cross-talk between TLR- and BCR-pathway. CLL-BCRs, in particular the ones belonging to the U-CLL subset, can bind and internalize immunocomplexes containing TLR9-ligands leading to activation of the TLR-pathway.

To further explore the role of TLR-signals in CLL cell growth and expansion, we tested the activity of R191, a novel IRAK1/4 inhibitor, to inhibit TLR-derived signals in Eμ-TCL1 murine CLL and human RS-patient-derived xenograft (PDX) cells. Experiments performed with primary leukemic cells isolated from four different Eμ-TCL1 mice showed that R191 completely inhibits proliferation induced by the TLR ligands CpG or LPS (Figure 24A and B).

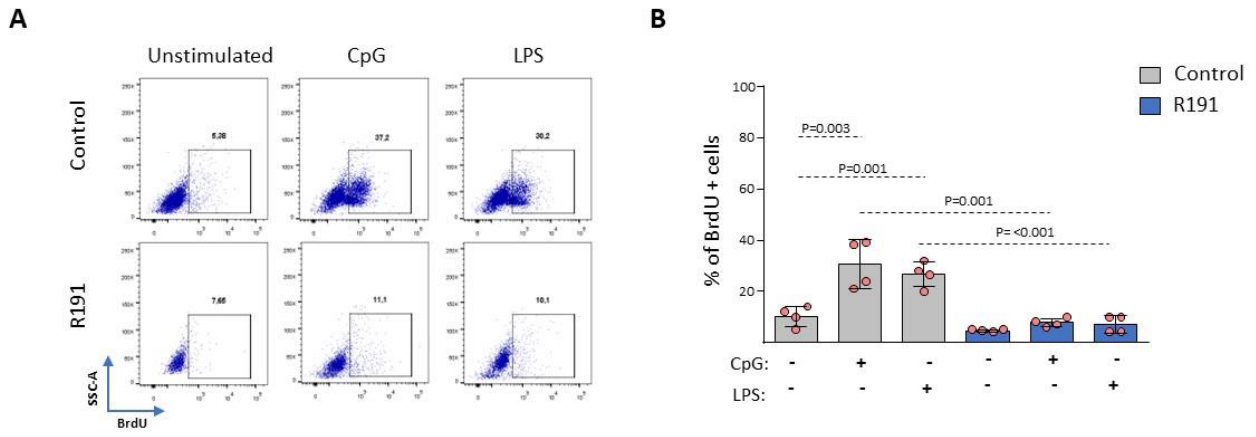

Figure 24. The IRAK1/4 inhibitor R191 blocks TLR-induced proliferation in murine Eμ-TCL1 CLL cells *in vitro*. A) and B) Effect of R191 on proliferation of TLR-stimulated Em-TCL1 CLL cells. The percentage of proliferating cells was determined by analysis of BrdU incorporation in viable Eμ-TCL1 leukemia cells that were cultured for 28 hours in the presence or absence of CpG-1668 (1 μM), LPS (5 μg/ml) and R191 (1 μM) and then for additional 20 hours in the presence of BrdU (10 μM). One representative experiment with TCL1-333 cells is shown in A and a summary of 4 experiments with CLL cells derived from 4 different Em-TCL1 transgenic mice is shown in B. Statistical analysis was done using One Way Repeated Measures ANOVA with Tukey test for multiple comparisons.

Treatment with R191 also inhibited the proliferation of human RS-PDX cells induced by stimulation with CpG while having only a modest effect on proliferation induced by CD40L/IL-4/IL-21 stimulation (Figure 25). R191 was also modestly cytotoxic against unstimulated TCL1 and RS-PDX cells, whereas it was not toxic for unstimulated human CLL cells. However, CpG-stimulated or CD40L/IL-4/IL-21-stimulated human CLL cells underwent apoptosis in the presence of R191 (Figure 26).

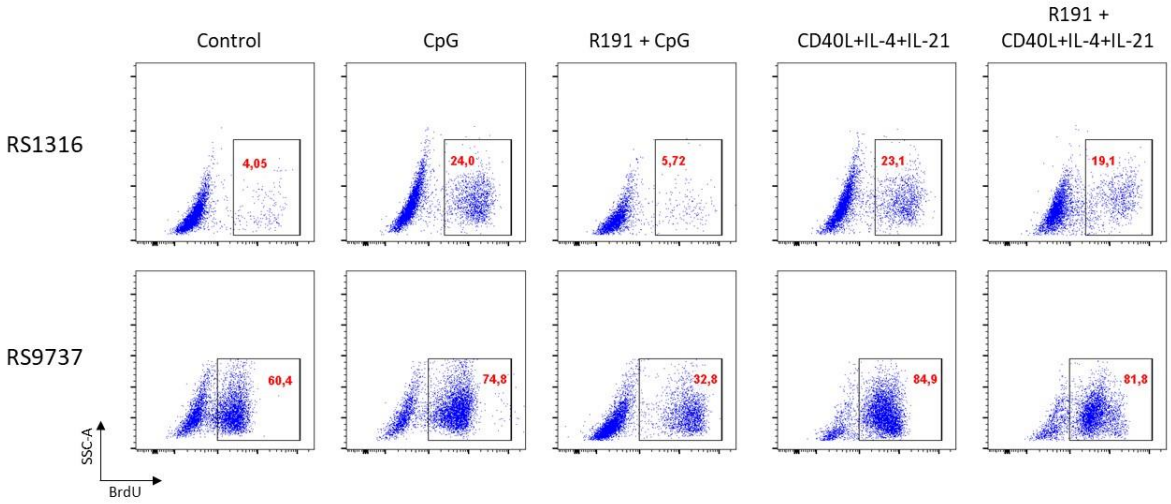

Figure 25. Effects of R191 on CpG- or CD40L/IL-4/IL-21- induced proliferation of RS-PDX cells. The percentage of proliferating cells was determined by analysis of BrdU incorporation in viable RS cells that were cultured for 28 hours in the presence or absence of CpG-2006 (1 μM) or CD40L expressing fibroblasts + IL-4 (25 ng/ml) + IL-21 (25 ng/ml) and then for additional 20 hours in the presence of BrdU (10 μM). R191 (1 μM) was added at the beginning of the culture.

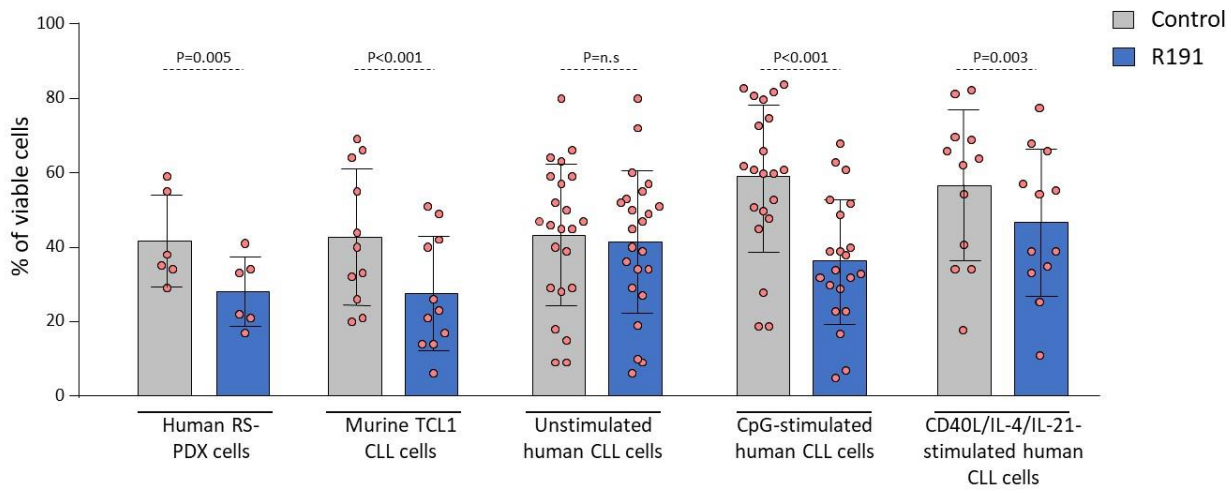

Figure 26. Effect of R191 on viability of human and murine CLL and RS cells in vitro. Cells were treated with 1μM R191 for 48 hours and cell viability was evaluated by annexin V/PI staining. The investigated samples included human CLL cells from 23 different patients, murine CLL cells from 11 different TCL1 transgenic mice and the three human RS-PDX cell lines that were investigated on two separate occasions. Statistical analysis was done using the paired t test.

Next, to investigate the effect of inhibition of TLR-signaling with this drug *in vivo*, we performed adoptive transfer experiments using two primary leukemic cells isolated from different Eμ-TCL1 mice (TCL1-355 and TCL1-333). $3x10^7$ murine CLL cells were inoculated intraperitoneally in syngeneic C57BL/6 mice and after 3 days mice were fed with the R191-prodrug R221 or with vehicle control. Analysis of leukemic cell count in peripheral blood showed no differences until day 20 of treatment, but a significant reduction was observed after 35 days in R221-treated mice (Figure 27A). Consistent with the reduced number of circulating leukemic cells, the R221-treated mice also exhibited a significantly longer survival than control mice (Figure 27B).

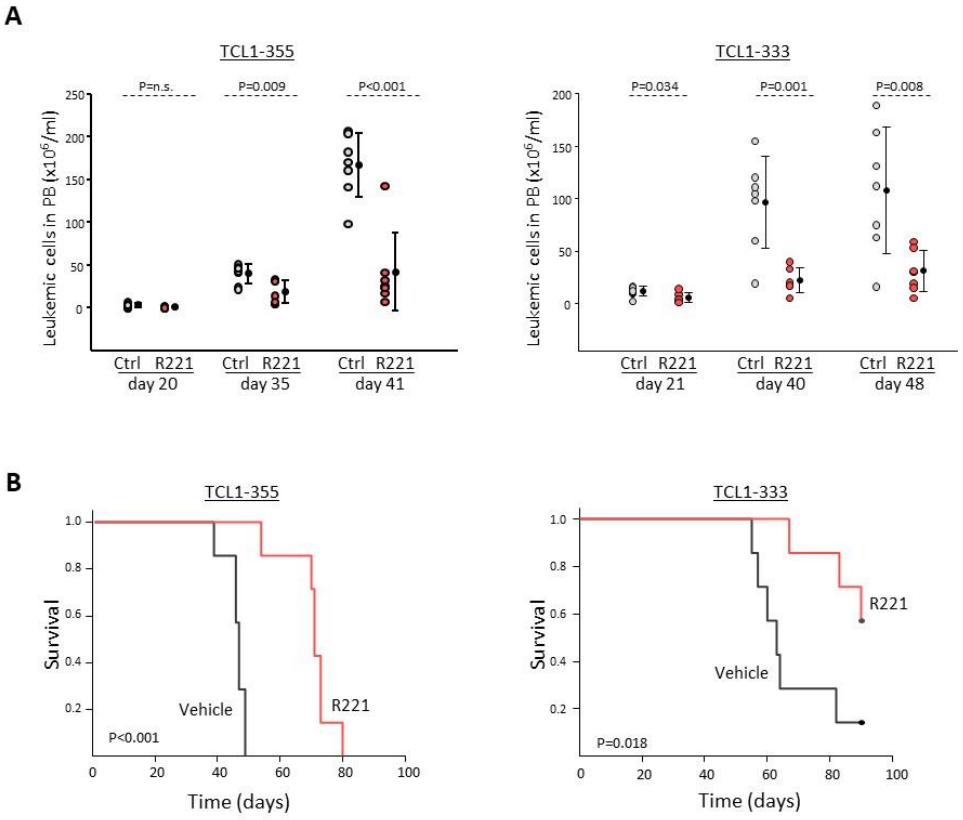

Figure 27. R221 treatment delays expansion of murine CLL cells *in vivo* and prolongs the survival of the R221-treated animals. A) Analysis of leukemia cell counts (CD5+/CD19+) in peripheral blood of mice inoculated with TCL1-355 or TCL1-333 leukemia cells and treated with R221 or vehicle control (n=7/group). Statistical analysis was done using the t test or Mann-Whitney test, as appropriate. B) Survival analysis of mice treated with R221 or vehicle control. Treatment was started 3 days after tumor transfer. X-axis indicates days from tumor transfer. Survival curves were estimated using the Kaplan–Meier method and curve differences were assessed using the log-rank test.

4.2.2 Genetic disruption of MyD88 does not affect the growth of adoptively transferred Eμ-TCL1 murine CLL cells

In addition to inhibiting its primary targets IRAK1 and IRAK4 (IC50 of 3 nmol/L), R191 has been reported to inhibit the kinase activity of 13 other kinases by >80% at concentrations ranging from 50 nmol/L to 250 nmol/L (*Ni H et al. 2018*). Therefore, to determine whether the effect of R221 treatment was caused because of inhibition of TLR-signal in the malignant cells themselves, we targeted the MyD88 gene in the Eμ-TCL1 leukemias TCL1-355 and TCL1-333 by CRISPR/Cas9 editing (Figure 28).

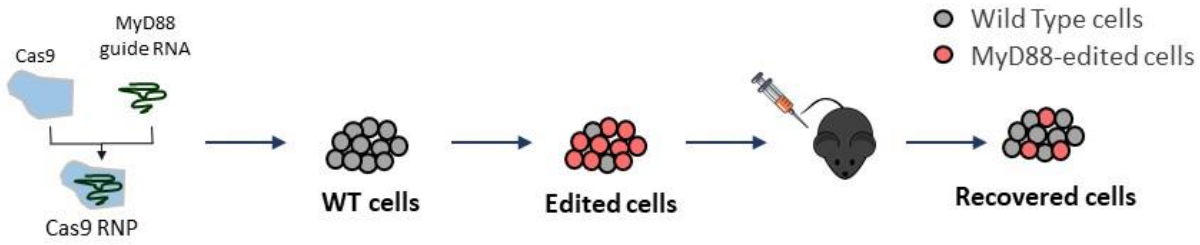

Figure 28. Schematic representation of the procedure to investigate the impact of CRISPR/Cas9-mediated disruption of the MyD88 gene on the growth of adoptively transferred Eμ-TCL1 CLL cells. The scheme illustrates expected outcome in case TLR signals are required for leukemia growth in vivo.

Targeting of the MyD88 gene was done by nucleofection-mediated delivery of a ribonucleoprotein complex containing recombinant Cas9 and a guide RNA against MyD88, resulting in an editing efficiency of 50% to >90% in different experiments and almost complete loss of MyD88 protein expression (Figure 29A and B).

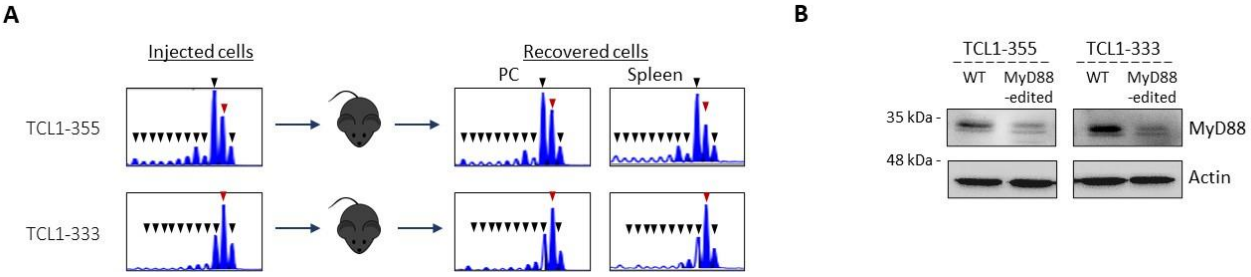

Figure 29. Analysis of the editing efficiency of targeting of MyD88 gene in TCL1-355 and -333 leukemia cells. A) Indel analysis by amplicon capillary electrophoresis of the targeted region of MyD88 in TCL1-355 and TCL1-333 injected and recovered leukemia cells isolated from peritoneal cavity (PC) and spleen. The wild type allele is indicated by a red arrow, mutant alleles are indicated by black arrows. B) Immunoblotting analysis of wild type (WT) and MyD88-edited TCL1-355 and TCL1-333 leukemia cells.

To test whether the MyD88 knockout cells were resistant to TLR stimulation, we stimulated TCL1-699 MyD88 wild-type and knockout cells with the TLR9-ligand CpG and investigated the effect on proliferation. We observed that the leukemic cells with disrupted MyD88 were not responsive to TLR stimulation, as evidenced by the lack of an increase in BrdU incorporation or phosphorylation of the NF-kB subunit p65 following stimulation with CpG (Figure 30A and B).

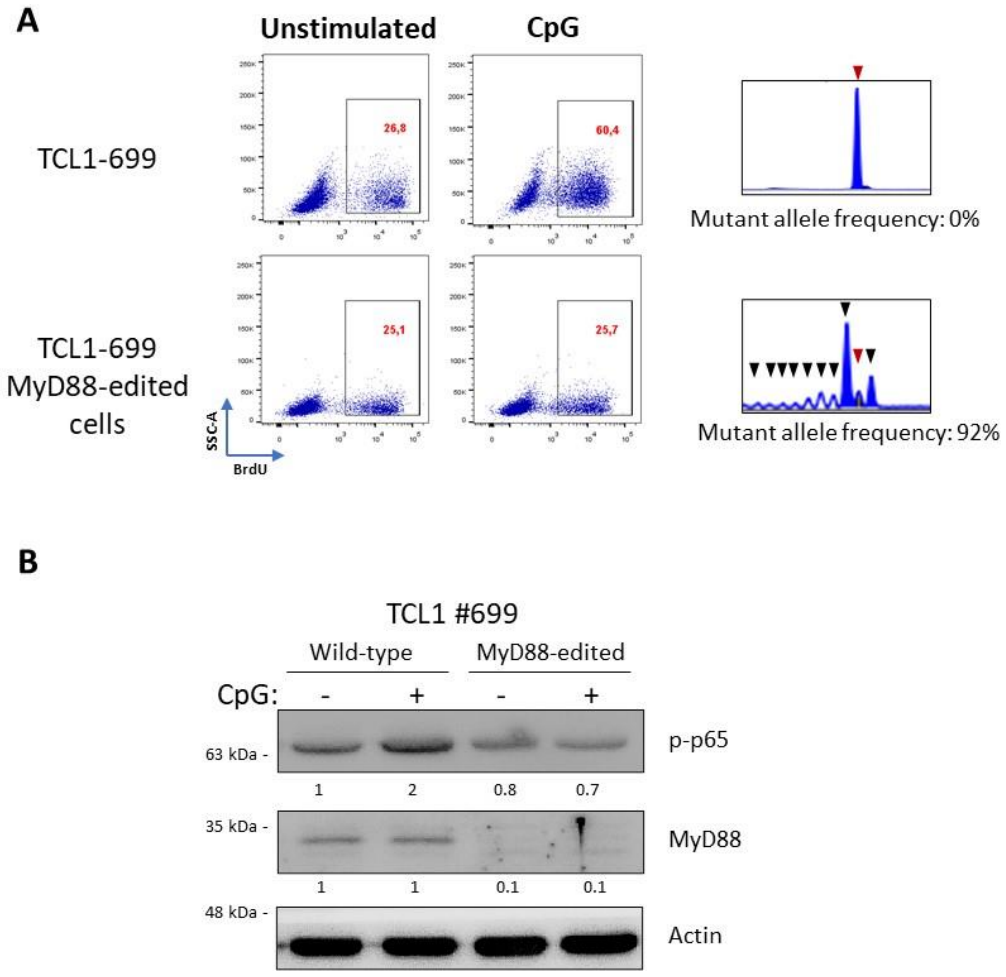

Figure 30. TLR9 stimulation increases proliferation and induces p65 phosphorylation in wild-type but not in MyD88-knockout TCL1 leukemia cells. A) Analysis of BrdU incorporation of MyD88-wild-type and MyD88-edited TCL1-699 leukemia cells after 48 hours in culture with or without CpG-1668. The percentage of BrdU+ cells is indicated in each flow chart. The right panel shows the amplicon capillary electrophoresis analysis of the MyD88-wt and MyD88-edited cells (wt allele is indicated with a red arrow, mutant alleles with black arrows). B) Immunoblotting analysis of p65 phosphorylation in wild type and MyD88-edited TCL1-699 cells stimulated for 2 hrs with 1 μM CpG 1668.

To investigate the impact of MyD88 genetic disruption *in vivo*, the Eμ-TCL1 MyD88-edited cells were injected in the peritoneal cavity of recipient mice and recovered 5 weeks later for analysis of the proportion of mutant and wild type alleles. Surprisingly, no negative selection of MyD88-mutant alleles was observed, suggesting that cells with a disrupted TLR signaling pathway do not have a growth disadvantage *in vivo*. To expand these findings and exclude possible off-target effects, a separate set of experiments using another MyD88 guide RNA and leukemia cells derived from 6 other Eμ-TCL1 transgenic mice was performed (Figure 31A). In addition, to investigate whether there is a difference in the behaviour of cells from the CLL and RS phase of the disease, we included two recently established Eμ-TCL1-derived lines that model RS (TCL1-355 TKO and TCL1-699 TKO) (*Chakraborty S et al. 2021*). The results of 17 independent experiments with the 8 Eμ-TCL1-derived CLL and 2 Eμ-TCL1-derived RS lines are summarized in Figure 31B. Comparison of the mutant allele frequency of the injected and recovered cells again showed no negative selection of cells with MyD88-mutant alleles in any of the three investigated compartments (peritoneal cavity, spleen and peripheral blood).

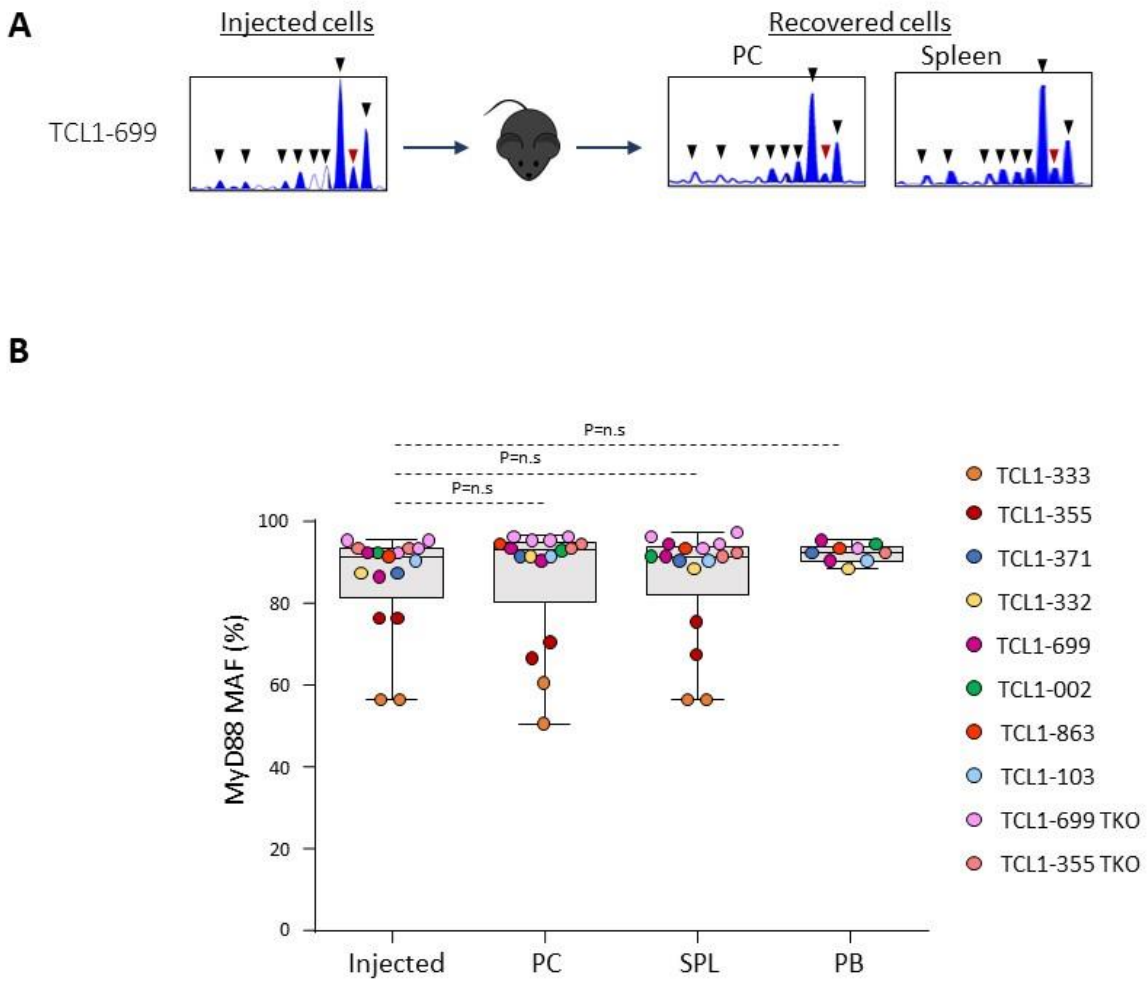

Figure 31. MyD88 edited murine leukemia cells are not negatively selected *in vivo*. A) Amplicon capillary electrophoresis of the targeted region of MyD88 in TCL1-699 injected and recovered leukemia cells isolated from peritoneal cavity (PC) and spleen. Experiment was performed with the 2nd MyD88 guide RNA. B) MyD88 mutant allele frequency (MAF) in injected leukemia cells and cells isolated from the PC, spleen (SPL) and peripheral blood of mice 21-35 days after adoptive transfer. Seventeen independent experiments were performed with the 8 TCL1-derived CLL and the 2 TCL1-derived RS lines. MAF was calculated by dividing the area of the mutated alleles with the total area of all amplified alleles (mutant +WT) detected in the amplicon capillary electrophoresis. Statistical analysis was done using One Way Repeated Measures ANOVA.

4.2.3 Different effects of pharmacological inhibition and genetic disruption of IRAK4 on the growth of xenografted human Richter Syndrome cells

The results of the above described experiments confirmed previously reported findings that treatment with an IRAK1/4 inhibitor delays leukemia progression in the Eμ-TCL1 model (*Gimenez N at al. 2020*), but also suggested that this effect is not caused by disruption of TLR signalling in the malignant cells themselves, because leukemia cells with disrupted TLR-pathway showed no growth disadvantage. To validate these findings in a human setting, we repeated these experiments using 4 recently established RS-PDX models (*Vaisitti T et al. 2018; Vaisitti T et al. 2021*). These RS-PDX models cannot be propagated *in vitro* because of spontaneous apoptosis but grow efficiently in immunodeficient NSG mice, suggesting that they receive and are responsive to microenvironmental growth and/or survival signals *in vivo*.

To test whether the 4 RS cell lines still respond to TLR-stimulation, RS cells were stimulated with CpG-2006 and the effects on proliferation were evaluated by BrdU incorporation analysis, which showed a significant increase in the percentage of proliferating tumor cells in presence of CpG (Figure 32A and B).

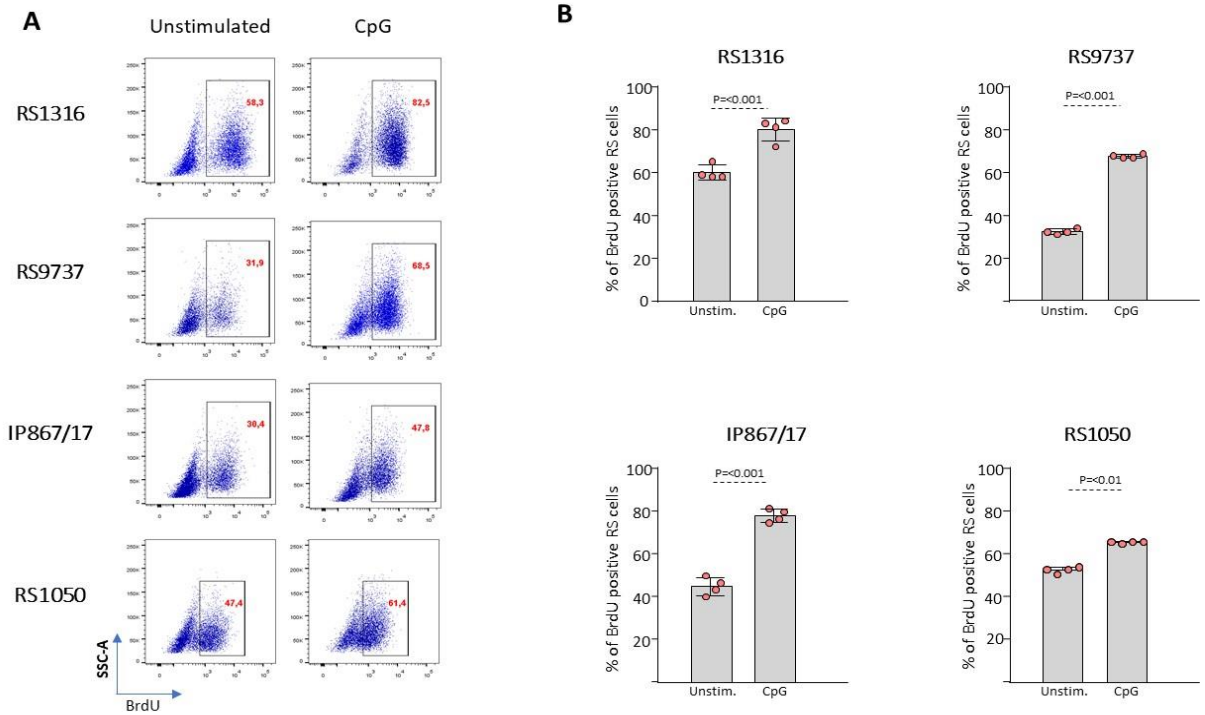

Figure 32. TLR9 stimulation increases the proliferation of Richter Syndrome patient-derived xenograft lines RS9737, RS1316, IP867/17 and RS1050 *in vitro*. Analysis of BrdU incorporation after 48 hours in culture with or without CpG-2006. Flow charts show one representative experiment for each RS tumor. The percentage of BrdU+ cells is indicated in each flow chart. B) Graphs show summary of results from 4 independent experiments performed with each RS line. Significance of differences were evaluated by t test.

To investigate whether TLR signals are required for the growth of these cells *in vivo*, we first tested the activity of R221 against the xenografted RS-PDX models RS9737 and RS1316. Since the malignant cells at different anatomical sites may receive different microenvironmental signals, these cells were xenografted both intraperitoneally and subcutaneously in each mouse. After 27 days of treatment, the total number of malignant B cells was evaluated in the subcutaneous tumor, peritoneal cavity and spleen of vehicle and R221-treated mice. Interestingly, in both experiments a significant reduction in the number of malignant B cells was observed in the subcutaneous tumor and spleen but not in the peritoneal cavity of R221-treated mice, suggesting that IRAK1/4 inhibitor treatment differently affects the growth of the malignant cells in different anatomical compartments (Figure 33).

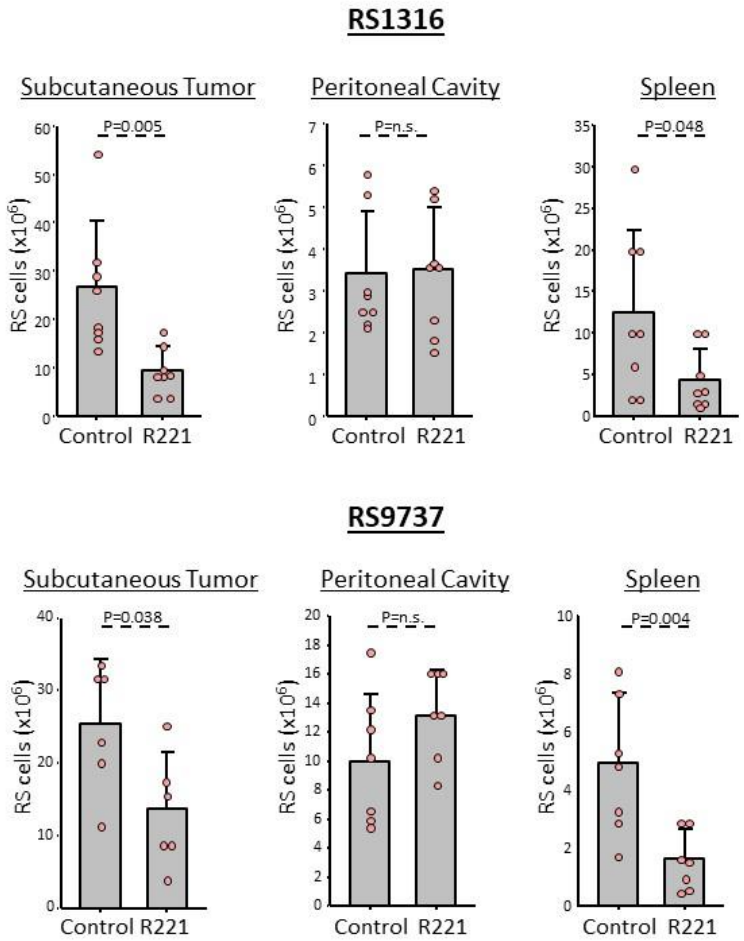

Figure 33. R221 treatment reduces the growth of RS cells *in vivo*. Treatment with R221 results in reduced growth of RS1316 and RS9737 cells in subcutaneous tumor and spleen but not in PC of xenografted NSG mice. Graphs show absolute number of tumor cells at each site. Statistical analysis was done using the t test or Mann-Whitney test, as appropriate.

To determine whether these effects are caused by disruption of IRAK1/4 signaling in the malignant B cells, we targeted exon 4 of the human IRAK4 gene by CRISPR/Cas 9. Targeting of the IRAK4 gene was done by nucleofection-mediated delivery of a RNP-complex containing recombinant Cas9 and a guide RNA against IRAK4, resulting in an editing efficiency of 50% to 80% in different experiments and in a reduction of the expression of the IRAK4 protein (Figure 34A and B). IRAK4-edited cells were xenografted intraperitoneally and in the subcutaneous tissue of immunodeficient NSG mice.

Consistent with the previous experiments using murine Eμ-TCL1 leukemia cells, no negative selection of IRAK4-mutant alleles was observed in any of the three investigated compartments. Figure 34C summarizes the results of 11 independent experiments with the four RS-PDX models showing no reduction in mutant allele frequency (MAF) of injected cells versus those isolated from the PC, spleen or subcutaneous tumor 4-5 weeks later.

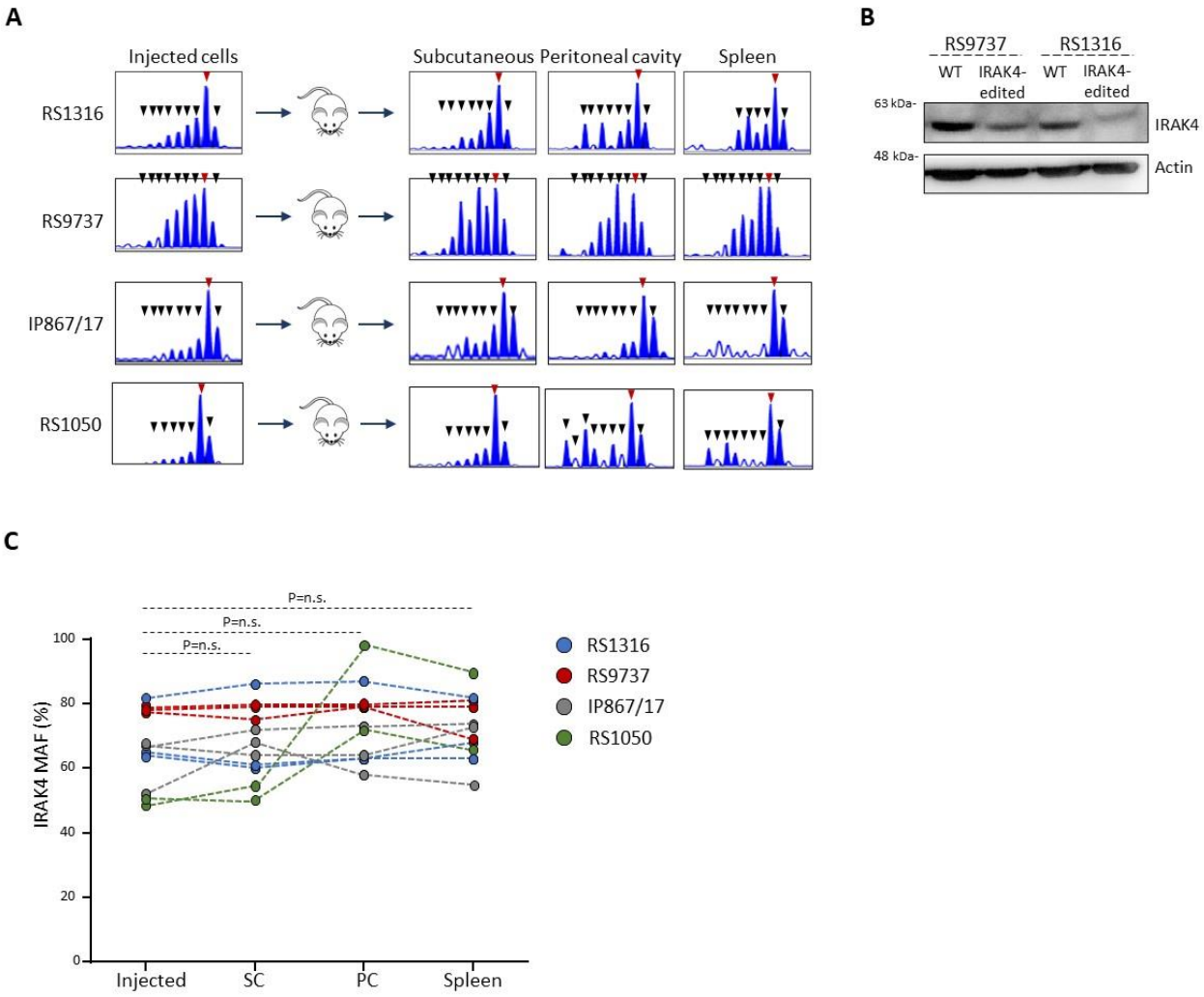

Figure 34. IRAK4-edited RS cells are not negatively selected *in vivo*. A) Indel analysis by amplicon capillary electrophoresis of the targeted region of IRAK4 in injected and recovered leukemia cells isolated from subcutaneous tumor, PC and spleen. The wild type allele is indicated by a red arrow, mutant alleles are indicated by black arrows. B) Immunoblotting analysis of IRAK4 expression in wild type (WT) and IRAK4-edited RS9737 and RS1316 cells. C) IRAK4 MAF in injected leukemia cells and cells isolated from subcutaneous tumors, PCs and spleens of NSG mice. The tumor cells were recovered between 27 and 34 days after transplantation. Eleven independent experiments were performed, 3 each with RS1316, RS9737 and IP867/17 and 2 with RS1050 cells. Statistical analysis was done using One Way Repeated Measures ANOVA.

4.2.4 BCR signals drive the growth of RS-PDX cells *in vivo*

To further validate our experimental approach, we targeted the exon 4 of the human IgM constant region gene (IGHM) in RS9737, RS1316, IP867/17 and RS1050 cells and investigated changes in MAF following *in vivo* propagation. In contrast to the IRAK4-knockout experiment, we observed a significant reduction in the proportion of mutant IgM alleles in all three investigated compartments, which was accompanied with selective loss of leukemic cells lacking surface IgM expression (Figure 35A, B and C).

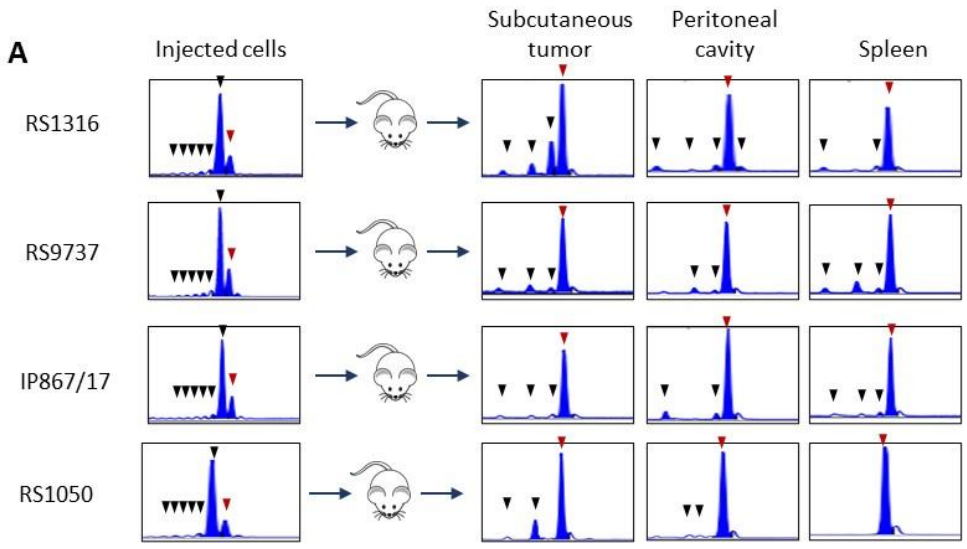

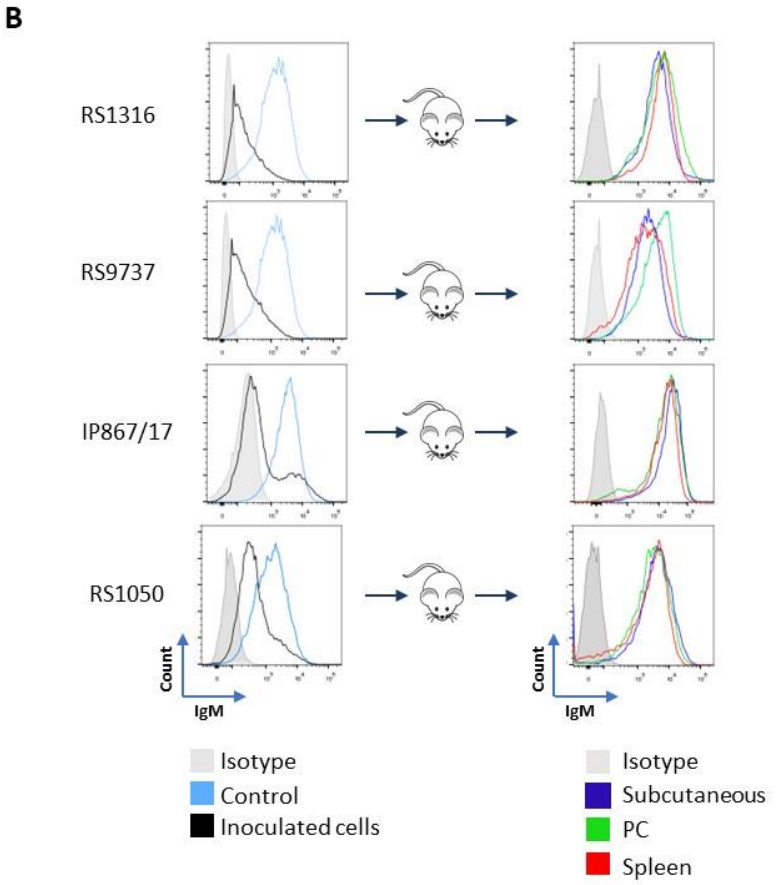

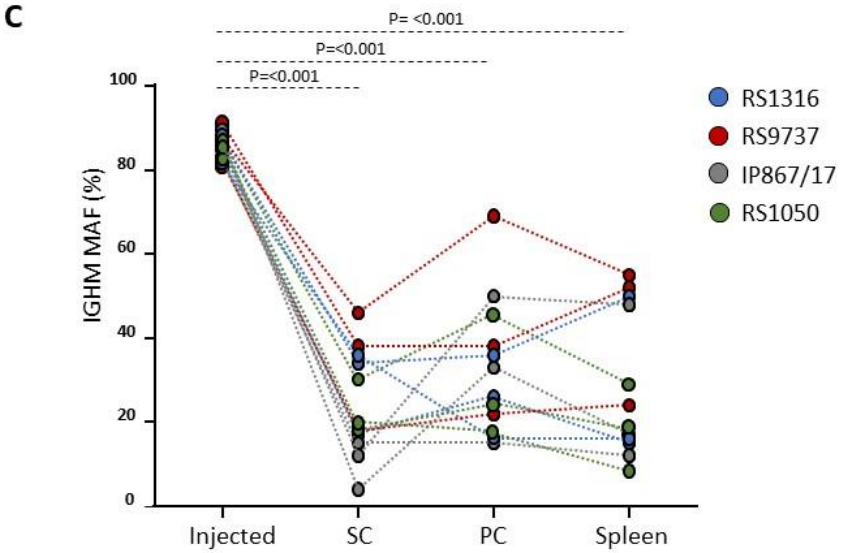

Figure 35. RS-PDX cells with CRISPR/Cas9-disrupted IgM heavy chain (IGHM) gene are negatively selected *in vivo.* A) Indel analysis of the targeted region of the IGHM gene in injected and recovered leukemia cells isolated from subcutaneous tumor, PC and spleen of xenografted NSG mice. The wild type allele is indicated by a red arrow, mutant alleles are indicated by black arrows. B) Flow cytometry analysis of surface IgM expression in IGHM-edited tumor cells before injection and after recovery from subcutaneous tumor, PC and spleen of xenografted NSG mice. C) IGHM MAF in injected leukemia cells and cells isolated from subcutaneous tumors, PCs and spleens of NSG mice. The tumor cells were recovered 30-31 days after transplantation. Twelve independent experiments were performed, 3 each with RS1316, RS9737, IP867/17 and RS1050 cells. Statistical analysis was done with One Way Repeated Measures ANOVA with Tukey test for multiple comparisons.

To further validate this result, a separate set of experiments using another IgM guide RNA, which targeted the exon 2 of the IGHM gene in RS9737, RS1316, IP867/17 cells, yielded identical results, providing further evidence that RS cells depend on BCR signals for their growth and/or survival (Figure 36A and B).

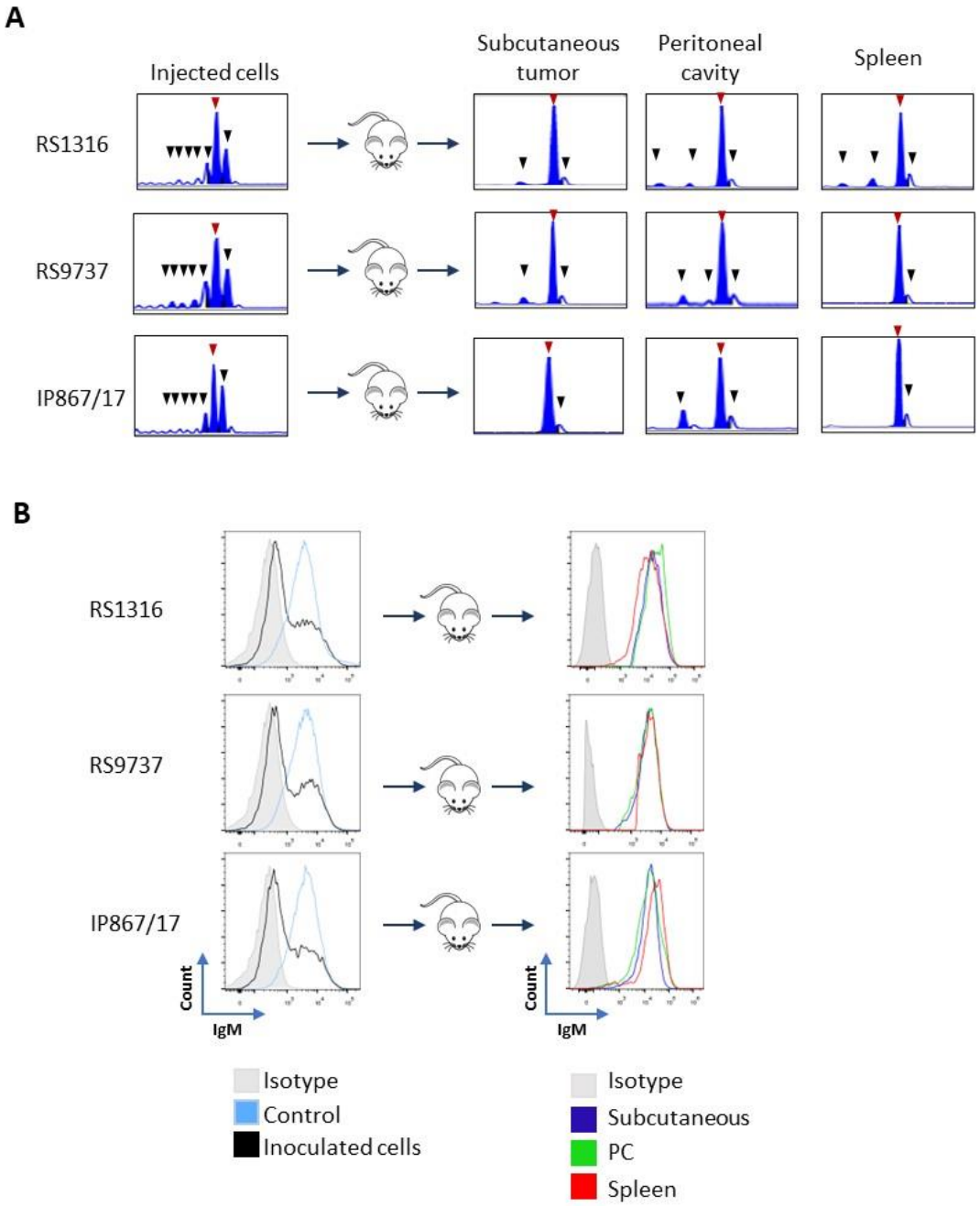

Figure 36. CRISPR/Cas9-editing of RS-PDX cells with a second IgM heavy chain (IGHM) gene crRNA results in negative selection of cells with a disrupted BCR in vivo. A) Indel analysis of the targeted region of the IGHM gene in injected and recovered leukemia cells isolated from subcutaneous tumor, PC and spleen of xenografted NSG mice 35-38 days after transplantation. The wild type allele is indicated by a red arrow, mutant alleles are indicated by black arrows. B) Flow cytometry analysis of surface IgM expression in IGHM-edited tumor cells before injection and after recovery from subcutaneous tumor, PC and spleen of xenografted NSG mice.

4.2.5 BCR and TLR signals do not affect the growth of the human CLL cells in vivo

To determine whether the findings from the human RS models are applicable to human CLL cells, we investigated the impact of IRAK4 and IgM knockout in the human CLL cell lines MEC1, C1 and HG3 (Figure 37). We targeted the IRAK4 and IgM genes in these human CLL cell lines and IRAK4- or IgM-edited cells were xenografted in immunodeficient NSG mice. To investigate the effects of genetic inactivation of IRAK4- or IgM- in leukemia cells located in different anatomical compartments, tumor cells were injected intraperitoneally, intravenously and in the subcutaneous tissue. The xenografted cells were recovered from the peritoneal cavity, spleen and subcutaneous tissue between 27 to 37 days after xenografting and the proportion of cells with mutant and wild type IRAK4 or IgM alleles was evaluated by amplicon capillary electrophoresis. Analysis of the mutant allele frequency showed no negative selection of IRAK4-knockout cells following propagation *in vivo*, but also did not show negative selection of IGHM-knockout cells. The lack of negative selection of IgM-knockout cells in this experiment can be explained by the fact that all of these cells lines are infected by the Epstein Barr Virus and express the LMP2A protein, which is a BCR mimic that can substitute for the BCR (*Mancao C et al. 2007*).

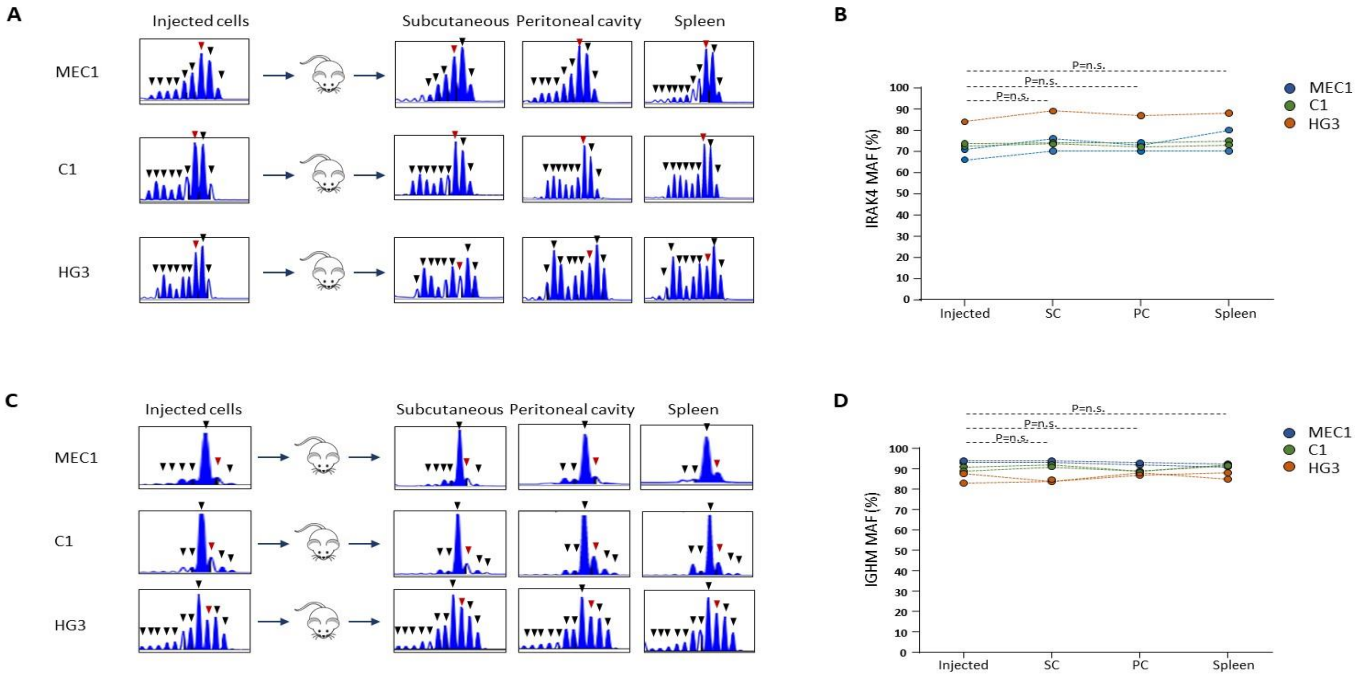

Figure 37. Analysis of changes in IGHM or IRAK4 MAF following in vivo propagation of human CLL cell lines MEC1, C1 and HG3. A) Indel analysis of the targeted region of the IRAK4 gene or C) IGHM gene in injected and recovered leukemia cells isolated from subcutaneous tumor, PC and spleen of xenografted NSG mice. The wild type allele is indicated by a red arrow, mutant alleles are indicated by black arrows. B) and D) IRAK4 and IGHM MAF in injected leukemia cells and cells isolated from subcutaneous tumors, PCs and spleens of NSG mice. The tumor cells were recovered 24-37 days after transplantation. Each circle represents an independent experiment. Statistical analysis was done with One Way Repeated Measures ANOVA with Tukey test for multiple comparisons.

4.2.6 IRAK4 inhibitor treatment depletes macrophages in NSG and wild type mice

The previous experiments showed that treatment with R221 reduces the growth of the murine and human malignant B cells *in vivo*, but also that this effect is not caused by disruption of TLR signaling in the malignant B cells themselves. Considering that the reduction in tumor growth occurred only after prolonged R221 treatment, we investigated whether it could be related to an effect on some other cellular subset present in the tumor microenvironment. We focused in particular on monocytes and macrophages, which rely for their activity on TLR-mediated signals and have been shown to support CLL cell survival *in vitro* and *in vivo* (*Reinart N et al. 201; Hanna BS et al. 2016; Galletti G et al 2016*). In NSG mice xenografted with RS9737 that had been treated for 18 days with R221, we observed a significant reduction in the absolute number of granulocytes ($CD11b^{+}F4/80^{-}$), monocytes ($CD11b^{+}F4/80^{int}$) and almost complete disappearance of macrophages ($CD11b^{low}F4/80^{hi}$) (Figure 38).

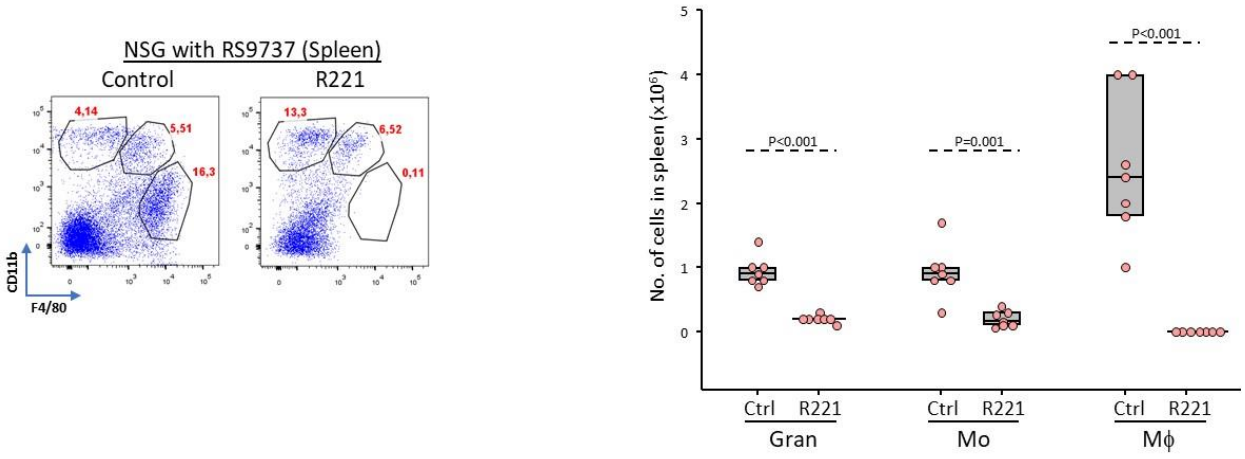

Figure 38. **R221 treatment affects myeloid cells in the spleen of NSG mice.** Representative flow cytometry analysis showing the percentage of granulocytes ($CD11b^{+}F4/80^{-}$), monocytes ($CD11b^{+}F4/80^{int}$) and monocyte-derived macrophages ($CD11b^{low}F4/80^{hi}$) gated on viable $CD45^{+}$ cells isolated from the spleen of R221- or vehicle control-treated NSG mice (n=7/group) xenografted with RS9737 cells. Cell populations were defined as described by Hanna et al. (2016). The box plot shows the absolute number of granulocytes (Gran), monocytes (Mo) and macrophages (Mϕ) in the spleen of vehicle control- and R221-treated NSG mice. Statistical analysis was done using the t test or Mann-Whitney test, as appropriate.

A separate experiment with wild type C57BL/6 mice that had not been inoculated with leukemia cells also showed depletion of macrophages and a significant reduction in the number of granulocytes in the spleen of R221-treated mice (Figure 39).

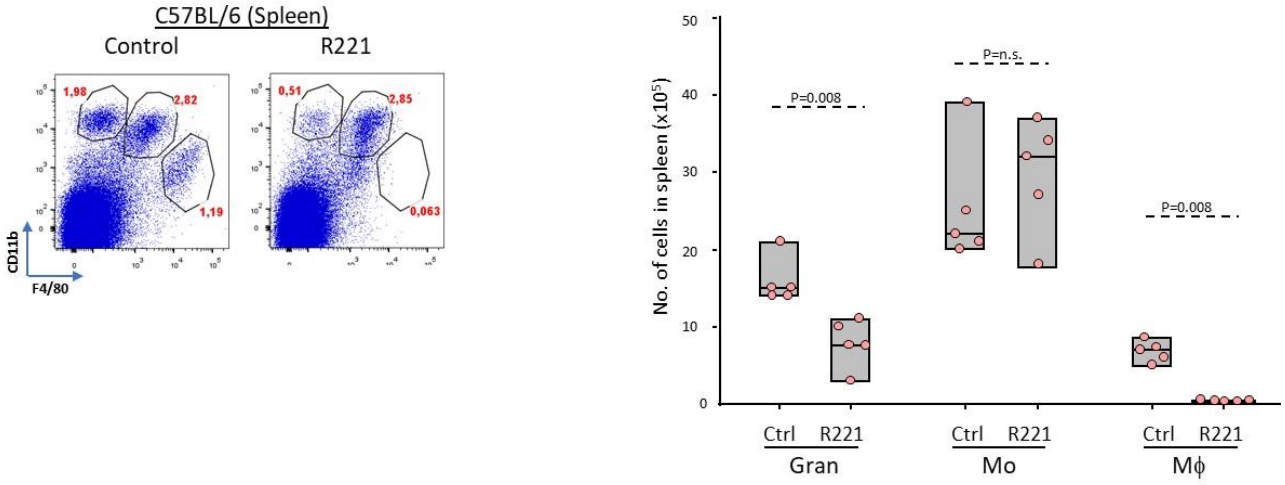

Figure 39. R221 treatment affects myeloid cells in the spleen of C57BL/6 mice. Flow cytometry dot plots and box plot showing the percentage (left panels) and the absolute number (right panel) of Gran, Mo and Mϕ in the spleen of R221- or vehicle control-treated C57/BL6 mice. Statistical analysis was done using the t test or Mann-Whitney test, as appropriate.

In contrast, R221 treatment did not affect the number or percentage of macrophages in the peritoneal cavity, where no effect on the growth of the malignant B cells had been observed (Figure 40).

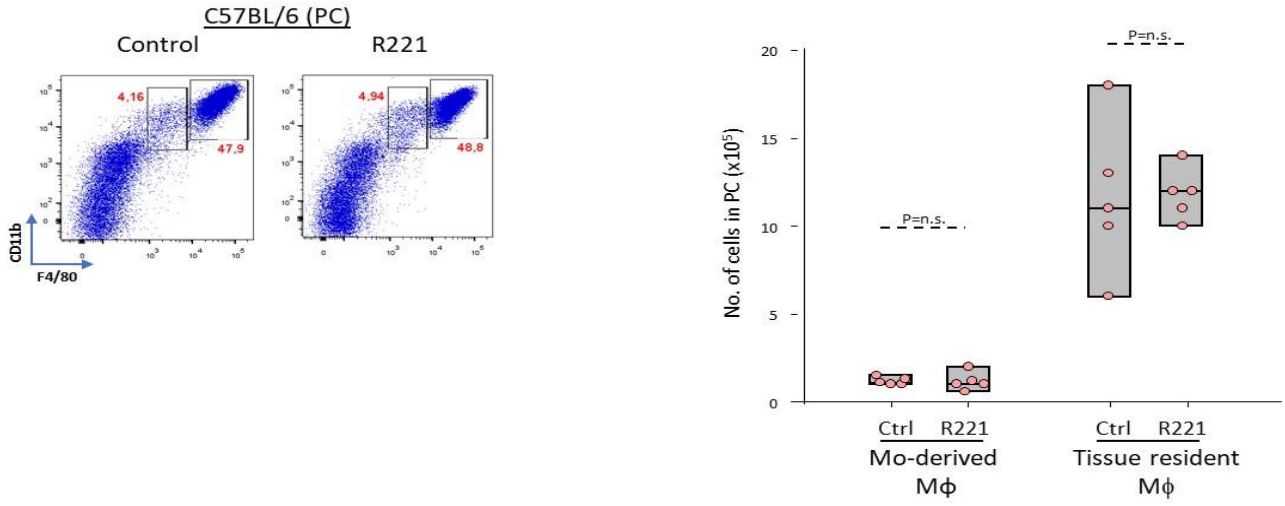

Figure 40. R221 treatment does not affect macrophages in the peritoneal cavity. Flow cytometry dot plots and box plot showing the percentage (left panels) and the absolute number (right panel) of monocyte-derived Mϕ ($CD11b^{+}F4/80^{int}$) and tissue-resident Mϕ ($CD11b^{+}F4/80^{hi}$) in the PC of R221 and vehicle control C57/BL6 mice. Statistical analysis was done using the t test or Mann-Whitney test, as appropriate.

To investigate the reason for this different sensitivity to R221 of splenic and peritoneal cavity macrophages, we treated *in vitro* for 24 hours both peritoneal cavity and bone marrow-derived macrophages with 1 μM R191. We observed that R191 treatment selectively kills both types of macrophages, whereas B (CD19+) or T (CD5+) cells were not affected by R191 treatment. These findings suggest that the lack of an effect *in vivo* against peritoneal cavity macrophages is most likely insufficient bioavailability of R221 in this compartment (Figure 41A and B).

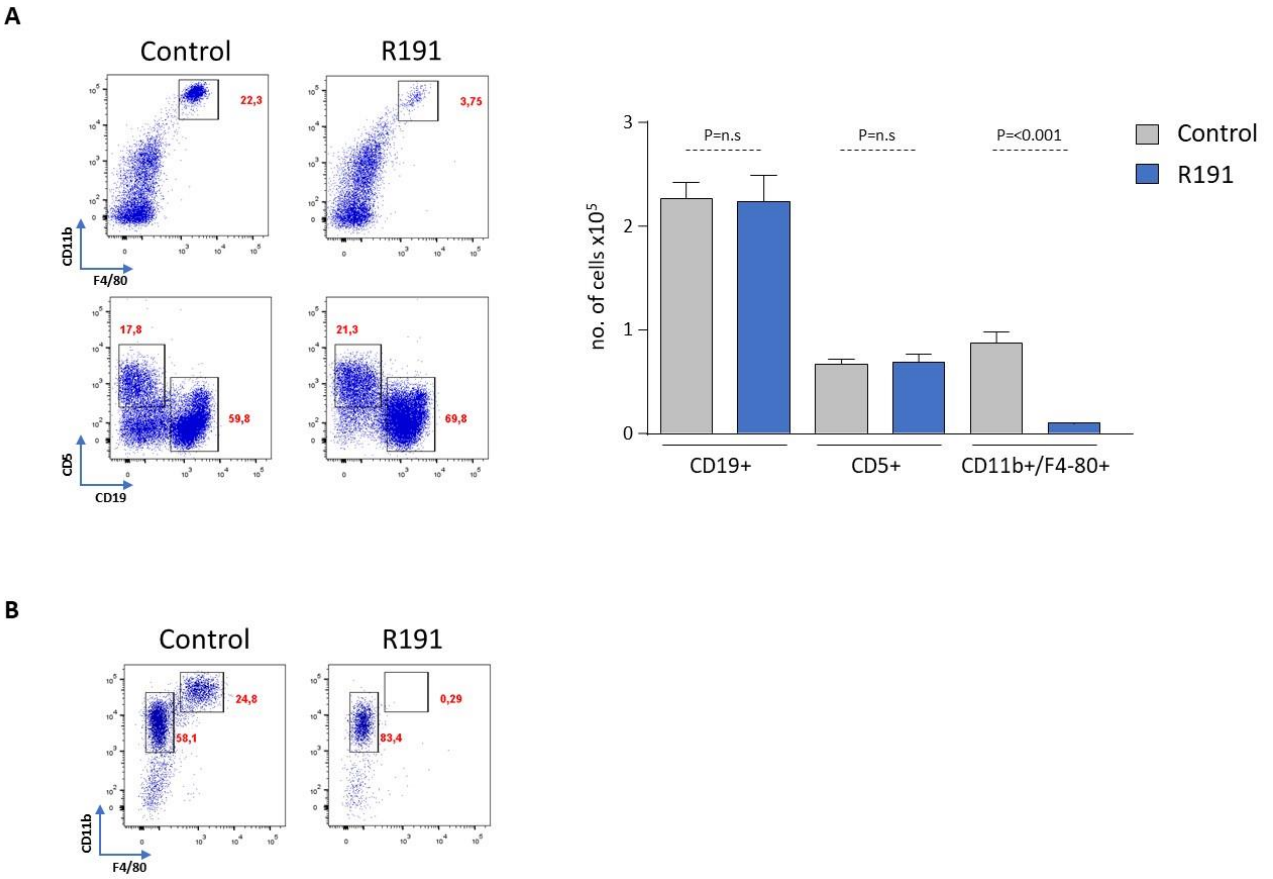

Figure 41. Peritoneal cavity and bone-marrow derived macrophages are sensitive to R191 treatment *in vitro*. A) Representative flow charts showing CD11b+/F4-80+ (upper panel) and CD5+/CD19+ (lower panel) cells isolated from the PC of a wild-type mouse. Cells were treated with 1 μM R191 for 24h prior to flow cytometry analysis, which was done on viable cells (PI negative). Summary of three independent experiments is shown on the right in the bar plot. B) BM-derived cells from one NSG mouse were differentiated for 4 days in presence of 10 ng/ml macrophage colony–stimulating factor (M-CSF) and then treated with 1 μM R191 for 24 h prior to flow cytometry analysis. Analysis was done on viable cells (PI negative). Flow charts show one representative of 3 independent experiments. Statistical analysis was done using the t test or Mann-Whitney test, as appropriate.

4.2.7 Macrophages sustain the survival of murine TCL1 and human RS leukemia cells

In the previous experiments we found that IRAK4/1 inhibitor treatment delays tumor growth because it selectively kills macrophages. To investigate the capacity of murine macrophages to support the survival of human RS cells, we co-cultured RS1316 and RS9737 cells with peritoneal cavity or bone marrow-derived macrophages from NSG mice. In both sets of experiments, co-culture with macrophages significantly protected the malignant B cells from spontaneous apoptosis (Figure 42A and B).

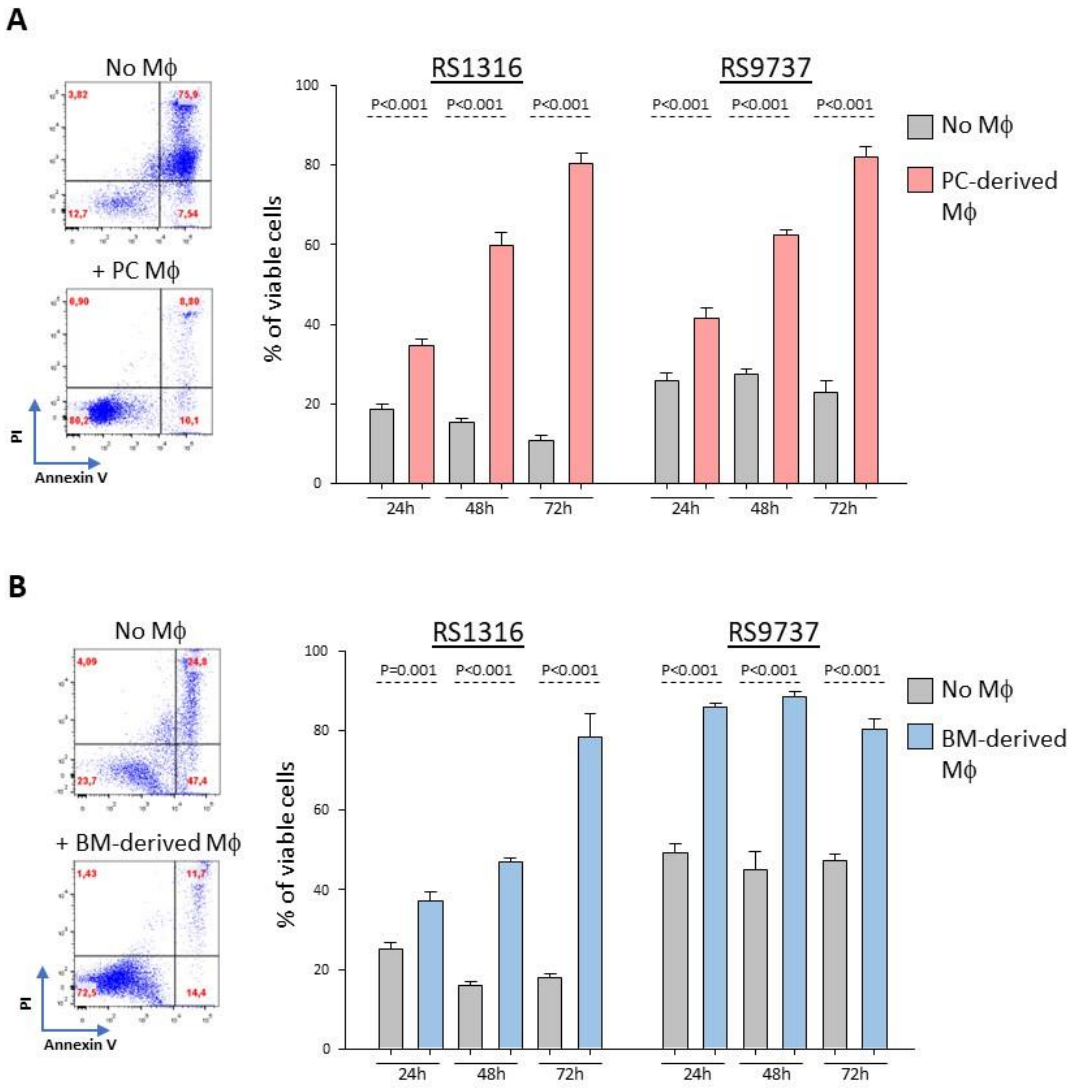

Figure 42. Macrophages prolong the survival of PDX-RS cells in vitro. A) Representative annexin V/PI analysis of RS1316 cells cultured for 72 hours in the presence or absence of PC-isolated Mϕ (left panels). Summary of three independent experiments using RS1316 and RS9737 cells is shown in right panel. B) Representative annexin V/PI analysis of RS1316 cells cultured for 72 hours in the presence or absence of bone marrow (BM)-derived Mϕ generated by differentiating bone marrow mononuclear cells for 4 days in culture with M-CSF (left panels). Summary of three independent experiments using RS1316 and RS9737 cells is shown in right panel.

The effects on the survival of the tumor cells were abrogated when macrophages were pre-treated for 24 hours with R191 prior co-culture with RS cells, suggesting that the drug impacts on the capacity of the macrophages to support the survival of the malignant cells (Figure 43).

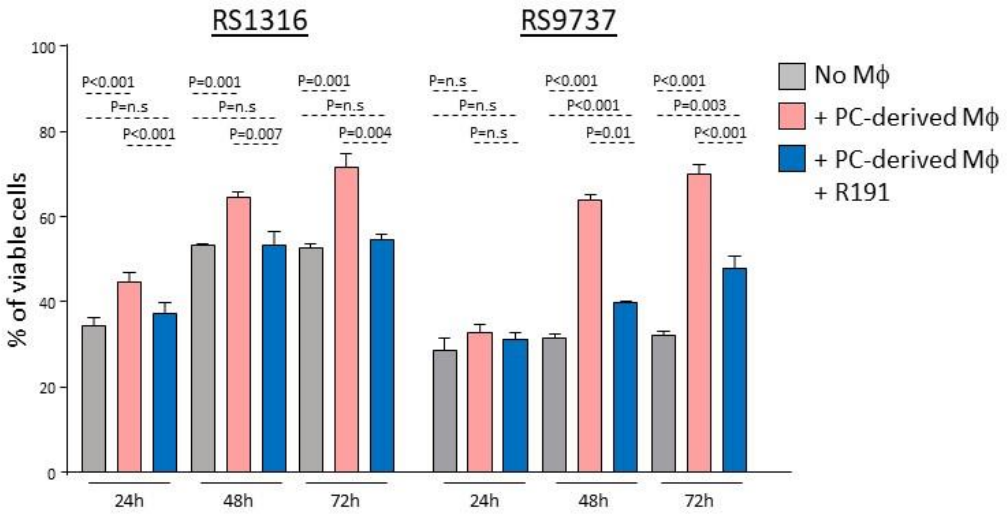

Figure 43. R191 treatment abrogates the capacity of macrophages to support the survival of the RS cells. Percentage of viable RS1316 or RS9737 cells following co-culture with peritoneal cavity-derived macrophages that had previously been exposed to R191 for 24 hours. Macrophages were washed to remove R191 prior to co-culture with the RS-PDX cells. Viability was assessed by Annexin V/PI staining. Graph represents summary of 3 independent experiments. Statistical analysis was done with One Way Repeated Measures ANOVA with Tukey test for multiple comparisons.

Moreover, to investigate the effect of macrophages on tumor cell proliferation, we co-cultured the 3 RS-PDX cell lines (RS1316, RS9737 and IP867/17) with peritoneal cavity macrophages, which were used because of the ease of isolation. BrdU incorporation analysis showed that macrophages can induce the proliferation of the RS cells, in contrast to primary human CLL cells which did not proliferate (Figure 44A and B). The capacity of macrophages to support the growth of RS cells was further validated in a separate set of coculture experiments showing that RS cells can be maintained in culture for extended periods (>10 days) if supplemented every 3-4 days with viable macrophages (Figure 44C).

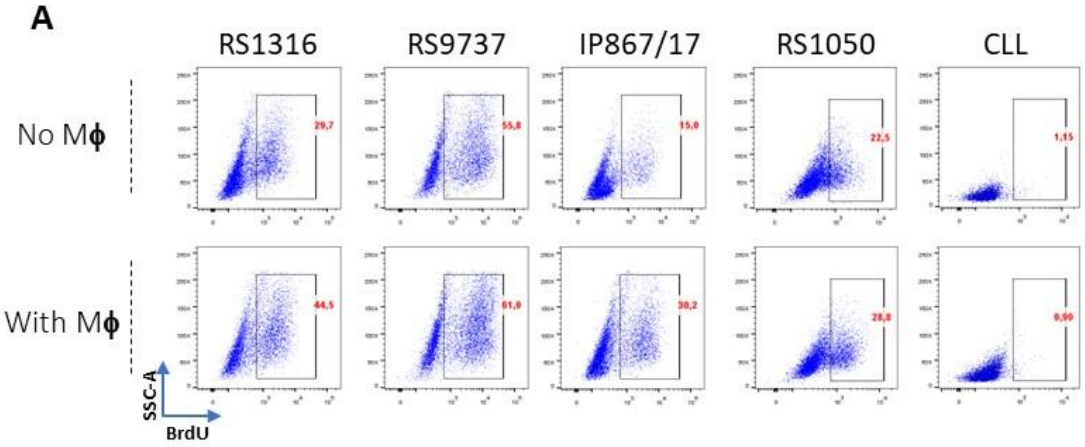

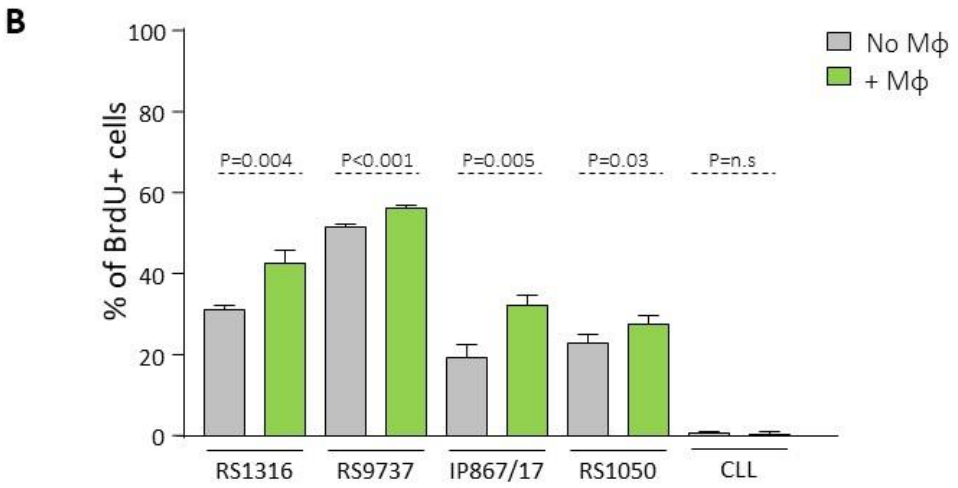

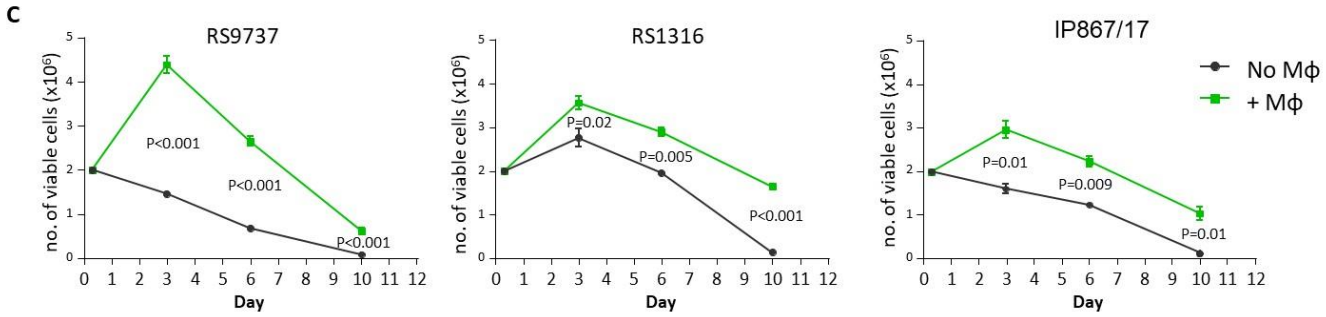

Figure 44. Macrophages enhance and sustain the proliferation of RS-PDX cells *in vitro*. A) Proliferation analysis of RS-PDX tumor cells that were cultured for 28 hours in the presence or absence of PC macrophages and then for additional 5 hours in the presence of BrdU (10 µM). One of 3 independent experiments with each RS-PDX primary line is shown. The percentage of proliferating BrdU+ cells is indicated in the plot. B) Summary of the proliferation analysis for each RS-PDX line and 6 different CLL primary samples. Three independent experiments with RS1316 and IP867/17 and four with RS9737 and RS1050 were performed. Statistical analysis was done with the t test. C) Time course analysis of absolute number of viable RS9737, RS1316 and IP867/17 cells cultured with or without PC macrophages. The number of viable cells was determined by manual counting of the cells and analysis of cell viability by propidium iodide staining and flow cytometry. Each data point represents 3 independent experiments with RS9737, RS1316 and IP867/17 cells**.**

A separate experiment with peritoneal cavity macrophages from C57BL/6 mice and the murine leukemias TCL1-355 and TCL1-863 also showed that macrophages can both sustain the survival and enhance the proliferation of murine TCL1 CLL cells (Figure 45A and B).

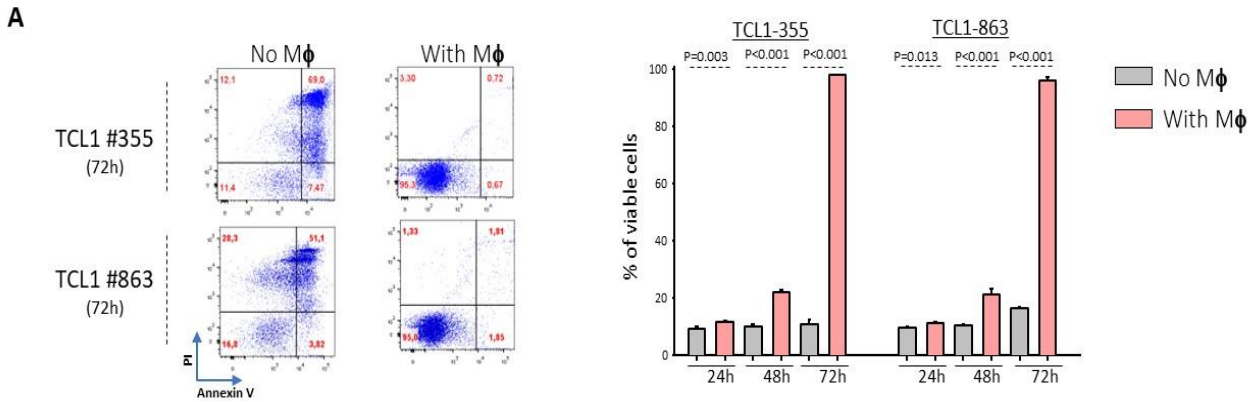

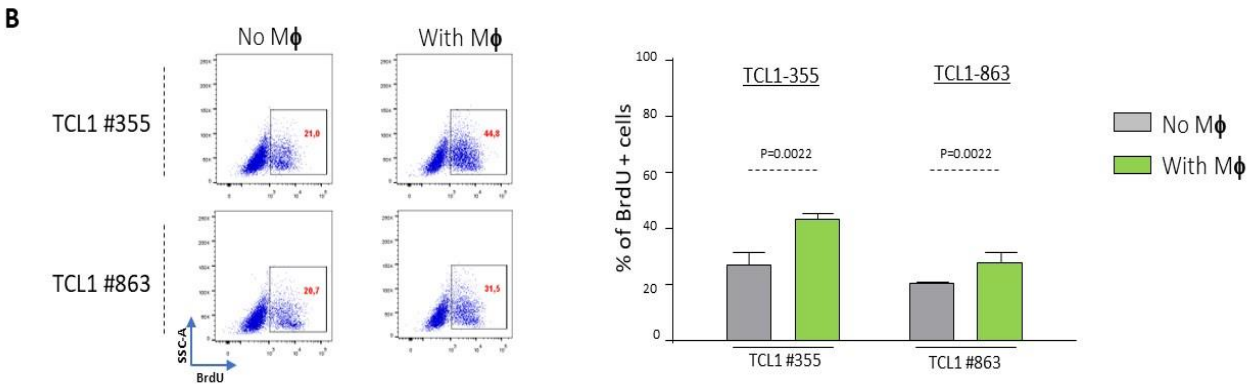

Figure 45. Macrophages protect murine Eμ-TCL1 leukemia cells from spontaneous apoptosis and induce their proliferation *in vitro*. A) Representative annexin V/PI analysis (left panels) and summary of three independent experiments (right panel) with 2 different Em-TCL1 leukemia primary cell lines cultured for the indicated time points in the presence or absence of PC-isolated Mϕ. B) Representative BrdU incorporation analysis (left panels) and summary of three independent experiments (right panel) using 2 different Eμ-TCL1 leukemia primary cell lines cultured in the presence or absence of PC-isolated Mϕ. Statistical analysis was done using the t test.

To investigate whether the supportive effect of macrophages was contact-dependent or caused by soluble factors, we separated the RS-PDX cells from macrophages with well inserts to prevent them from directly interacting. Analysis of viability of the RS-PDX cells showed that the effect on survival of the macrophages is primarily contact-dependent (Figure 46).

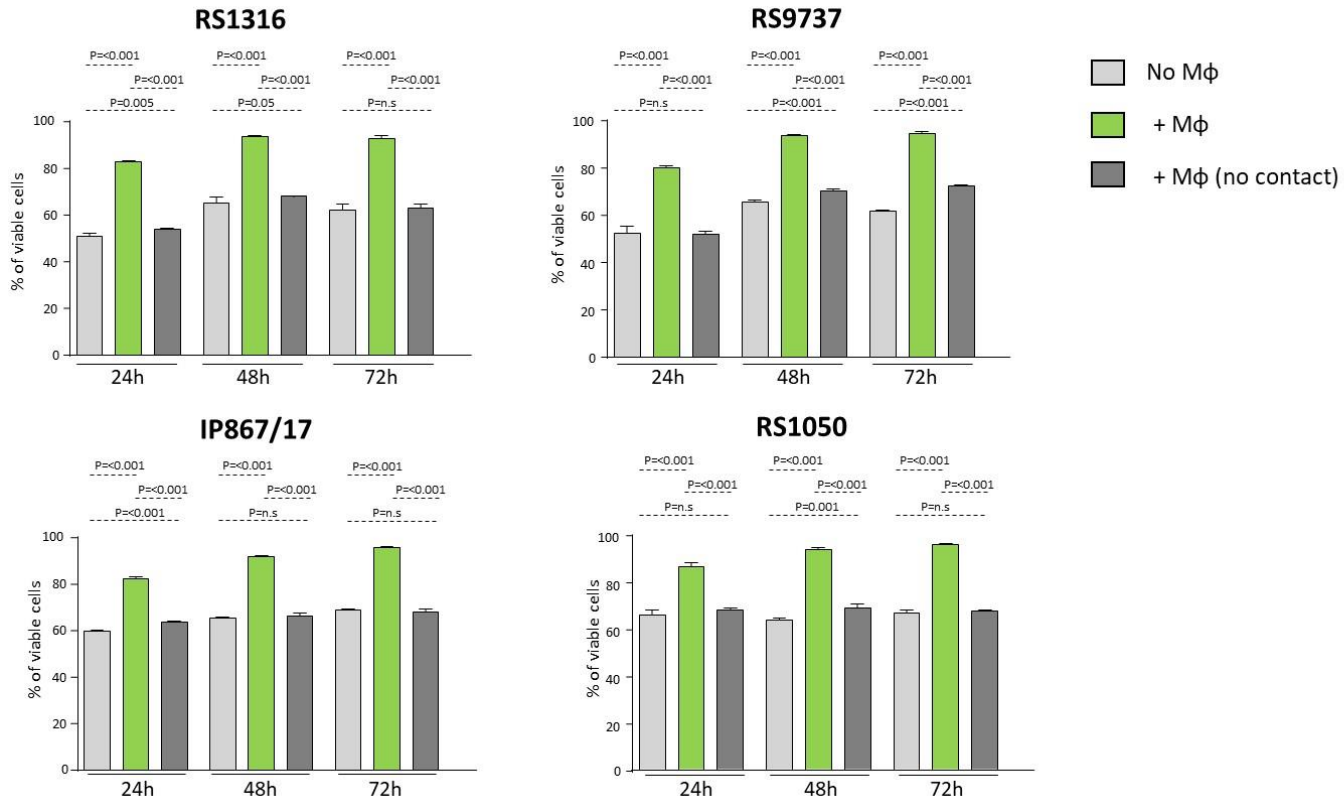

Figure 46. Cell-cell interactions and soluble factors sustain the survival of RS-PDX cells co-cultured with macrophages. Flow cytometric analysis (Annexin/PI) of viable RS-PDX cells co-cultured with murine PC-derived macrophages, with or without 0.4 mm pore inserts. Macrophages isolated from the peritoneal cavities of 2 NSG mice were co-cultured for the indicated time points with the 4 RS-PDX cell lines. Graphs show the summary of three independent experiments with each RS-PDX cell line.

To explore the possibility that soluble factors also contribute to the increased survival of macrophage-cocultured RS-PDX cells, we investigated the viability of all four RS-PDX models in the presence of various cytokines and chemokines that had previously been reported to support the survival of human CLL cells, including IL-15, CXCL12, WNT5a and BAFF (*Hasan MK et al. 2018; Endo T et al. 2007*). A small increase in viability was observed when RS-PDX cells were cultured with recombinant BAFF and IL-15 but not with the other soluble macrophage-derived factors, further suggesting that the supportive effect of macrophages on the survival of RS cells is mainly mediated by cell-cell interactions (Figure 47).

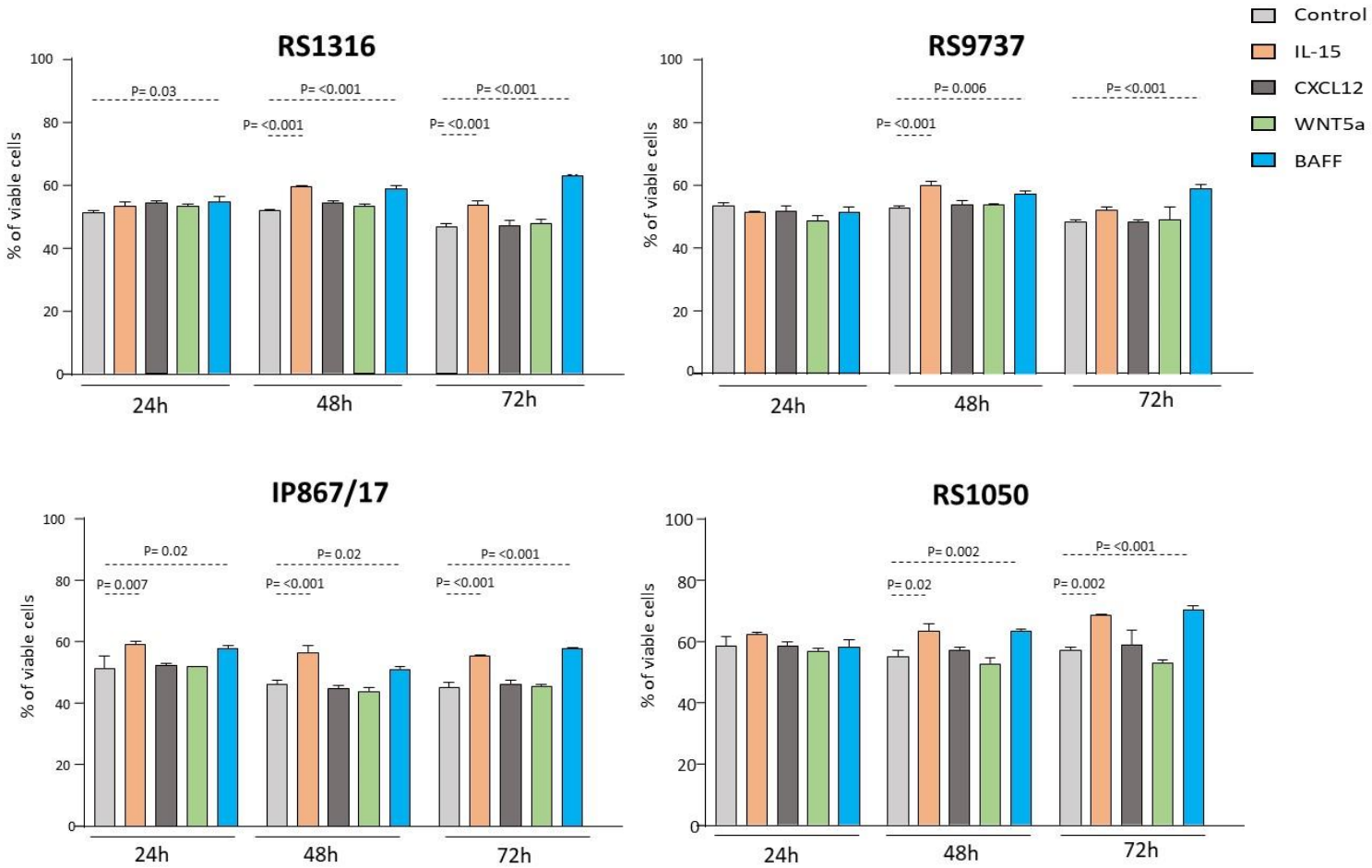

Figure 47. BAFF and IL1-15 support the survival of RS-PDX cells. RS-PDX cells were cultured in presence or absence of h-IL15 (25ng/ml) or CXCL12 (200 ng/ml) or h-WNT5a (100ng/ml) or h-BAFF (100ng/ml) for the indicated time points. Viability of the cells was assessed by flow cytometry using Annexin V/PI staining. Statistical analysis was done using One Way ANOVA with Tukey test for multiple comparisons.

4.2.8 Depletion of macrophages delays the growth of adoptively-transferred murine TCL1 leukemia cells

The initial tumor transfer experiments showed a delay in the growth of adoptively transferred TCL1 leukemia cells only upon prolonged treatment of mice with R221 (Figure 27). This finding, together with the observations that R221-treatment depletes macrophages and that MyD88 knockout does not inhibit the growth of the leukemic cells, suggested that the antileukemic activity of R221 may be primarily caused by deprivation of the malignant B cells from macrophage-derived growth and survival signals. To further evaluate this possibility, we repeated the experiment described in Figure 27B, except that this time we included an additional group of mice in which macrophages were depleted by R221 pre-treatment for 14 days prior to injection of TCL1-355 leukemia cells. Treatment was continued thereafter in both groups for 21 days, when mice were sacrificed for analysis of tumor burden. In contrast to mice that had not received pre-treatment, a significant reduction in the number of leukemic cells was observed in the peripheral blood and spleen of the R221-pretreated mice in comparison to the untreated mice (Figure 48). Consistent with the lack of an effect on peritoneal cavity macrophages, no reduction in the number of leukemic cells at this site was observed.

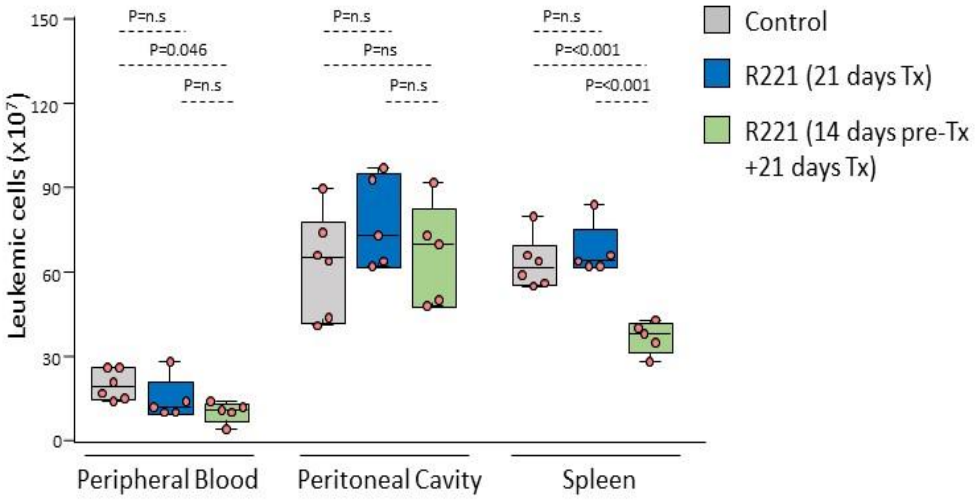

Figure 48. Depletion of macrophages by R221 treatment reduces the growth of leukemic cells in vivo. Analysis of leukemia cell counts (CD5+/CD19+) in peripheral blood, peritoneal cavity and spleen of mice treated with vehicle control (n=6), mice treated for 21 days with R221 (n=5), or mice pre-treated for 14 days with R221 prior to tumor transfer and then treated for additional 21 days (n=5). Statistical analysis was done using One Way ANOVA with Tukey test for multiple comparisons.

Chapter 5. Discussion

Chronic Lymphocytic Leukemia for long time has been considered as a disease of clonal accumulation rather than proliferation of malignant B cells. However, *in vivo* labeling studies have shown that CLL cells proliferate at a substantial rate which exceeds the proliferation rate of normal B cells (*Messmer BT et al. 2005; Herndon TM et al. 2017*).

Although BCR stimulation in normal B cells induces proliferation, *in vitro* BCR stimulation of CLL cells with anti-IgM transmits survival signals with activation of NF-κB, ERK and AKT pathways but does not lead to proliferation, suggesting that other signals are required for cell-cycle progression (*Longo PG et al. 2008, Slinger E et al. 2017*).

Cell-cycle progression is highly regulated by a complex interplay which involves different cyclins, cyclin-dependent kinases (CDKs) and CDK inhibitors. The CDK4 and CDK6 proteins are activated by the D-type cyclins CCND1,CCND2 and CCND3 and inhibited by the CDK inhibitors CDKN1A, CDKN1B, CDKN2A, and CDKN2B. The levels of expression of these cell-cycle regulators is highly dependent by growth factors and various external signals which can induce cell-cycle progression (*Piatelli M et al 2003*). Previous studies have shown that BCR stimulation induces the expression of several positive regulators of the cell cycle in human and murine B cells, including MYC, CCND1, CCND2, and CDK4, which results in entrance into the G1 phase of the cell cycle but is insufficient for further progression (*Deglesne PA et al. 2006; Krysov S et al. 2012; Guarini A et al. 2008*).

The first main finding of this thesis is that BCR stimulation does not induce the proliferation of human and murine CLL cells because in addition to inducing the expression of positive regulators of the cell cycle, such as MYC, CCND1, CCND2, and CDK4, it simultaneously induces also the expression of the negative regulators of the cell-cycle CDKN1A, CDKN2A and CDKN2B, which cause cell-cycle arrest. This block in cell-cycle progression can be overcome *in vitro* by providing costimulatory signals such as TLR or CD40 signals, which have been shown to induce upregulation of CCND3 and downregulation of CDKN1B, thus shifting the balance in favor of positive regulators of the cell cycle. (*Lam EW et al. 200; Longo PG et al. 2008; Bomben R et al. 2012*). The data presented in this thesis show that another mechanism to bypass the block in cell-cycle progression are inactivating lesions in the negative regulators of the cell-cycle TP53, which regulates CDKN1A, and CDKN2A/2B. Importantly, genetic lesions that downregulate these negative regulators are found in approximately 30-50% of Richter syndrome cases *(Chigrinova E et al. 2013*). By preventing the

induction of CDKN1A, CDKN2A and CDKN2B, these lesions can substitute for costimulatory signals from the microenvironment and allow for spontaneous proliferation of the malignant B cells. Importantly, we show that genetic inactivation of the IGHM gene in these spontaneously proliferating murine tumor cells results in negative selection of cells that do not express IgM, suggesting that the proliferation of these cells is still BCR dependent. Consistent with this possibility, previous immunogenetic studies have shown a higher risk for Richter transformation in stereotyped CLL subsets characterized by broad autoreactivity (*Leeksma AC et al. 2021; Rossi D et al. 2013*).

The BCR is also involved in the activation of the TLR-pathway delivering DNA-associated complexes to TLR9, that is located in the endosomes with activation of several downstream signaling pathways, such as MAPK/ ERK, PI3K/AKT/mTOR, and NF-kB resulting in induction of CLL cell proliferation (*Catera R et al. 2008; Crassini K et al. 2017*).

Links between TLR and BCR signaling have also been described, as for example *in vitro* stimulation of CLL cells with CpG induced phosphorylation of CD79A, LYN and SYK which appears to depend on the expression of the kinase ZAP-70 (*Wagner M et al. 2016*). Moreover, *in vitro* response to TLR9 stimulation is correlated with progression-free survival, time to treatment and overall survival in mutated-CLL and the strong correlation between CpG-induced proliferation and IGHV mutation status may argue that TLR stimulation is modulated by BCR signaling (*Tarnani M et al. 2010; Longo PG et al. 2007).*

In vivo TLR9 pathway activation has been suggested by gene expression profiling analysis showing enrichment of TLR9-target genes in LN CLL cells compared to PB CLL cells and by proximality ligation assay (PLA) that showed interaction of pIkBa with TLR9, MYD88 or IRAK1. However, the overexpressed genes identified as TLR9-target genes are also regulated by other pathways, such as BCR pathway, which is known to be activated in the lymph node compartment. In addition, the TLR-signaling complex activation was observed only in 2 out of 14 analysed LN CLL samples by PLA, suggesting that it may be a relatively rare event (*Herishanu Y et al. 2011; Dadashian EL et al. 2019).*

Here, to further define the role of the TLR pathway in the pathogenesis of CLL and RS, we performed *in vivo* pharmacological inhibition and CRISPR/Cas9 gene editing of a broad range of murine and human PDX models. In contrast to our initial expectation, we find that TLR-signals do not influence the growth of the tumor cells *in vivo* in any of the investigated models.

The negative findings of our study cannot completely exclude the possibility for a less important role of TLR signals in CLL pathogenesis or progression. In particular, considering that both the murine TCL1 and the human RS models are characterized by rapid tumor growth, a more subtle effect of

TLR pathway disruption may have remained undetected. For example, a recent study by Kennedy et al suggested that mitochondrial DNA, which is present at higher levels in the plasma of CLL patients compared with healthy controls, increases by two-fold the propensity of the leukemic cells to migrate towards CXCL12 (*Kennedy E et al. 2021*). Such an effect is unlikely to have a major impact on the growth of rapidly proliferating tumors and would likely be missed in our experimental models. However, using the same experimental approach, we readily demonstrated strong negative selection of human IGHM-knockout RS-PDX cells, thus demonstrating that our experimental system is robust enough to identify signals that are essential for the growth of the malignant cells.

Another unexpected finding of this study was the compartment-restricted effect of R191/R221 treatment on the growth of the transplanted malignant B cells. R191 has been reported to induce cell-cycle arrest by downregulating MYC, CDK4 and CDK6 and thus inducing apoptosis in Waldenstrom Macroglobulinemia cell lines, suggesting that it could be selectively toxic for cycling cells (*Ni H et al. 2018*). In line with this possibility, we observed that R191 reduces the viability of RS, TCL1 and CpG- or CD40L/IL-4/IL-21-stimulated human CLL samples, which all contain a substantial proportion of cycling cells, but has no impact on the viability on unstimulated, resting CLL cells. However, considering that the difference in tumor growth *in vivo* was seen only after prolonged R221 treatment and coincided with a reduction in the number of macrophages, another non-mutually exclusive possibility is that the effect of treatment was a consequence of reduced availability of macrophage-derived growth and survival signals. This possibility was additionally supported by our *in vitro* co-culture experiments showing increased proliferation and survival of human RS cells and murine TCL1 leukemia cells in the presence of macrophages, as well as by the findings of Giménez et al, who using another IRAK4 inhibitor also observed a concomitant reduction in the number of monocytes, macrophages and adoptively transferred murine TCL1 leukemia cells in the spleens of treated mice (*Gimènez N et al. 2020*).

The mechanism causing macrophage depletion in IRAK4 inhibitor-treated mice is currently unknown. In the study of Giménez et al., IRAK4 inhibitor treatment was associated with reduced monocyte expression of the chemokine receptor CCR2, which is essential for the CCL-2 mediated recruitment of monocytes by CLL cells (*van Attekum MHA et al. 2017*). However, in our study the effect of IRAK4 inhibitor treatment was more direct, resulting in selective killing of monocytes and macrophages but not affecting B and T cells present in the same compartment. Whether the cytotoxic effect of R191 against macrophages is a consequence of inhibition of TLR signals, which

are required for the differentiation of blood monocytes into macrophages *(Jia L et al. 2014; Audrito V et al. 2015; Managò A et al. 2019)* or an unrelated pathway remains to be determined.

The capacity of macrophages to support CLL cell survival involves both soluble factors which are released by macrophages and direct cell-cell contacts. The nursing function of the macrophages has been well established in numerous i*n vitro* studies showing that co-culture of primary CLL cells with nurse-like cells sustains the survival of the leukemia cells. This supporting effect of macrophages has been further validated in *in vivo* studies with Eμ-TCL1-derived murine CLL cells or the human CLL cell line MEC1, where the macrophage nursing activity was inhibited by impairing NLC development or by drug treatment (*Burger JA et al 2000; Nishio M et al. 2005; Reinart N et al. 2013, Polk A et al. 2016; Hanna BS et al. 2016; Galletti G et al 2016; Nguyen PH et al. 2016; Edwards V DK et al. 2018; Merchand-Reyes G et al. 2022*). A novelty of our findings in this respect is that the same effect was seen with non-immortalized human RS-PDX cells, suggesting that therapeutic strategies based on interfering with macrophage-tumor cell interactions could provide a therapeutic benefit also in Richter syndrome.

Co-culture experiments of RS-PDX cells with macrophages showed enhanced *ex vivo* proliferation of the tumor cells, whereas no proliferation was detected with non-transformed human CLL cells (Figure 42). This finding, together with previous observations that human RS cells, unlike human CLL cells, can be grown efficiently in the absence of T cells in immunodeficient mice (*Bagnara et al. 2011; Patten PEM et al. 2021; Vaisitti T et al. 2018; Vaisitti T et al. 2021*) suggests that macrophage-derived signals, in combination with certain genetic lesions in cell cycle regulators, may substitute for T cell-derived signals in driving the proliferation of RS cells.

In conclusion, the presented data provide additional genetic evidence for a key role for BCR signals in driving the proliferation of CLL and RS cells and further emphasize an important role for macrophages in the pathogenesis of the disease. In addition, we describe a novel CRISPR/Cas9 genome editing approach that allows for rapid genetic disruption of intracellular signaling pathways involved in transducing different microenvironmental signals and allows the investigation of the relative relevance of such signals for the growth and survival of the malignant cells *in vivo*.

6. References

- Agathangelidis A et al. Stereotyped B cell receptors in one-third of chronic lymphocytic leukemia: a molecular classification with implications for targeted therapies. Blood. 2012; 119(19): 4467–75.
- Audrito V et al. Extracellular nicotinamide phosphoribosyl-transferase (NAMPT) promotes M2 macrophage polarization in chronic lymphocytic leukemia. Blood. 2015; 125(1):111-23.
- Austen B et al. Mutations in the ATM gene lead to impaired overall and treatment-free survival that is independent of IGVH mutation status in patients with B-CLL. Blood. 2005; 106:3175–3182.
- Autore F et al. Morphological, immunophenotypic, and genetic features of chronic lymphocytic leukemia with trisomy 12: a comprehensive review. Haematologica 2018; Volume 103(6):931-938.
- Bagnara D et al. A novel adoptive transfer model of chronic lymphocytic leukemia suggests a key role for T lymphocytes in the disease. Blood. 2011; 117(20):5463–72.
- Balatti V et al. NOTCH1 mutations in CLL associated with trisomy 12. Blood. 2012; 119(2):329-31.
- Binet JL et al. A new prognostic classification of chronic lymphocytic leukemia derived from a multivariate survival analysis. Cancer 1981; 48:198-206.
- Bomben R et al. The miR-17$92 family regulates the response to Toll-like receptor 9 triggering of CLL cells with unmutated IGHV genes. Leukemia. 2012;26(7):1584-1593.
- Browne E. Regulation of B-cell responses by Toll-like receptors. Immunology 2012 136, 370-379.
- Bulian P et al. CD49d is the strongest flow cytometry-based predictor of overall survival in chronic lymphocytic leukemia. J Clin Oncol. 2014; 32(9):897-904.
- Burger JA et al. B cell receptor signaling in chronic lymphocytic leukemia. Trends Immunol 2013; 34, 592–601.
- Burger JA et al. Blood-derived nurse-like cells protect chronic lymphocytic leukemia B cells from spontaneous apoptosis through stromal cell-derived factor-1. Blood. 2000; 96(8):2655–63
- Burger JA et al. Blood-derived nurse-like cells protect chronic lymphocytic leukemia B cells from spontaneous apoptosis through stromal cell-derived factor-1. Blood. 2000; 96(8):2655-63.
- Burger JA and Wiestner A. Targeting B cell receptor signalling in cancer: preclinical and clinical advances. Nat Rev Cancer. 2018; 18(3):148-167.

- Cambier JC et al. B-cell anergy: from transgenic models to naturally occurring anergic B cells? Nat Rev Immunol. 2007; 7(8): 633–643.
- Campo E et al. WHO Classification Of Tumours Of Haematopoietic And Lymphoid Tissues. Blood 2011; 117: 5019–5032.
- Catera R, et al. Chronic lymphocytic leukemia cells recognize conserved epitopes associated with apoptosis and oxidation. Mol Med. 2008; 14:665-74.20.
- Chen L et al. Expression of ZAP-70 is associated with increased B-cell receptor signaling in chronic lymphocytic leukemia. Blood. 2002; 100(13): 4609–14.
- Chen L et al. ZAP-70 enhances IgM signaling independent of its kinase activity in chronic lymphocytic leukemia. Blood. 2007; 111(5):2685-92.
- Chen SS et al. Autoantigen can promote progression to a more aggressive TCL1 leukemia by selecting variants with enhanced B-cell receptor signaling. Proc Natl Acad Sci USA. 2013;110(16): E1500-E1507.
- Chen SS et al. BTK inhibition results in impaired CXCR4 chemokine receptor surface expression, signaling and function in chronic lymphocytic leukemia. Leukemia. 2016; 30(4): 833-43
- Cheng S et al. BTK inhibition targets in vivo CLL proliferation through its effects on B-cell receptor signaling activity. Leukemia 2014; 28, 649–657.
- Chigrinova E et al. Two main genetic pathways lead to the transformation of chronic lymphocytic leukemia to Richter syndrome. Blood. 2013; 122(15):2673-82.
- Chiorazzi N et al. Chronic lymphocytic leukemia: a tale of one or two signals? Cell Res 2013; 23(2):182-5.
- Chiorazzi N et al. Chronic lymphocytic leukemia. NEJM. 2005; 352(8):804– 815.
- Cimmino A et al. miR-15 and miR-16 induce apoptosis by targeting BCL2. Proc. Proc Natl Acad Sci U S A. 2005; 102(39):13944–13949.
- Correa JMI, et al. Toll-like receptors in the pathogenesis of human B cell malignancies. Journal of Hematology & Oncology 2014, 7:57.
- Crassini K et al. Modeling the chronic lymphocytic leukemia microenvironment in vitro. Leuk Lymphoma 2017; 58(2):266–79
- Dadashian EL McAuley EM, Liu D, et al. TLR Signaling Is Activated in Lymph Node-Resident CLL Cells and Is Only Partially Inhibited by Ibrutinib. Cancer Res. 2019; 79(2):360-371.
- Dal Bo M et al. CD49d prevails over the novel recurrent mutations as independent prognosticator of overall survival in chronic lymphocytic leukemia. Leukemia. 2016; 30(10):2011-2018.

- Dal Bo M et al. The SIRT1/TP53 axis is activated upon B-cell receptor triggering via miR-132 up-regulation in chronic lymphocytic leukemia cells. Oncotarget. 2015; 6(22):19102-17.
- Dal Bo M et al. Microenvironmental interactions in chronic lymphocytic leukemia: the master role of CD49d. Semin Hematol. 2014; 51(3):168-176.
- Damle RN et al. Ig V gene mutation status and CD38 expression as novel prognostic indicators in chronic lymphocytic leukemia. Blood. 1999; 94(6):1840-7.
- Damm F et al. Acquired Initiating Mutations in Early Hematopoietic Cells of CLL Patients. Cancer Discov. 2014; 4(9):1088-101.
- Dancescu M, et al. Interleukin 4 protects chronic lymphocytic leukemic B cells from death by apoptosis and upregulates Bcl-2 expression. J Exp Med. 1992; 176(5):1319–26.
- Deglesne PA et al. Survival response to B-cell receptor ligation is restricted to progressive chronic lymphocytic leukemia cells irrespective of Zap70 expression. Cancer Res. 2006; 66(14):7158-7166
- Del Gaizo Moore V et al. Chronic lymphocytic leukemia requires BCL2 to sequester prodeath BIM, explaining sensitivity to BCL2 antagonist ABT-737. J Clin Invest. 2007; 117(1):112-21.
- Dicker F et al. The detection of TP53 mutations in chronic lymphocytic leukemia independently predicts rapid disease progression and is highly correlated with a complex aberrant karyotype. Leukemia. 2009; 23(1):117–124.
- Dohner H et al. Genomic Aberrations and Survival in Chronic Lymphocytic Leukemia. N Engl J Med. 2000; 343(26):1910-6.
- Dühren-von Minden M et al. Chronic lymphocytic leukaemia is driven by antigen-independent cell-autonomous signalling. Nature. 2012; 489(7415):309-12.
- Edwards V DK et al. Targeting of colony-stimulating factor 1 receptor (CSF1R) in the CLL microenvironment yields antineoplastic activity in primary patient samples. Oncotarget. 2018; 9(37):24576-24589.
- Efremov D et al. Mechanisms of B Cell Receptor Activation and Responses to B Cell Receptor Inhibitors in B Cell Malignancies. Cancers (Basel). 2020; 12(6):1396.
- Efremov D et al. Recent Advances in the Pathogenesis and Treatment of Chronic Lymphocytic Leukemia. Pril (Makedon Akad Nauk Umet Odd Med Nauki) 2014; 35(3):105-20.
- Endo T et al. BAFF and APRIL support chronic lymphocytic leukemia B-cell survival through activation of the canonical NF-kappaB pathway. Blood. 2007; 109(2):703-10.
- Fabbri G et al. Analysis of the chronic lymphocytic leukemia coding genome: role of NOTCH1 mutational activation. J. Exp. Med. 2011; 208, 1389–1401.

- Fabbri G et al. Genetic lesions associated with chronic lymphocytic leukemia transformation to Richter syndrome. J. Exp. Med. 2013; 210, 2273–2288.
- Friedberg JW et al. Inhibition of Syk with fostamatinib disodium has significant clinical activity in non-Hodgkin lymphoma and chronic lymphocytic leukemia. Blood. 2010; 115, 2578–2585.
- Furman RR et al. Idelalisib and rituximab in relapsed chronic lymphocytic leukemia. N Engl J Med. 2014; 370: 997–1007.
- Galletti G et al. Targeting Macrophages Sensitizes Chronic Lymphocytic Leukemia to Apoptosis and Inhibits Disease Progression. Cell Rep. 2016; 14(7):1748-1760.
- Ghia P et al. Microenvironmental influences in chronic lymphocytic leukaemia: the role of antigen stimulation. J Intern Med. 2008; 264:549-62.
- Giménez N et al. Targeting IRAK4 disrupts inflammatory pathways and delays tumor development in chronic lymphocytic leukemia. Leukemia. 2020; 34(1):100-114.
- Gobessi S et al. Inhibition of constitutive and BCR-induced Syk activation downregulates Mcl-1 and induces apoptosis in chronic lymphocytic leukemia B cells. Leukemia 2009; 23, 686–697.
- Gobessi S et al. ZAP-70 enhances B-cell-receptor signaling despite absent or inefficient tyrosine kinase activation in chronic lymphocytic leukemia and lymphoma B cells. Blood. 2007; 109:2032– 2039.
- Gonzalez D et al. Mutational status of the TP53 gene as a predictor of response and survival in patients with chronic lymphocytic leukemia: Results from the LRF CLL4 trial. J Clin Oncol. 2011; 29(16):2223–2229.
- Grandjenette C et al. Expression of functional toll-like receptors by B-chronic lymphocytic leukemia cells. Haematologica 2007; 92(9), 1279-81.
- Guarini A et al. BCR ligation induced by IgM stimulation results in gene expression and functional changes only in IgV H unmutated chronic lymphocytic leukemia (CLL) cells. Blood. 2008; 112(3):782-92.
- Hallek M et al. International Group of Investigators; German Chronic Lymphocytic Leukaemia Study Group. Addition of rituximab to fludarabine and cyclophosphamide in patients with chronic lymphocytic leukaemia: a randomised, open-label, phase 3 trial. Lancet. 2010; 376(9747): 1164–74.
- Hallek M et al. iwCLL guidelines for diagnosis, indications for treatment, response assessment, and supportive management of CLL. Blood. 2018;131(25):2745-2760.
- Hallek M et al. Guidelines for the diagnosis and treatment of chronic lymphocytic leukemia: a report from the International Workshop on Chronic Lymphocytic Leukemia updating the National Cancer Institute−Working Group 1996 guidelines. Blood. 2008; 111: 5446-5456.

- Hamblin TJ et al. Unmutated Ig V(H) genes are associated with a more aggressive form of chronic lymphocytic leukemia. Blood. 1999; 94:1848– 1854.
- Hanna BS et al. Depletion of CLL-associated patrolling monocytes and macrophages controls disease development and repairs immune dysfunction in vivo. Leukemia. 2016; 30(3):570-9.
- Hasan MK et al. Wnt5a induces ROR1 to recruit DOCK2 to activate Rac1/2 in chronic lymphocytic leukemia. Blood. 2018; 132(2):170-178.
- Herishanu Y et al. The lymph node microenvironment promotes B-cell receptor signaling, NFkappaB activation, and tumor proliferation in chronic lymphocytic leukemia. Blood. 2011; 117(2): 563–74.
- Herndon TM et al. Direct in vivo evidence for increased proliferation of CLL cells in lymph nodes compared to bone marrow and peripheral blood. Leukemia. 2017; 31(6):1340-1347.
- Herve M, et al. Unmutated and mutated chronic lymphocytic leukemias derive from self-reactive B cell precursors despite expressing different antibody reactivity. J Clin Invest 2005; 115(6):1636-43.
- Iacovelli S, et al. Two types of BCR interactions are positively selected during leukemia development in the Eμ-TCL1 transgenic mouse model of CLL. Blood 2015; 125(10):1578-88.
- Improgo MR et al. MYD88 L265P mutations identify a prognostic gene expression signature and a pathway for targeted inhibition in CLL. Br J Haematol. 2019; 184(6):925-936.
- Jia L et al. Extracellular HMGB1 promotes differentiation of nurse-like cells in chronic lymphocytic leukemia. Blood. 2014; 123(11):1709-19.
- Johnson SA, et al. Phoshorylated immunoreceptor signaling motifs (ITAMs) exhibit unique abilities to binf and active Lyn and Syk tyrosine kinases. J Immunol 1995; 155:4596-4603.
- Kennedy E et al. TLR9 expression in chronic lymphocytic leukemia identifies a promigratory subpopulation and novel therapeutic target. Blood. 2021; 137(22):3064-3078.
- Klein U, et al. Gene expression profiling of B cell chronic lymphocytic leukemia reveals a homogeneous phenotype related to memory B cells. J Exp Med. 2001; 194(11):1625-38.
- Knisbacher BA et al. Molecular map of chronic lymphocytic leukemia and its impact on outcome. Nat Genet. 2022. PMID: 35927489. Online ahead of print.
- Krysov S et al. Surface IgM stimulation induces MEK1/2-dependent MYC expression in chronic lymphocytic leukemia cells. Blood. 2012; 119(1):170-179.

- Kulis M, et al. Epigenomic analysis detects widespread gene-body DNA hypomethylation in chronic lymphocytic leukemia. Nat Genet 2012. 44, 1236–1242.
- Laine J et al. The protooncogene TCL1 is an Akt kinase coactivator. Mol Cell. 2000; 6(2):395-407.
- Lam EW et al. Cyclin D3 compensates for loss of cyclin D2 in mouse B-lymphocytes activated via the antigen receptor and CD40. J Biol Chem. 2000; 275(5):3479-3484.
- Lanemo Myhrinder A et al. A new perspective: molecular motifs on oxidized LDL, apoptotic cells, and bacteria are targets for chronic lymphocytic leukemia antibodies. Blood. 2008; 111:3838.
- Lannutti BJ, et al. CAL-101, a p110δ selective phosphatidylinositol-3-kinase inhibitor for the treatment of B-cell malignancies, inhibits PI3K signaling and cellular viability. Blood 2011; 117, 591–594.
- Leeksma AC et al. Genomic arrays identify high-risk chronic lymphocytic leukemia with genomic complexity: a multi-center study. Haematologica. 2021; 106(1):87-97.
- Lewis R et al. CXCR4 hyperactivation cooperates with TCL1 in CLL development and aggressiveness. Leukemia. 2021; 35(10):2895-2905.
- Longo PG et al. The Akt/Mcl-1 pathway plays a prominent role in mediating antiapoptotic signals downstream of the B-cell receptor in chronic lymphocytic leukemia B cells. Blood. 2008; 111(2):846-55.
- Longo PG et al. The Akt signaling pathway determines the different proliferative capacity of chronic lymphocytic leukemia B-cells from patients with progressive and stable disease. Leukemia. 2007; 21(1):110-20.
- Lovat F et al. miR-15b/16-2 deletion promotes B-cell malignancies. Proc Natl Acad Sci U S A. 2015; 112(37): 11636–11641.
- Malcikova J, et al. Monoallelic and biallelic inactivation of TP53 gene in chronic lymphocytic leukemia: selection, impact on survival, and response to DNA damage. Blood. 2009; 114(26):5307–5314.
- Managò A et al. Extracellular nicotinate phosphoribosyltransferase binds Toll like receptor 4 and mediates inflammation. Nat Commun. 2019; 10(1):4116.
- Mancao C, Hammerschmidt W. Epstein-Barr virus latent membrane protein 2A is a B-cell receptor mimic and essential for B-cell survival. Blood. 2007; 110(10):3715-21.
- Mansouri L et al. Functional loss of IkBε leads to NF-kB deregulation in aggressive chronic lymphocytic leukemia. J Exp Med. 2015; 212(6):833-43.
- Merchand-Reyes G et al. Disruption of Nurse-like Cell Differentiation as a Therapeutic Strategy for Chronic Lymphocytic Leukemia. J Immunol. 2022. 15;209(6):1212-1223.

- Messmer BT et al. In vivo measurements document the dynamic cellular kinetics of chronic lymphocytic leukemia B cells. J Clin Invest. 2005; 115(3):755-64.
- Mongini P, et al. TLR-9 and IL-15 Synergy Promotes the In Vitro Clonal Expansion of Chronic Lymphocytic Leukemia B Cells. The Journal of Immunology. 2015; 195 901-923.
- Ngo VN et al. Oncogenically active MYD88 mutations in human lymphoma. Nature. 2011; 470:115–119.
- Nguyen PH et al. LYN Kinase in the Tumor Microenvironment Is Essential for the Progression of Chronic Lymphocytic Leukemia. Cancer Cell. 2016; 30(4):610-622.
- Ni H et al. Targeting myddosome signaling in Waldenstrom's macroglobulinemia with the interleukin-1 receptor-associated kinase 1/4 inhibitor R191. Clin Cancer Res. 2018;24(24): 640
- Niiro H Clark EA. Regulation of B-cell fate by antigen-receptor signals. Nat Rev Immunol 2002; 2:945-56.
- Nishio M et al. Nurselike cells express BAFF and APRIL, which can promote survival of chronic lymphocytic leukemia cells via a paracrine pathway distinct from that of SDF-1alpha. Blood. 2005; 106(3):1012-20.)
- O'Brien SM et al. Results of the fludarabine and cyclophosphamide combination regimen in chronic lymphocytic leukemia. J Clin Oncol. 2001; 19(5): 1414-20.
- Panayiotidis P et al. Human bone marrow stromal cells prevent apoptosis and support the survival of chronic lymphocytic leukaemia cells in vitro. Br J Haematol. 1996; 92(1):97–103.
- Parikh SA et al. How we treat Richter syndrome. Blood. 2014; 123(11):1647-57.
- Pascutti MF et al. IL-21 and CD40L signals from autologous T cells can induce antigen-independent proliferation of CLL cells. Blood. 2013; 122(17):3010-9.
- Patten PEM et al. A Detailed Analysis of Parameters Supporting the Engraftment and Growth of Chronic Lymphocytic Leukemia Cells in Immune-Deficient Mice. Front Immunol. 2021; 12:627020.
- Petlickovski A et al. Sustained signaling through the B-cell receptor induces Mcl-1 and promotes survival of chronic lymphocytic leukemia B cells. Blood. 2005; 105:4820-4827.
- Piatelli M et al. Cell cycle control mechanisms in B-1 and B-2 lymphoid subsets. Immunol Res. 2003; 27(1): 31-52
- Polk A et al. Colony-Stimulating Factor-1 Receptor Is Required for Nurse-like Cell Survival in Chronic Lymphocytic Leukemia. Clin Cancer Res. 2016; 22(24):6118-6128.
- Ponader S et al. The Bruton tyrosine kinase inhibitor PCI-32765 thwarts chronic lymphocytic leukemia cell survival and tissue homing in vitro and in vivo. Blood. 2012; 119(5):1182-9.

- Puente XS et al. Whole-genome sequencing identifies recurrent mutations in chronic lymphocytic leukaemia. Nature. 2011; 475(7354):101–105.
- Quesada V et al. Exome sequencing identifies recurrent mutations of the splicing factor SF3B1 gene in chronic lymphocytic leukemia. Nat Genet. 2011; 44(1):47–52.
- Rai KR et al. Fludarabine compared with chlorambucil as primary therapy for chronic lymphocytic leukemia. N Engl J Med. 2000; 343(24): 1750-7.
- Rai KR et al. Clinical staging of chronic lymphocytic leukemia. Blood 1975; 46:219-234.
- Reinart N et al. Delayed development of chronic lymphocytic leukemia in the absence of macrophage migration inhibitory factor. Blood. 2013; 121(5):812-21.
- Richardson SJ et al. ZAP70 expression is associated with enhanced ability to respond to migratory and survival signals in B-cell chronic lymphocytic leukemia (B-CLL), Blood. 2006; 107(9):3584-92.
- Riches JC et al. Trisomy 12 chronic lymphocytic leukemia cells exhibit upregulation of integrin signaling that is modulated by NOTCH1 mutations. Blood. 2014; 123(26):4101-10.
- Roberts AW et al. Targeting BCL2 with Venetoclax in Relapsed Chronic Lymphocytic Leukemia. N Engl J Med. 2016; 374(4):311-22.
- Rosati E et al. Constitutively activated Notch signaling is involved in survival and apoptosis resistance of B-CLL cells. Blood. 2009; 113(4):856-65.
- Rossi D et al. Association between molecular lesions and specific B-cell receptor subsets in chronic lymphocytic leukemia. Blood. 2013; 121(24):4902-4905.
- Rossi D et al. Disruption of BIRC3 associates with fludarabine chemorefractoriness in TP53 wild-type chronic lymphocytic leukemia. Blood. 2012; 119(12):2854-62.
- Rossi D et al. Mutations of NOTCH1 are an independent predictor of survival in chronic lymphocytic leukemia. Blood 2012; 119(2): 521–529.
- Rossi D et al. The genetics of Richter syndrome reveals disease heterogeneity and predicts survival after transformation. Blood 2011; 117(12):3391-401
- Sameer A t al. How we treat Richter syndrome. Blood. 2014; 123(11):1647-1657.
- Scielzo C et al. The functional in vitro response to CD40 ligation reflects a different clinical outcome in patients with chronic lymphocytic leukemia. Leukemia 2011; 25(11):1760-7.
- Seiffert M. et al. Cellular origin and pathophysiology of chronic lymphocytic leukemia. J Exp Med. 2012. 209, 2183–2198.
- Slinger E et al. Targeting antigen-independent proliferation in chronic lymphocytic leukemia through differential kinase inhibition. Leukemia. 2017; 31(12):2601–7.

- Stachelscheid Jet al. The proto-oncogene TCL1A deregulates cell cycle and genomic stability in CLL. Blood. 2022 (Online ahead of print).
- Stevenson FK et al. B-cell receptor signaling in chronic lymphocytic leukemia. Blood 2011; 18: 4313-4320.
- Suljagic M et al. The Syk inhibitor fostamatinib disodium (R788) inhibits tumor growth in the Eμ-TCL1 transgenic mouse model of CLL by blocking antigen-dependent B-cell receptor signaling. Blood 2010; 116: 4894-4905.
- Tam CS et al. Long-term results of the fludarabine, cyclophosphamide, and rituximab regimen as initial therapy of chronic lymphocytic leukemia. Blood. 2008; 112(4): 975–80.
- Tarnani M et al. The proliferative response to CpG-ODN stimulation predicts PFS, TTT and OS in patients with chronic lymphocytic leukemia. Leuk Res. 2010; 34 (9):1189–94.
- Tissino E et al. CD49d promotes disease progression in chronic lymphocytic leukemia: new insights from CD49d bimodal expression. Blood. 2020; 135(15):1244-1254.
- Tissino E et al. Functional and clinical relevance of VLA-4 (CD49d/CD29) in ibrutinib-treated chronic lymphocytic leukemia. J Exp Med. 2018; 215(2):681-697.
- Vaisitti T et al. ROR1 targeting with the antibody-drug conjugate VLS-101 is effective in Richter syndrome patient-derived xenograft mouse models. Blood. 2021; 137(24):3365-3377.
- Vaisitti T et al. Novel Richter Syndrome Xenograft Models to Study Genetic Architecture, Biology, and Therapy Responses. Cancer Res. 2018; 78(13):3413-3420.
- van Attekum MHA et al. CD40 signaling instructs chronic lymphocytic leukemia cells to attract monocytes via the CCR2 axis. Haematologica. 2017; 102(12):2069-2076.
- Wagner M et al. Integration of innate into adaptive immune responses in ZAP-70-positive chronic lymphocytic leukemia. Blood. 2016. 127(4):436–48.)
- Wang L et al. SF3B1 and other novel cancer genes in chronic lymphocytic leukemia. N Engl J Med. 2011; 365(26):2497–2506.
- Wiestner A et al. ZAP-70 expression identifies a chronic lymphocytic leukemia subtype with unmutated immunoglobulin genes, inferior clinical outcome, and distinct gene expression profile. Blood. 2003; 101(12):4944–51.
- Xinfang Yu et al. MYD88 L265P Mutation in Lymphoid Malignancies. Cancer Res 2018; 78(10).
- Zenz T. et al. TP53 mutation and survival in chronic lymphocytic leukemia. J. Clin. Oncol. 2010; 28, 4473–4479.

PUBLICATIONS DIRECTLY FROM THESIS PROJECT:

- Chakraborty S, **Martines C**, Porro F, Fortunati I, Bonato A, Dimishkovska M, Piazza S, Yadav BS, Innocenti I, Fazio R, Vaisitti T, Deaglio S, Zamò A, Dimovski AJ, Laurenti L, Efremov DG. B-cell receptor signaling and genetic lesions in TP53 and CDKN2A/CDKN2B cooperate in Richter transformation. Blood. 2021 Sep 23;138(12):1053-1066. doi: 10.1182/blood.2020008276. PMID: 33900379.

- **Martines C**, Chakraborty S, Vujovikj M, Gobessi S, Vaisitti T, Deaglio S, Laurenti L, Dimovski AJ, Efremov DG. Macrophage- and BCR- but not TLR-derived signals support the growth of CLL and Richter Syndrome murine models in vivo. Blood. 2022 Sep 9:blood.2022016272. doi: 10.1182/blood.2022016272. Epub ahead of print. PMID: 36084319.

blood®
Regular Article

LYMPHOID NEOPLASIA

B-cell receptor signaling and genetic lesions in TP53 and CDKN2A/CDKN2B cooperate in Richter transformation

Supriya Chakraborty,[1] Claudio Martines,[1] Fabiola Porro,[1] Ilaria Fortunati,[1] Alice Bonato,[1] Marija Dimishkovska,[2] Silvano Piazza,[3] Brijesh S. Yadav,[4] Idanna Innocenti,[5] Rosa Fazio,[1] Tiziana Vaisitti,[6] Silvia Deaglio,[6] Alberto Zamò,[7] Aleksandar J. Dimovski,[2] Luca Laurenti,[5] and Dimitar G. Efremov[1]

[1]Molecular Hematology Unit, International Center for Genetic Engineering and Biotechnology, Trieste, Italy; [2]Research Center for Genetic Engineering and Biotechnology, Macedonian Academy of Sciences and Arts, Skopje, North Macedonia; [3]Computational Biology Unit, International Center for Genetic Engineering and Biotechnology, Trieste, Italy; [4]University of Information Science & Technology St Paul the Apostle, Ohrid, North Macedonia; [5]Department of Hematology, Catholic University Hospital A. Gemelli, Rome, Italy; [6]Department of Medical Sciences, University of Turin, Turin, Italy; and [7]Institute of Pathology, University of Würzburg, Würzburg, Germany

KEY POINTS

- **Biallelic inactivation of TP53 and CDKN2A/CDKN2B allows for BCR-dependent/costimulatory signal-independent proliferation of CLL cells.**
- **BCR and CDK4/6 inhibitors display synergistic activity against RS models with genetic lesions in TP53 and CDKN2A/CDKN2B.**

B-cell receptor (BCR) signals play a critical role in the pathogenesis of chronic lymphocytic leukemia (CLL), but their role in regulating CLL cell proliferation has still not been firmly established. Unlike normal B cells, CLL cells do not proliferate in vitro upon engagement of the BCR, suggesting that CLL cell proliferation is regulated by other signals from the microenvironment, such as those provided by Toll-like receptors or T cells. Here, we report that BCR engagement of human and murine CLL cells induces several positive regulators of the cell cycle, but simultaneously induces the negative regulators CDKN1A, CDKN2A, and CDKN2B, which block cell-cycle progression. We further show that introduction of genetic lesions that downregulate these cell-cycle inhibitors, such as inactivating lesions in CDKN2A, CDKN2B, and the CDKN1A regulator TP53, leads to more aggressive disease in a murine in vivo CLL model and spontaneous proliferation in vitro that is BCR dependent but independent of costimulatory signals. Importantly, inactivating lesions in CDKN2A, CDKN2B, and TP53 frequently co-occur in Richter syndrome (RS), and BCR stimulation of human RS cells with such lesions is sufficient to induce proliferation. We also show that tumor cells with combined TP53 and CDKN2A/2B abnormalities remain sensitive to BCR-inhibitor treatment and are synergistically sensitive to the combination of a BCR and cyclin-dependent kinase 4 and 6 (CDK4/6) inhibitor both in vitro and in vivo. These data provide evidence that BCR signals are directly involved in driving CLL cell proliferation and reveal a novel mechanism of Richter transformation.

Introduction

Chronic lymphocytic leukemia (CLL) is a common B-cell malignancy characterized by the expansion and progressive accumulation of mature autoreactive B lymphocytes. Studies conducted over the past 15 to 20 years have provided compelling evidence that the disease is driven by a complex interplay of recurrent genetic defects and signals that the leukemic cells receive from the microenvironment.[1,2] Among the latter, signals that the leukemic cells receive through the B-cell receptor (BCR) have proven to play a particularly important role in the pathogenesis of the disease.[3] Evidence for this includes the frequent expression of BCRs with stereotyped structural properties, the strong correlation between the clinical course and the mutational status of the genes encoding for the immunoglobulin portion of the BCR, the high expression of BCR target genes in lymph node CLL cells, and, above all, the significant clinical activity of drugs that inhibit BCR signal transduction.[4-10] Moreover, a recent study by our group showed that chronic autoantigen stimulation induces CLL in the Eμ-TCL1–transgenic mouse model, providing further in vivo evidence that BCR signals drive the expansion of the malignant cells.[11]

Despite the evidence supporting a major role for the BCR in the pathogenesis of CLL, the malignant B cells, unlike normal B cells, do not proliferate in vitro upon engagement of the BCR by external ligand. Instead, they can be induced to proliferate by other signals from the microenvironment, such as the Toll-like receptor (TLR) ligand cytosine guanine dinucleotide (CpG) DNA or the T-cell–derived combination of CD40L, interleukin 21 (IL-21), and IL-4.[12-14] These data suggest that CLL cell proliferation is regulated by BCR-independent signals and that the BCR plays only an indirect role in this process, presumably by facilitating the recruitment, internalization, and/or processing of the proliferation signals. However, the rapid reduction in the percentage of proliferating leukemic cells in lymph node biopsies from patients with CLL or in spleens from Eμ-TCL1–transgenic mice treated with a Bruton tyrosine kinase (BTK) or SYK inhibitor suggests that the BCR may be more directly involved, at least in a subset of

cases.[15-20] In further support of this possibility, gene-expression and cell-cycle analyses have shown that stimulation of surface immunoglobulin M (IgM) induces an increase in the expression of the G_1-phase cell-cycle regulators MYC, CCND2, and CDK4 and an increase in the percentage of CLL cells in the G1 phase of the cell cycle in samples from patients with poor prognostic features.[21-23] However, no increase in the percentage of cells in the S phase of the cell cycle was observed,[22] suggesting that the BCR can only provide the initial signal required for cell-cycle entry, whereas subsequent cell-cycle progression is driven by costimulatory signals.

To further understand the role of the BCR pathway in regulating CLL cell proliferation, we investigated in more detail the effects of BCR stimulation on the expression of cell-cycle regulators in human and murine CLL cells. Surprisingly, we observed that BCR stimulation induces not only the expression of positive regulators of the cell cycle, but also expression of the negative regulators CDKN1A and CDKN2B. This finding was interesting for 2 reasons: first, it provided a possible explanation for the inability of BCR signals to induce the entry of CLL cells into the S phase of the cell cycle and, second, it raised the possibility that certain genetic lesions associated with CLL progression may function by reducing the requirement for costimulatory signals in driving CLL proliferation. Such lesions most notably include deletions of the CDKN2A/2B locus and mutations/deletions of the CDKN1A regulator TP53, which co-occur in approximately one-quarter of cases with clonally related Richter syndrome (RS), an aggressive B-cell lymphoma arising from transformation of CLL B cells.[24-26]

To address the possibility that genetic lesions in CDKN2A/2B and TP53 cooperate with BCR signals in the pathogenesis of RS, we used clustered regularly interspaced short palindromic repeats (CRISPR)/CRISPR-associated protein 9 (Cas9) technology to simultaneously target the CDKN2A, CDKN2B, and TP53 genes in primary Eμ-TCL1–derived murine CLL cells expressing different autoreactive BCRs.[11] We show that the genetically modified leukemia cells acquire the capacity to proliferate spontaneously in vitro but remain dependent on BCR signals.

Materials and methods

CLL samples

Blood samples were collected from CLL patients after obtaining informed consent according to the Declaration of Helsinki. Approval for the study was obtained from the institutional review board committee at Catholic University Hospital A. Gemelli (14563/15). CLL cells were purified, cultured, and stimulated with immobilized anti-IgM as described elsewhere.[27] Ibrutinib, idelalisib, R406, and GS-9973 (all from Selleckchem), and palbociclib (kindly provided by Pfizer), were used as indicated in the figures or figure legends.

CRISPR/Cas9 editing of murine CLL cells

Murine CLL cells with autoreactive BCRs had previously been isolated from Eμ-TCL1–transgenic mice that had been backcrossed for >10 generations on a C57BL/6J background.[11] Cells were thawed and cultured in RPMI 1640 supplemented with 10% heat-inactivated fetal bovine serum, 100 U/mL penicillin, 0.1 mg/mL streptomycin, 2 mM L-glutamine, 1 mM sodium pyruvate (Invitrogen), and 1 μM CpG-1668 (InvivoGen) at a concentration of 1×10^7 cells per mL for 20 hours prior to CRISPR/Cas9 editing with the Alt-R system (Integrated DNA Technologies [IDT]). Predesigned crispr RNAs (cr-RNAs) were used for targeting the TP53, CDKN2A, CDKN2B, MGA, and MyD88 genes, whereas the immunoglobulin heavy constant μ (IGHM) cr-RNA was designed using the IDT web tool (https://eu.idtdna.com/site/order/designtool/index/CRISPR_CUSTOM). To generate the Cas9 ribonucleoprotein (RNP) complexes, the cr-RNAs (1.5 μM) were combined with 1.5 μM ATTO 550-labeled trans-activating cr-RNA, 0.75 μM recombinant Cas9 protein, and 1.5 μM Alt-R Cas9 electroporation enhancer in 5 μL of nuclease-free duplex buffer (IDT). Cas9 RNP complexes were then electroporated using the Amaxa Nucleofector II device and the Z-001 program into 5×10^6 leukemic cells resuspended in 100 μL of mouse B-cell nucleofector solution (Lonza). Control cells were nucleofected with Cas9 RNPs without cr-RNA. Transfection efficiency was evaluated 3 hours after nucleofection by flow cytometry and ranged from 60% to 90% based on the percentage of ATTO 550–positive cells (supplemental Figure 1, available on the *Blood* Web site). Analysis of editing efficiency was performed on an aliquot of the nucleofected cells collected after 24 hours in culture and purified with the EasySep Mouse CD19 Positive Selection Kit II (StemCell Technologies). Editing efficiency was evaluated by amplicon capillary electrophoresis on a 3500 Genetic Analyzer (Applied Biosystems) of polymerase chain reaction (PCR) fragments spanning the region of genomic DNA around the targeted site.[28] Editing efficiency was additionally analyzed by Sanger sequencing followed by analysis with the ICE v2 CRISPR tool (https://www.synthego.com/). cr-RNA and PCR primer sequences are provided in supplemental Tables 1-3.

In vivo adoptive transfer experiments

All animal procedures were performed under a protocol approved by the Italian Ministry of Health (no. 347/2017-PR). CRISPR/Cas9-edited Eμ-TCL1 leukemia cells were transferred by intraperitoneal injection in NSG or C57BL/6 mice immediately after the nucleofection without any prior sorting or antibiotic selection. Leukemia cell expansion was analyzed by white blood cell counts and CD5/CD19 staining. For the in vivo treatment experiment, C57BL/6 mice were randomly assigned to each of the 4 experimental cohorts 3 days after adoptive transfer. Mice were treated with palbociclib at a daily dose of 50 mg/kg and/or ibrutinib at a daily dose of 25 mg/kg. Both drugs were administered in 2 divided doses by intraperitoneal injection as described elsewhere.[29-31]

Additional details regarding cell culture and stimulation, cell-proliferation assays, histology, immunohistochemistry, real-time quantitative PCR (RQ-PCR), immunoblotting, flow cytometry, whole-exome sequencing, and statistical analysis are provided in the supplemental Materials and methods.

Results

Biallelic disruption of TP53, CDKN2A, and CDKN2B results in spontaneous proliferation of autoreactive Eμ-TCL1 leukemia cells

To further explore the role of the BCR in CLL cell proliferation, we reanalyzed a gene-expression data set of unstimulated and immobilized anti-IgM–stimulated CLL cells that we had previously used to identify targets of BCR-regulated micro-RNAs.[32] A total of 735 genes were found to be differentially expressed based on fold

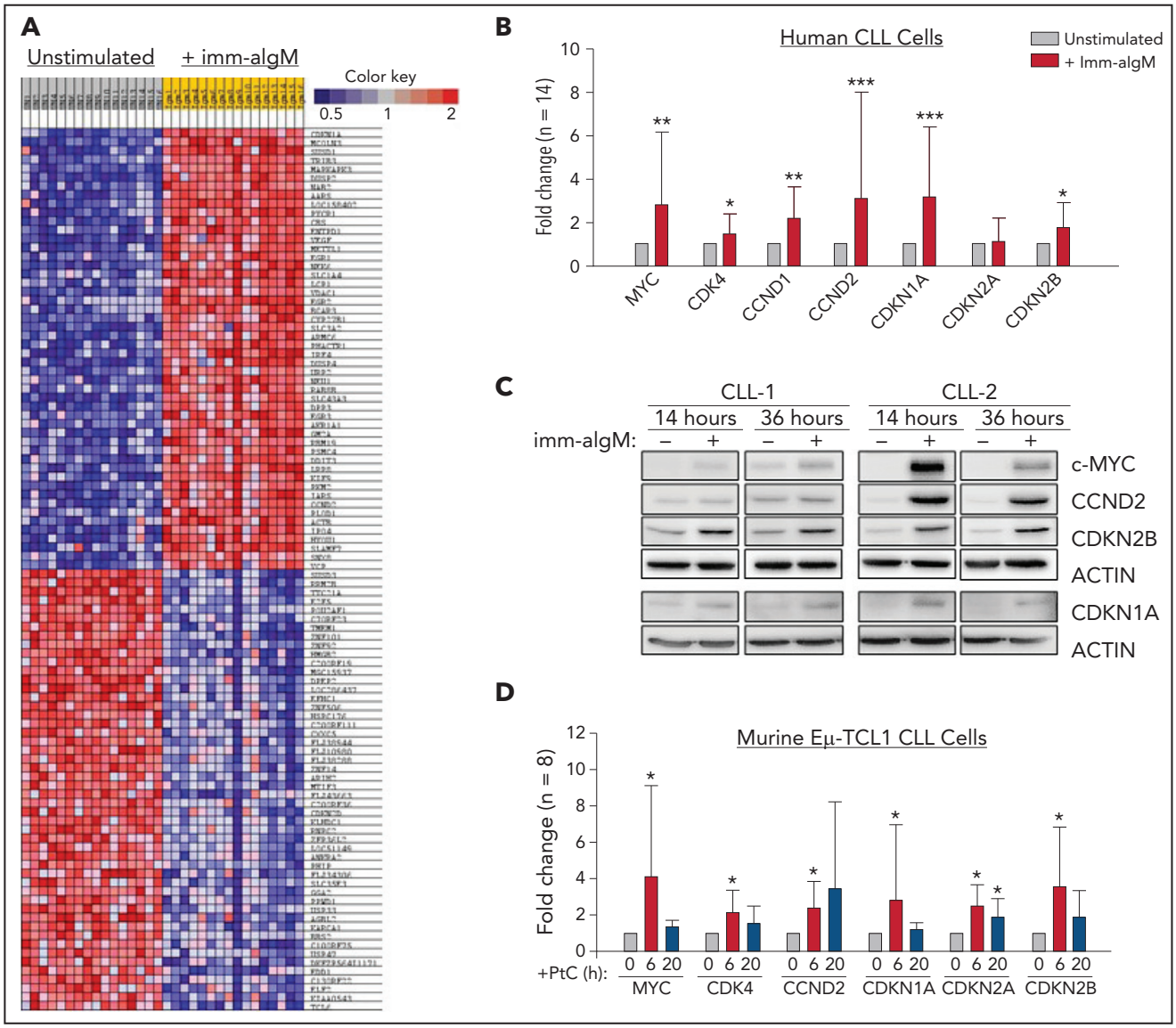

Figure 1. Positive and negative G_1-phase cell-cycle regulators are induced in BCR-stimulated CLL cells. (A) Differentially expressed genes between unstimulated CLL cells and CLL cells stimulated for 20 hours with immobilized anti-IgM (imm-algM; n = 16) and analyzed on the Agilent Whole Human Genome Microarray 4x44K platform (GEO accession number GSE52776). The top 50 upregulated and top 50 downregulated genes are shown. (B) RQ-PCR analysis of an independent series of human CLL samples (n = 14) cultured for 20 hours with or without immobilized anti-IgM prior to RNA extraction. Significant differences with respect to unstimulated CLL cells are indicated with asterisks: *$P < .05$, **$P < .01$, ***$P < .001$. Analysis was performed using the paired Student *t* test or Wilcoxon signed-rank test, as appropriate. (C) Time-course analysis of changes in MYC, CCND2, CDKN1A, and CDKN2B protein expression in human CLL cells stimulated with immobilized anti-IgM. Analysis of CLL cells from 2 different patients is shown. (D) RQ-PCR analysis of changes in expression of positive and negative cell-cycle regulators in PtC-stimulated murine Eμ-TCL1–derived CLL cells expressing an anti-PtC BCR.

change > 2.0 and $P < .001$. Pathway-enrichment analysis using the BIOCARTA database identified gene sets involved in G1-phase cell-cycle regulation as the most differentially expressed between unstimulated and anti-IgM–stimulated CLL cells (supplemental Table 4). The differentially expressed genes included MYC, CCND1, CCND2, and CDK4, which were all upregulated, and CDKN2D, which was downregulated in anti-IgM–stimulated CLL cells, consistent with entry of the leukemic cells into the G1 phase of the cell cycle. However, upregulation of the negative regulators CDKN1A and CDKN2B was also observed, with CDKN1A appearing as the most differentially expressed gene in this analysis (Figure 1A). The change in the expression of these cell-cycle inhibitors was further validated by RQ-PCR and immunoblotting analysis of an independent set of primary CLL samples (Figure 1B-C).

To investigate whether BCR engagement induces similar changes in murine CLL cells, we used Eμ-TCL1–derived leukemia cells reactive with the autoantigen phosphatidylcholine (PtC). PtC is a membrane phospholipid that is exposed on the surface of senescent or apoptotic cells and is recognized by the leukemic BCR in up to 30% of spontaneously arising Eμ-TCL1 leukemias.[15,33,34] Stimulation of PtC-binding leukemia cells with PtC liposomes resulted in significant induction of CDKN1A and CDKN2B (Figure 1D). In addition, the cell-cycle inhibitor CDKN2A, which lies

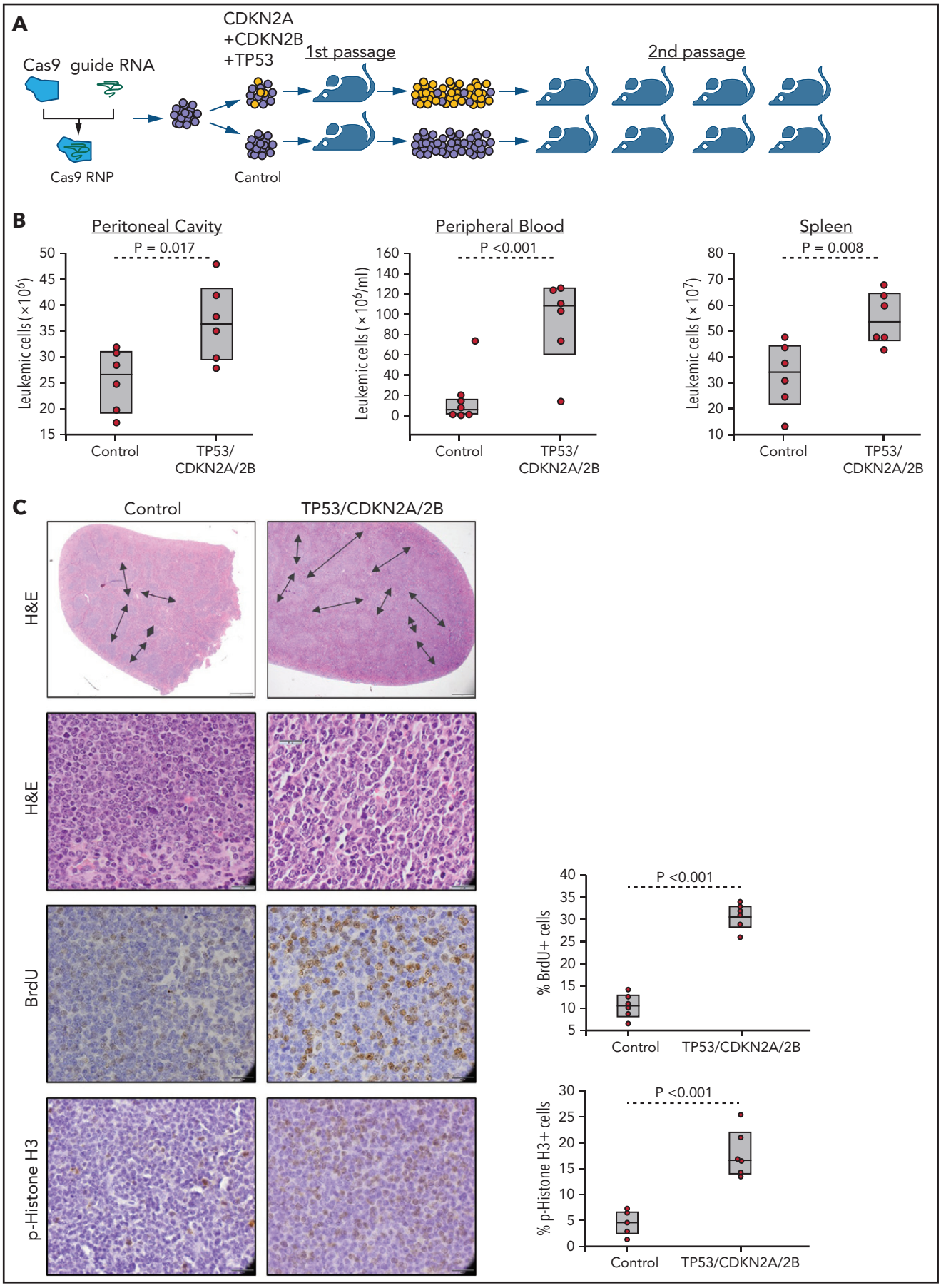
A
Cas9 guide RNA
Cas9 RNP
CDKN2A
+CDKN2B
+TP53
Cantrol
1st passage
2nd passage
B
Peritoneal Cavity
P = 0.017
Leukemic cells (×10^6)
Control
TP53/
CDKN2A/2B
Peripheral Blood
P <0.001
Leukemic cells (×10^6/ml)
Spleen
P = 0.008
Leukemic cells (×10^7)
C
Control
TP53/CDKN2A/2B
H&E
H&E
BrdU
p-Histone H3
P <0.001
% BrdU+ cells
P <0.001
% p-Histone H3+ cells

Figure 2.

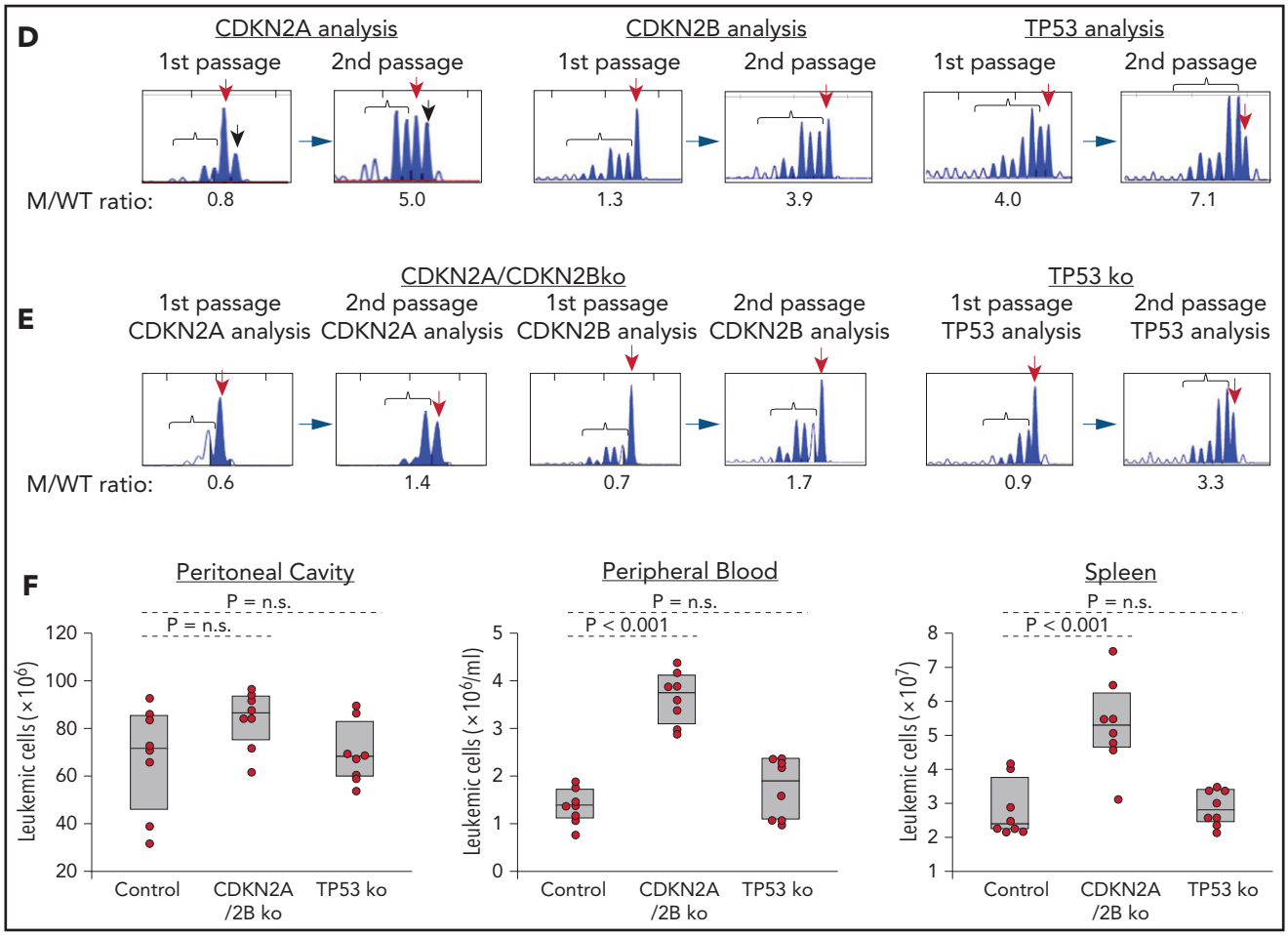

Figure 2. Combined CDKN2A, CDKN2B, and TP53 disruption accelerates tumor growth in the Eμ-TCL1 adoptive transfer model. (A) Schematic representation of the CRISPR/Cas9 procedure to target the CDKN2A, CDKN2B, and TP53 genes in primary Eμ-TCL1–derived murine CLL cells. (B) Box plots with data points showing absolute numbers of $CD5^+/CD19^+$ leukemia cells in peritoneal cavity, peripheral blood, and spleen of mice at 21 days after receiving CDKN2A/2B/TP53-targeted or control leukemia cells (n = 6 mice per group). Statistical analysis was performed using the Student *t* test. (C) Hematoxylin-and-eosin (H&E) staining and immunohistochemistry analysis of proliferating $BrdU^+$ and phosphohistone $H3^+$ cells in spleens of mice 21 days after receiving CDKN2A/2B/TP53-targeted or control leukemia cells. Images were captured with an Olympus BX53 microscope using an Olympus UC90 camera and CellSens Entry software. Statistical analysis was performed using the Student *t* test. Top row: scale bars, 500 μm; rows 2-4: scale bars, 20 μm. (D) Indel analysis by amplicon capillary electrophoresis of CDKN2A/2B/TP53-targeted leukemia cells isolated from spleens of mice after the first and second passage. Wild-type alleles are indicated by a red arrow; mutant alleles are indicated by a black arrow or brackets. The mutant/wild-type (M/WT) ratio was calculated by dividing the sum of the peak areas of the mutant alleles with the peak area of the wild-type allele. (E) Amplicon capillary electrophoresis analysis of indels in CDKN2A, CDKN2B, and TP53 in leukemia cells with independent targeting of CDKN2A/2B or TP53. (F) Box plots with data points showing absolute numbers of $CD5^+/CD19^+$ leukemia cells in peritoneal cavity, peripheral blood, and spleen of mice injected with CDKN2A/2B-targeted, TP53-targeted, or control leukemia cells (n = 8 mice per group).

adjacent to CDKN2B on chromosome 9p21, was also induced in these experiments.

The finding that the cell-cycle inhibitors CDKN1A, CDKN2A, and CDKN2B are induced upon BCR engagement suggested that upregulation of these proteins could represent a mechanism to prevent the proliferation of antigen-stimulated CLL cells in the absence of costimulatory signals. On the other hand, the fact that these genes are often directly or indirectly inactivated in RS because of deletions involving the CDKN2A/2B locus (>30% of cases) and mutations or deletions the CDKN1A transcriptional activator TP53 (>50% of cases) suggested that genetic defects in these genes may contribute to CLL progression by allowing for costimulatory signal-independent proliferation. To further explore this possibility, we simultaneously targeted CDKN2A, CDKN2B, and TP53 in 1 Eμ-TCL1–derived leukemia expressing an anti-PtC BCR (TCL1-355). Targeting of CDKN2A, CDKN2B, and TP53 was performed by nucleofection-mediated delivery of RNP complexes containing recombinant Cas9 and a pool of guide RNAs (Figure 2A). The targeted and control cells were then expanded in immunodeficient NSG mice and were subsequently transferred in syngeneic recipients to evaluate the effects of CDKN2A/2B/TP53 knockdown on leukemia growth and proliferation. Combined targeting of CDKN2A, CDKN2B, and TP53 resulted in accelerated leukemia growth, as evidenced by the significantly higher number of leukemic cells in the peritoneal cavity, peripheral blood, and spleen of mice that received Cas9-edited vs control TCL1-355 leukemia cells (Figure 2B). The spleens of mice with Cas9-edited tumors showed morphological changes consistent with Richter transformation, including more diffuse infiltration, larger and more pleomorphic cells, a larger percentage of cells with macronucleoli and a significantly higher percentage of

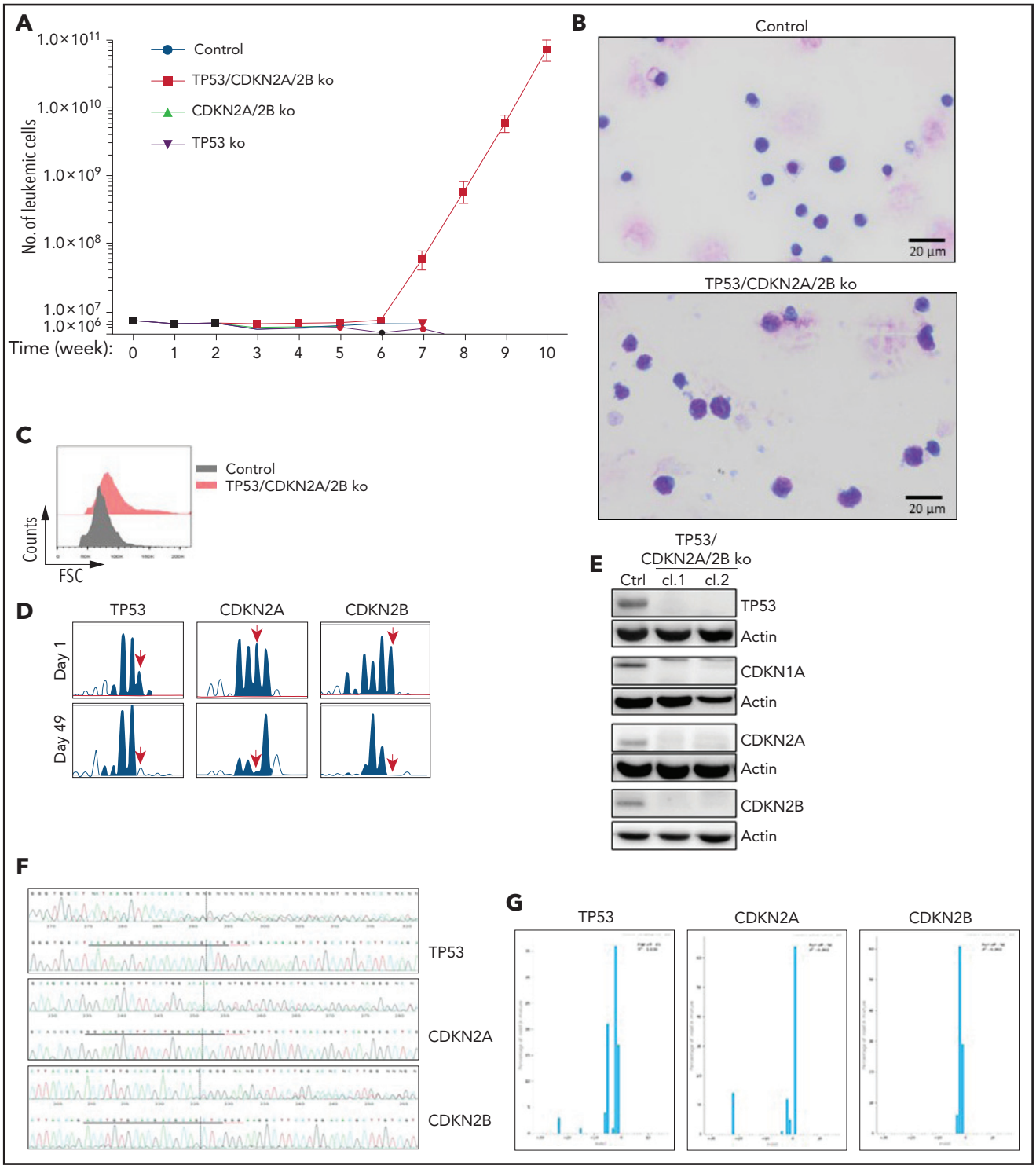

Figure 3. Eμ-TCL1 leukemia cells with biallelic loss of CDKN2A, CDKN2B, and TP53 proliferate spontaneously in vitro. (A) Absolute number of viable CDKN2A/2B/TP53-targeted, CDKN2A/2B-targeted, TP53-targeted, or control TCL1-355 leukemia cells at different time points in culture. A total of 5×10^6 leukemia cells of each genotype were isolated from spleens of corresponding mice and placed in culture. The number of viable cells was calculated by evaluating the ratio of the percentage of propidium iodide (PI)-negative cells out of the total number of cells. Each data point represents an average of 5 independent experiments with CDKN2A/2B/TP53-targeted and 3 independent experiments with CDKN2A/2B-targeted, TP53-targeted, and control leukemia cells. (B) May-Grünwald-Giemsa staining of control TCL1-355 leukemia cells and TCL1-355 leukemia cells with biallelic CDKN2A/2B/TP53 disruption. Scale bars, 20 μm. (C) Forward scatter (FSC) analysis of control TCL1-355 leukemia cells and TCL1-355 leukemia cells with biallelic CDKN2A/2B/TP53 disruption. (D) Indel analysis by amplicon capillary electrophoresis of CDKN2A/2B/TP53-targeted leukemia cells at day 1 and day 49 in culture. The position of the wild-type allele is indicated by a red arrow. (E) Immunoblotting analysis of TP53, CDKN1A, CDKN2A, and CDKN2B protein expression in 2 different clones of spontaneously proliferating TCL1-355 leukemia cells with biallelic CDKN2A/2B/TP53 disruption. (F) Alignment of mutant and wild-type nucleotide sequences (upper and lower panel, respectively) of the Cas9-targeted region using the Inference of CRISPR Edits (ICE) software tool. Analysis was performed on TP53/CDKN2A/2B-ko leukemia cells collected after 7 weeks in culture. (G) Analysis of the percentage of individual indels in the whole population using the ICE software tool. Wild-type allele corresponds to position 0 and is absent in all 3 panels.

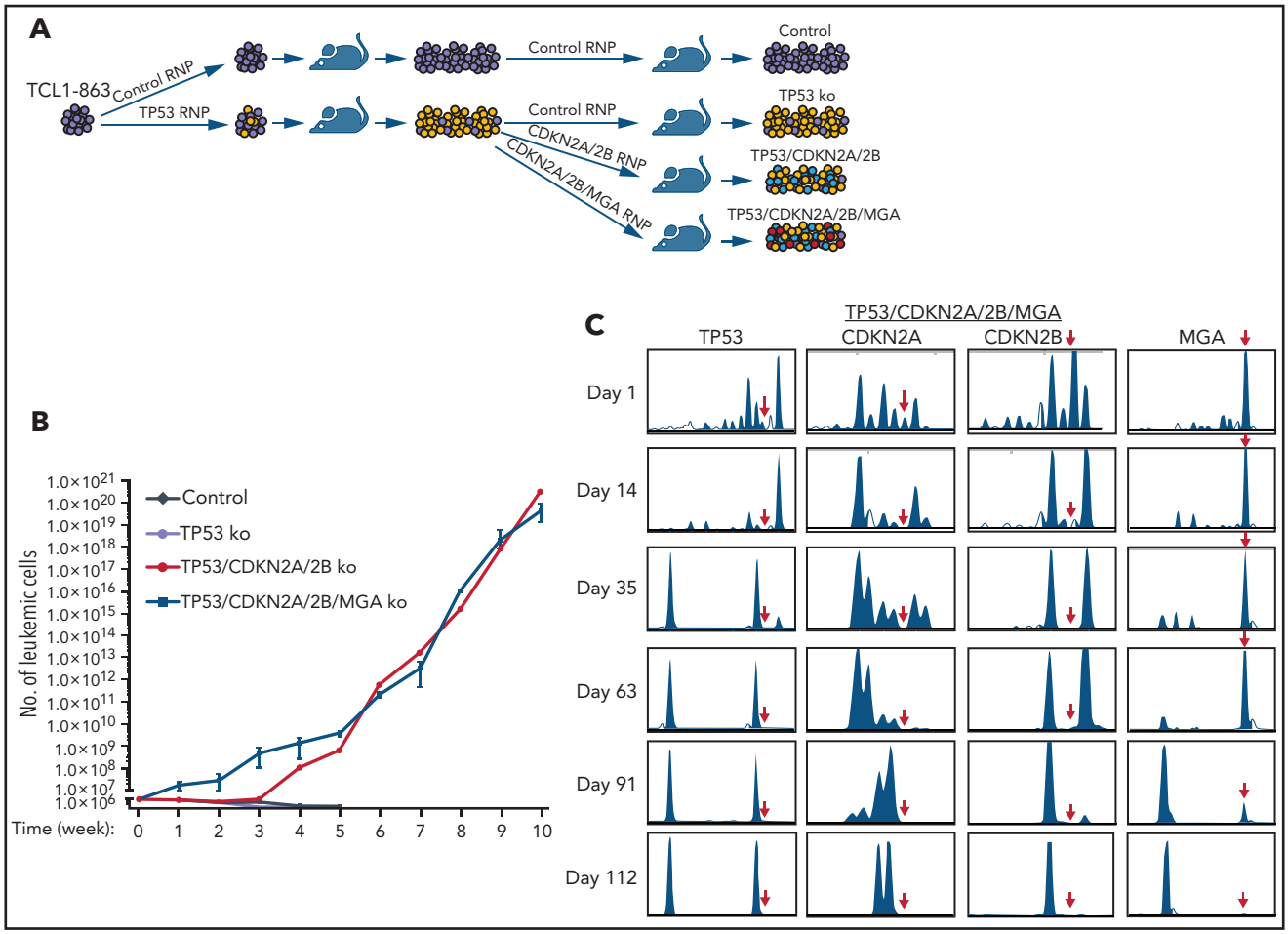

Figure 4. In vitro growth of Eμ-TCL1 leukemia cells with combined disruption of TP53, CDKN2A, CDKN2B, and MGA. (A) Schematic representation of the CRISPR/Cas9 procedure to target the TP53, CDKN2A, CDKN2B, and MGA genes in TCL1-863 leukemia cells. (B) Absolute number of viable TCL1-863 cells with TP53-targeted, TP53/CDKN2A/2B-targeted, TP53/CDKN2A/2B/MGA-targeted, or control TCL1-355 leukemia cells at different time points in culture. Each data point represents an average of 3 technical replicates. (C) Indel analysis by amplicon capillary electrophoresis of TP53/CDKN2A/2B/MGA-targeted leukemia cells at different time points in culture. The position of the wild-type allele is indicated by a red arrow.

proliferating 5-bromo-2′-deoxyuridine-positive ($BrdU^+$) or phosphohistone $H3^+$ cells (Figure 2C). Moreover, indel analysis by amplicon capillary electrophoresis of Cas9-edited cells showed an increase in the ratio of CDKN2A, CDKN2B, and TP53 mutant vs wild-type alleles during in vivo propagation, further suggesting that cells with combined TP53/CDKN2A/2B deficiency have a growth advantage compared with wild-type CLL cells (Figure 2D). A separate experiment with independent knockdown of CDKN2A/2B and TP53 also revealed selection of the mutant alleles during in vivo propagation, although only CDKN2A/2B knockdown resulted in a significant increase in tumor burden (Figure 2E-F).

To investigate whether cells with combined CDKN2A/2B/TP53 deficiency are capable of spontaneous proliferation, we analyzed in vitro the growth of control, CDKN2A/2B-, TP53- and TP53/CDKN2A/2B-targeted leukemia cells, each isolated from spleens of 3 different mice. The percentage of viable leukemic cells dropped by 70% to 95% within the first week of culture in each of the 4 genotypes, but a small percentage of leukemic cells remained viable during the subsequent 4 to 5 weeks. Strikingly, starting from the sixth week of culture, the number of TP53/CDKN2A/2B-targeted cells started to increase (Figure 3A). By this time all of the control, CDKN2A/2B-, and TP53-targeted cells had died. The cells that started to proliferate were larger than the control TCL1-355 cells and displayed pleomorphic features (Figure 3B-C). Importantly, amplicon capillary electrophoresis showed complete disappearance of the wild-type CDKN2A, CDKN2B, and TP53 alleles in these cells, suggesting that biallelic loss of all 3 genes is required for spontaneous growth in vitro (Figure 3D). Consistent with this finding, immunoblotting analysis revealed no detectable expression of TP53, CDKN1A, CDKN2A, and CDKN2B protein in the spontaneously proliferating cells (Figure 3E). Nucleotide sequencing of the CRISPR/Cas9-targeted region further confirmed that both alleles of TP53, CDKN2A, and CDKN2B had been inactivated (Figure 3F-G).

To more accurately model the temporal occurrence of genetic lesions in TP53 and CDKN2A/2B during Richter transformation, an independent experiment was performed using another Eμ-TCL1 leukemia line with an anti-PtC BCR (TCL1-863). In this experiment, the leukemia cells were first transfected with the TP53 Cas9-RNP complex, and after 1 round of in vivo expansion were transfected with the pool of CDKN2A/2B Cas9-RNP complexes (Figure 4A). Because cases of RS with CDKN2A/2B/TP53 lesions have frequently co-occurring MYC abnormalities, such as

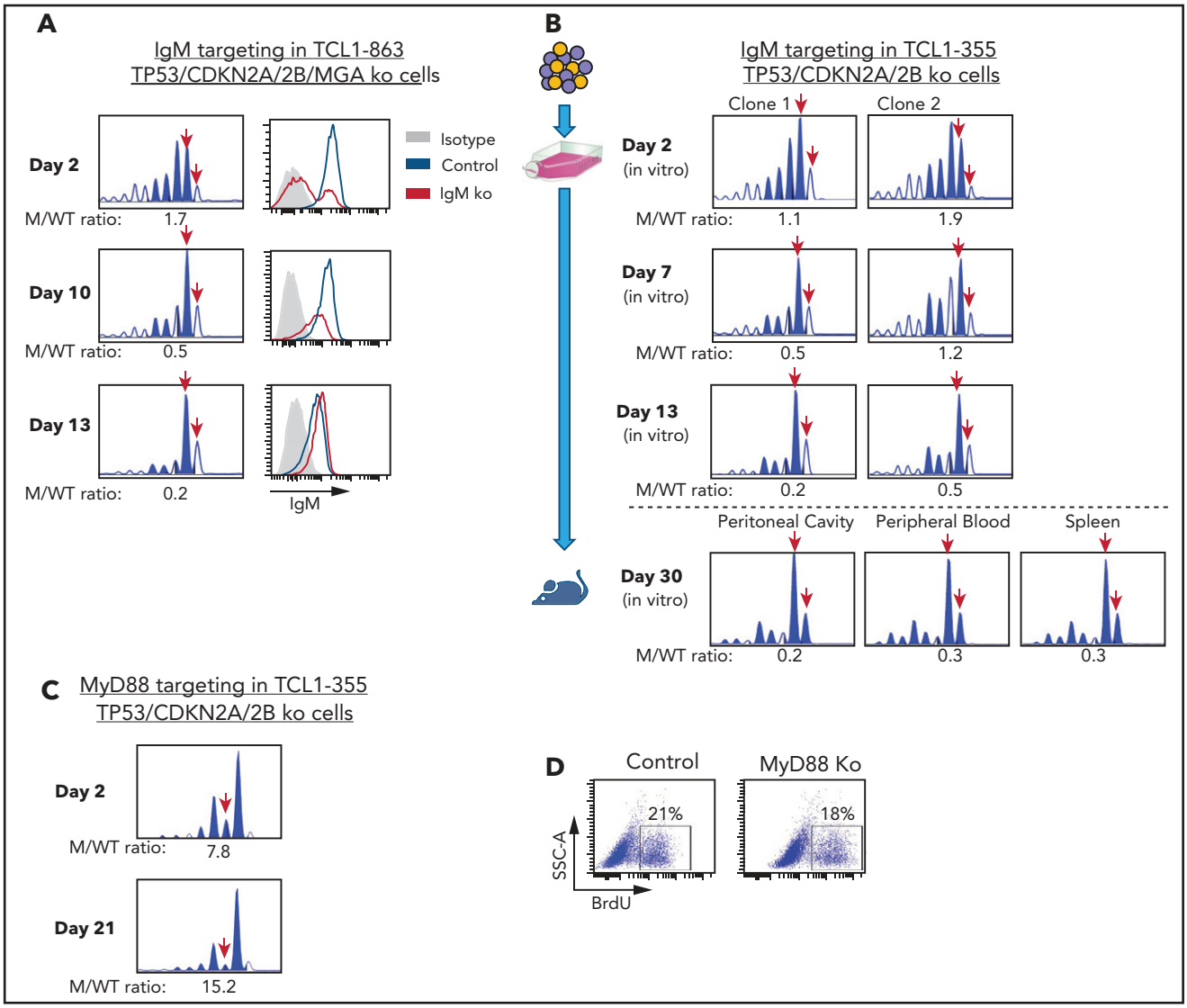

Figure 5. Effects of IgM or MyD88 targeting on growth of TP53/CDKN2A/2B-ko cells. (A) Time-course analysis of changes in IgM mutant vs wild-type allele ratio and surface IgM expression in TCL1-863 TP53/CDKN2A/2B/MGA-ko cells. The presence of 2 bands corresponding to the wild-type IgM heavy chain constant region gene (red arrows) is a result of the occasional nontemplated addition of a nucleotide at the 3′ end of PCR-amplified products by the Taq DNA polymerase.[60] (B) Changes in IgM mutant vs wild-type allele ratio in TCL1-355 TP53/CDKN2A/2B-ko cells grown in vitro or in vivo. Cells were transfected with the RNP complex targeting the IgM heavy chain constant region gene and placed in culture. After 48 hours, cells were split and continued to be grown in vitro or were injected in the peritoneal cavity of an NSG mouse that was euthanized 28 days later. One of 2 experiments with identical results is shown. (C) Time-course analysis of changes in MyD88 mutant vs wild-type allele ratio in TCL1-355 TP53/CDKN2A/2B-ko cells. (D) BrdU-incorporation analysis of TCL1-355 TP53/CDKN2A/2B-ko cells with wild-type or mutated MyD88. Analysis was performed on cells collected 21 days after transfection with the MyD88 or control RNP complex.

amplification of MYC or deletion of the MYC antagonists MGA or MNT,[24,25,35,36] the TP53-targeted cells were transfected in parallel with a pool of CDKN2A/2B/MGA Cas9 RNP complexes. The resulting TP53/CDKN2A/2B- and TP53/CDKN2A/2B/MGA-targeted cells, as well as control and TP53-targeted TCL1-863 leukemia cells, were expanded in syngeneic recipients and analyzed for spontaneous growth in vitro. In accordance with the previous experiment, the control and TP53-targeted cells died within a few weeks in culture, whereas the TP53/CDKN2A/2B- and TP53/CDKN2A/2B/MGA-targeted cells started to spontaneously proliferate (Figure 4B). The spontaneously proliferating cells showed biallelic loss of TP53, CDKN2A, and CDKN2B, whereas MGA was disrupted in only a minor proportion of cells (Figure 4C; supplemental Figures 2-5). However, cells with biallelic loss of MGA were selected after prolonged culture, suggesting that this genetic lesion provides a growth advantage but is not required for spontaneous proliferation.

To investigate whether biallelic loss of TP53, CDKN2A, and CDKN2B can induce spontaneous proliferation of leukemia cells with a different BCR specificity, a separate experiment was performed using a previously established Eμ-TCL1 leukemia (TCL1-699) expressing a transgenic BCR reactive with the Smith (Sm) autoantigen.[11] Targeting TP53, CDKN2A, and CDKN2B in these cells also resulted in the establishment of spontaneously proliferating leukemia cells with biallelic loss of all 3 genes (supplemental Figure 6). Importantly, whole-exome sequencing of the TCL1-355, TCL1-863, and TCL1-699 TP53/CDKN2A/2B knockout (ko)

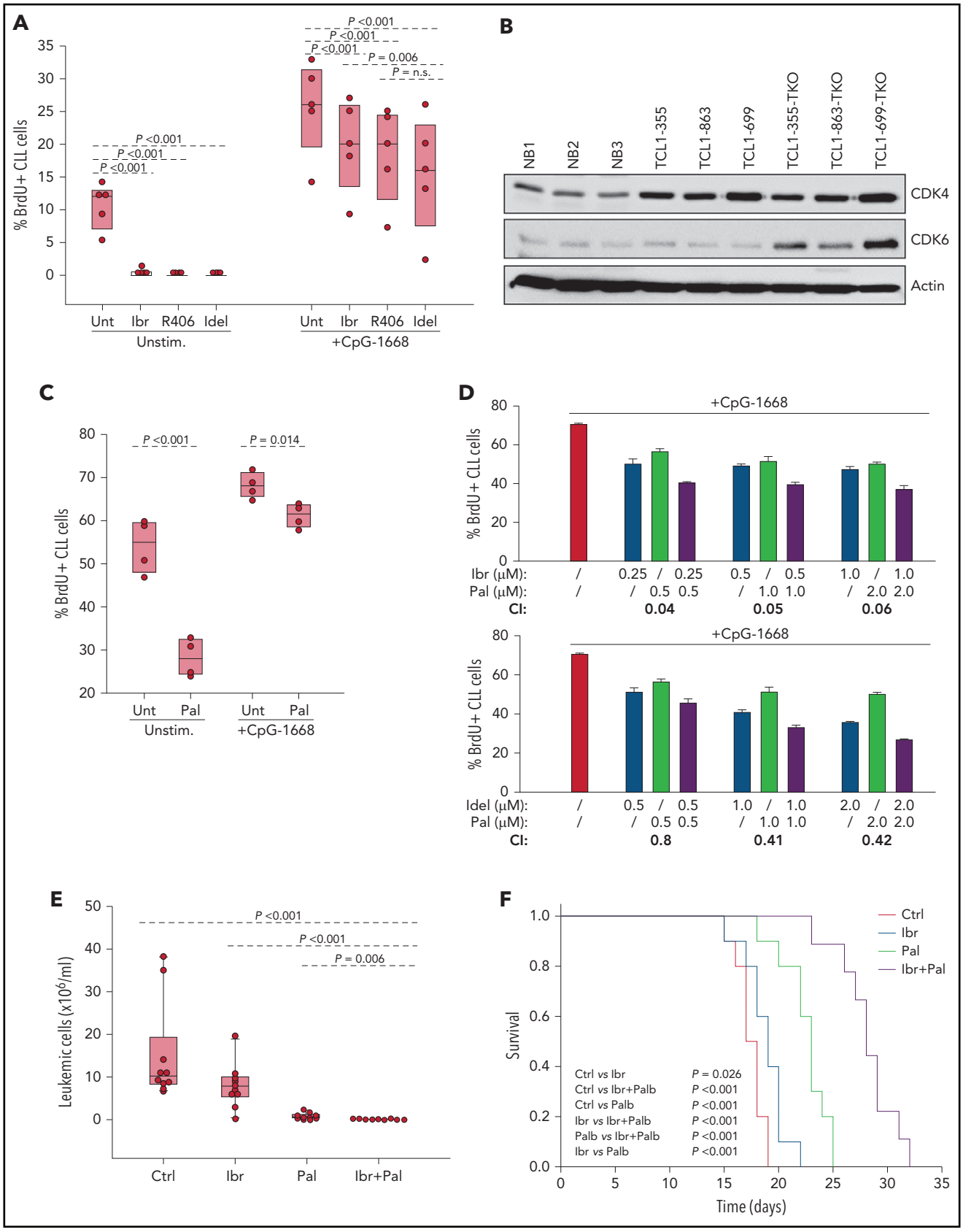
A
% BrdU+ CLL cells
P <0.001
P <0.001
P <0.001
P <0.001
P <0.001
P = 0.006
P = n.s.
Unt Ibr R406 Idel
Unstim.
Unt Ibr R406 Idel
+CpG-1668
B
NB1 NB2 NB3 TCL1-355 TCL1-863 TCL1-699 TCL1-355-TKO TCL1-863-TKO TCL1-699-TKO
CDK4
CDK6
Actin
C
% BrdU+ CLL cells
P <0.001
P = 0.014
Unt Pal
Unstim.
Unt Pal
+CpG-1668
D
+CpG-1668
% BrdU+ CLL cells
Ibr (μM): / 0.25 / 0.25 0.5 / 0.5 1.0 / 1.0
Pal (μM): / / 0.5 0.5 / 1.0 1.0 / 2.0 2.0
CI: 0.04 0.05 0.06
+CpG-1668
% BrdU+ CLL cells
Idel (μM): / 0.5 / 0.5 1.0 / 1.0 2.0 / 2.0
Pal (μM): / / 0.5 0.5 / 1.0 1.0 / 2.0 2.0
CI: 0.8 0.41 0.42
E
Leukemic cells (x10⁶/ml)
P <0.001
P <0.001
P = 0.006
Ctrl Ibr Pal Ibr+Pal
F
Survival
Time (days)
Ctrl
Ibr
Pal
Ibr+Pal
Ctrl vs Ibr P = 0.026
Ctrl vs Ibr+Palb P <0.001
Ctrl vs Palb P <0.001
Ibr vs Ibr+Palb P <0.001
Palb vs Ibr+Palb P <0.001
Ibr vs Palb P <0.001

Figure 6.

leukemias and their wild-type counterparts did not identify any additional shared acquired mutations in the CRISPR/Cas9-edited leukemic clones, excluding the possibility that spontaneous proliferation of these cells is caused by off-target mutations introduced during CRISPR/Cas9 editing (supplemental Table 5).

To determine the impact of biallelic TP53/CDKN2A/2B deficiency on leukemia behavior in vivo, wild-type and TP53/CDKN2A/2B-ko TCL1-355, TCL1-863, and TCL1-699 cells were adoptively transferred by intraperitoneal injection in C57BL/6-recipient mice. In all cases, mice that received TP53/CDKN2A/2B-ko cells had significantly shorter survival compared with controls (supplemental Figure 7). Interestingly, mice that received TCL1-699 TP53/CDKN2A/2B-ko cells had almost no circulating leukemia cells and much smaller spleens than their wild-type counterparts but instead developed large intraperitoneal tumors (supplemental Figure 8). The TP53/CDKN2A/2B-ko tumors were characterized by larger cells with less condensed chromatin and a larger percentage of $BrdU^+$ or phosphohistone $H3^+$ cells compared with their wild-type counterparts (supplemental Figures 9-11). Flow cytometry analysis did not reveal any immunophenotypic differences between the TP53/CDKN2A/2B-ko and wild-type tumors (supplemental Figure 12).

TP53/CDKN2A/2B-ko cells require BCR signals for proliferation

The previous experiments showed that biallelic loss of TP53, CDKN2A, and CDKN2B overcomes the need for costimulatory signals in driving proliferation of Eμ-TCL1 leukemia cells in vitro, but did not prove that this proliferation is BCR dependent. To further address this issue, we targeted the IgM constant region gene by CRISPR/Cas9 in TCL1-863 leukemia cells with biallelic TP53/CDKN2A/2B deficiency (Figure 5A). An editing efficiency of ∽60% was observed by indel analysis, consistent with the detection of a similar proportion of surface IgM^- cells by flow cytometry. The surface IgM^- cells became undetectable within 10 days of culture and were outgrown by cells with retained surface IgM expression. In parallel, a reduction in the ratio of IgM mutant vs wild-type alleles was observed. A small proportion of indels remained detectable even after prolonged culture, presumably reflecting the presence of cells with monoallelic IgM disruption and normal surface IgM expression. A separate experiment using 2 different TCL1-355 leukemia clones with TP53/CDKN2A/2B deficiency showed identical results (Figure 5B). Transfer of these cells in NSG mice showed that cells with a disrupted IgM heavy chain gene are also negatively selected in vivo (Figure 5B).

To exclude the possibility that in vitro the leukemic cells receive costimulatory proliferation signals from TLR ligands released in the culture medium by apoptotic cells, such as the TLR9 ligand DNA, we targeted by CRISPR/Cas9 the TLR adaptor protein MyD88. In contrast to cells with IgM disruption, cells with MyD88 knockdown were not negatively selected and proliferated at the same rate as cells with wild-type MyD88 (Figure 5C-D). Considering that T-cell–derived costimulatory signals are not present in the culture conditions, these experiments further establish that proliferation of Eμ-TCL1 leukemia cells with biallelic TP53/CDKN2A/2B deficiency is BCR dependent and costimulatory signal independent.

TP53/CDKN2A/2B-ko cells are sensitive to BCR-inhibitor treatment

The finding that cells with combined TP53/CDKN2A/2B deficiency require BCR expression indicated that they should be sensitive to treatment with a BCR inhibitor. To evaluate this possibility further, TCL1-355 TP53/CDKN2A/2B-ko cells were treated in vitro with the BTK inhibitor ibrutinib, the phosphatidylinositol 3-kinase δ inhibitor idelalisib, or the SYK inhibitor R406 (active substance of the drug fostamatinib). BrdU incorporation experiments showed almost complete growth inhibition, further suggesting that proliferation of these cells is dependent on BCR signals (Figure 6A).

To investigate how BCR inhibitors affect the growth of CDKN2A/2B/TP53-ko cells exposed to other proliferative stimuli, BrdU incorporation experiments were performed with cells stimulated with the TLR9 ligand CpG-1668 (Figure 6A). Stimulation with CpG-1668 resulted in an increase in the percentage of $BrdU^+$ cells that was only partially inhibited by treatment with ibrutinib, idelalisib, or R406. Considering that CDKN2A/2B/TP53 disruption results in cell-cycle dysregulation, we investigated the activity of palbociclib, a US Food and Drug Administration (FDA)-approved inhibitor of the kinases CDK4 and CDK6, both of which were found to be overexpressed in the CDKN2A/2B/TP53-ko leukemia compared with normal B cells (Figure 6B). Palbociclib inhibited the proliferation of unstimulated CDKN2A/2B/TP53-ko cells but was only modestly effective against CpG-1668–stimulated cells (Figure 6C). However, combining palbociclib with ibrutinib or idelalisib resulted in significantly greater inhibition of leukemic cell proliferation compared with each agent alone and displayed a combination index consistent with a synergistic effect (Figure 6D).

To compare in vivo the activity of the single and combination treatments, we treated 4 groups of mice with adoptively

Figure 6. Evaluation of activity of BCR and CDK4/6 inhibitors against Eμ-TCL1 leukemia cells with combined TP53/CDKN2A/2B deficiency. (A) Effects of ibrutinib, R406, and idelalisib on proliferation of unstimulated or CpG-stimulated TCL1-355 leukemia cells with biallelic TP53/CDKN2A/2B disruption. Cells were cultured for 6 hours with BrdU prior to harvesting for flow cytometry analysis. All inhibitors were used at 1 μM concentration. Statistical analysis was performed using 1-way repeated measures analysis of variance (ANOVA) with the Holm-Šidak test for multiple comparisons. (B) Immunoblotting analysis of CDK4 and CDK6 protein expression in 3 normal splenic B-cell samples (NB1-NB3), the 3 CDKN2A/2B/TP53-ko leukemias (TCL1-355-TKO, TCL1-863-TKO, and TCL1-699-TKO), and their non-CDKN2A/2B/TP53–aberrated counterparts (TCL1-355, TCL1-863, TCL1-699). (C) Effects of palbociclib (Pal.) on proliferation of unstimulated or CpG-stimulated TCL1-355 leukemia cells with biallelic TP53/CDKN2A/2B disruption. Cells were cultured with BrdU for 20 hours prior to harvesting. Statistical analysis was performed using the paired Student *t* test. (D) Analysis of effects of palbociclib in combination with ibrutinib or idelalisib on proliferation of CpG-stimulated TCL1-355 leukemia cells with biallelic TP53/CDKN2A/2B disruption. The combination index (CI) was calculated using CompuSyn software (Paramus, NJ) according to the Chou-Talalay method.[61] Mean values from 3 technical replicates were used in the equation. CI values below 1.0 indicate synergistic activity. (E) A total of 1×10^7 TCL1-355 TP53/CDKN2A/2B-ko cells were engrafted in C57BL/6 mice via intraperitoneal injection and randomly assigned to each of the 4 experimental cohorts. Treatment with palbociclib, ibrutinib, or palbociclib plus ibrutinib was started 3 days later. The number of leukemic cells in peripheral blood after 10 days of treatment is shown. (F) Survival analysis of mice treated with palbociclib, ibrutinib, or palbociclib plus ibrutinib. The x-axis indicates days from adoptive transfer. Survival curves were estimated using the Kaplan-Meier method and curve differences among groups were assessed using the log-rank test and the Holm-Šidak method for multiple comparisons. Ibr, ibrutinib; Idel, idelalisib; Unt, untreated.

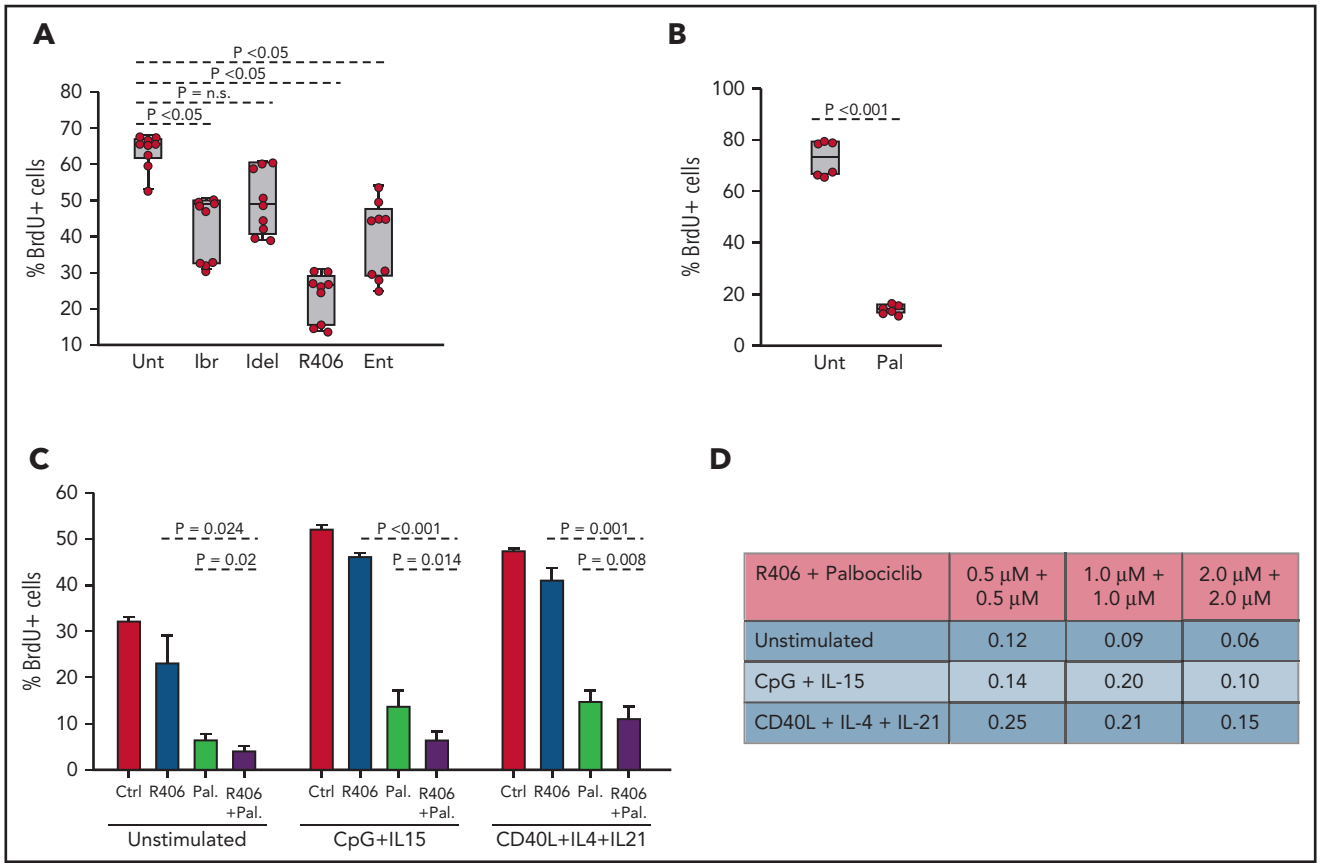

R406 + Palbociclib	0.5 μM + 0.5 μM	1.0 μM + 1.0 μM	2.0 μM + 2.0 μM
Unstimulated	0.12	0.09	0.06
CpG + IL-15	0.14	0.20	0.10
CD40L + IL-4 + IL-21	0.25	0.21	0.15

Figure 7. Effects of BCR inhibitors and palbociclib on the proliferation of human RS cells. (A) Effects of BCR inhibitors on spontaneous proliferation of RS9737 cells after 48 hours in culture. All inhibitors were used at 1 μM concentration. Three independent experiments, each with 3 technical replicates, were performed. Statistical analysis was performed using 1-way repeated measures ANOVA with the post hoc Tukey test. (B) Effects of palbociclib (1 μM) on spontaneous proliferation of RS9737 cells after 48 hours in culture. Statistical analysis was performed using the paired Student *t* test. (C) Analysis of activity of R406 and palbociclib, alone or in combination, against unstimulated and CpG plus IL15 or CD40L plus IL4 plus IL21 stimulated RS9737 cells. (D) Analysis of CI for R406 plus palbociclib against RS9737 cells. The CI was calculated as described in Figure 6D.

transferred CDKN2A/2B/TP53-deficient leukemia cells (n = 10 per group) with palbociclib, ibrutinib, palbociclib plus ibrutinib or vehicle for a period of 3 weeks. Analysis of peripheral blood samples after 10 days of treatment showed significantly lower numbers of leukemic cells in mice treated with palbociclib plus ibrutinib compared with any other treatment group (Figure 6E). Consistent with this finding, survival of mice receiving combination treatment was significantly improved compared with control mice or mice receiving single-agent treatment (Figure 6F).

BCR signals induce proliferation of human TP53/CDKN2A/2B-deficient RS cells

To validate these findings in a human setting, we took advantage of 2 recently established RS patient-derived xenografts.[37] The RS9737 tumor has biallelic inactivation of TP53 and deletion of the genomic region encompassing CDKN2A and CDKN2B, whereas the RS1316 tumor has wild-type TP53 and CDKN2A/2B, but carries trisomy 12 and mutations in KRAS, MED12, and NOTCH2. Both tumors can be propagated in vivo using immunodeficient NSG mice but not in vitro because of spontaneous cell death by apoptosis.[37]

To investigate whether combined TP53 and CDKN2A/2B abnormalities allow for costimulatory signal-independent proliferation of human RS cells, RS9737 and RS1316 tumors were isolated from immunodeficient NSG mice, placed in culture, and analyzed by the BrdU-incorporation assay. Analysis of RS9737 cells showed spontaneous ex vivo proliferation until 96 hours, after which time point the cells started rapidly dying (supplemental Figure 13A). The percentage of proliferating RS9737 cells increased following stimulation with immobilized anti-IgM, suggesting that BCR stimulation alone is sufficient to induce proliferation of these cells. In contrast, RS1316 cells did not proliferate ex vivo and were not induced to proliferate by BCR stimulation, although they were induced to proliferate by stimulation with CpG plus IL-15 or CD40L plus IL-4 plus IL-21, stimuli that also increased the percentage of proliferating RS9737 cells (supplemental Figure 13B-C).

To determine whether the spontaneous ex vivo proliferation of RS9737 cells is BCR driven, BrdU-incorporation analysis was performed after 48-hour culture with ibrutinib, idelalisib, R406, or the SYK inhibitor entospletinib (Figure 7A). Treatment with R406, ibrutinib, or entospletinib significantly inhibited the proliferation of the malignant cells, with R406 displaying greatest inhibition. Palbociclib also significantly inhibited the proliferation of the malignant cells (Figure 7B) and demonstrated synergistic activity in combination with R406 (Figure 7C-D). This combination also displayed synergistic activity against CpG-2006 plus IL-15 or

CD40L plus IL-4 plus IL-21 stimulated cells, suggesting that the combination of a BCR and CDK4/6 inhibitor could be effective against RS tumors exposed to other microenvironmental proliferation signals.

Discussion

The rapid inhibition of CLL cell proliferation in patients treated with a BCR inhibitor and the absence of a proliferative response upon BCR engagement in vitro have raised questions regarding the role of the BCR in regulating CLL cell proliferation. We now show that BCR stimulation of human and murine CLL cells induces the expression of the positive regulators MYC, CCND1, CCND2, and CDK4, which are required for cell-cycle entry, but simultaneously induces the expression of the negative regulators CDKN1A, CDKN2A and CDKN2B, which block subsequent cell-cycle progression. We further show that combined deficiency of these negative regulators, as occurs in approximately one-quarter of RS tumors, leads to more aggressive disease in vivo and spontaneous proliferation in vitro that is BCR dependent but independent of costimulatory signals. Together, these data provide evidence that BCR signals are directly involved in regulating CLL cell proliferation and reveal a mechanism through which frequently co-occurring genetic lesions in TP53 and CDKN2A/2B contribute to Richter transformation.

Progression through the G1 phase and entry in the S phase of the cell cycle is regulated by a complex interplay between different cyclins, cyclin-dependent kinases (CDKs) and CDK inhibitors. The limiting enzymes for G_1-phase progression are CDK4 and CDK6, which are activated by the D-type cyclins CCND1, CCND2, and CCND3 and inhibited by the CDK inhibitors CDKN1A, CDKN1B, CDKN2A, and CDKN2B.[38] The levels of expression of these cell-cycle regulators are determined by various extracellular signals, which depending upon the stage of differentiation and the strength, duration, and timing of the signal can induce S-phase entry, reversion to quiescence, or trigger apoptosis. Previous studies have shown that BCR engagement induces the expression of several positive regulators of the cell cycle in human and murine B cells, including CCND1, CCND2, and CDK4.[21-23,38] In addition, studies in immature murine B cells have shown that BCR stimulation can also induce the negative cell-cycle regulators CDKN1A and CDKN1B.[39] In our study, CDKN1B was not identified as differentially expressed following BCR stimulation, but upregulation of CDKN1A and CDKN2B was observed in human BCR-stimulated CLL cells and CDKN1A, CDKN2A, and CDKN2B in murine BCR-stimulated CLL cells. These findings suggest that enhanced expression of CDK inhibitors could be a common mechanism to prevent cell-cycle progression of B cells that have been stimulated through the BCR but have not received a costimulatory signal.

In the case of CLL B cells, this block in proliferation can be bypassed by costimulatory signals provided by TLR or CD40 stimulation, which have been shown to induce the expression of CCND3 and downregulate CDKN1B,[40-43] thus shifting the balance in favor of positive cell-cycle regulators. The data presented in this study show that another mechanism to bypass this block is inactivating lesions in CDKN2A/2B and TP53, which have been reported in 1.7% and 17.7% of unselected CLL cases[44] and 30% and 50% of RS cases,[24,25] respectively. By preventing the induction of CDKN1A, CDKN2A, and CDKN2B, these lesions can substitute for costimulatory signals from the microenvironment and allow for BCR-dependent/costimulatory signal-independent proliferation of autoreactive B cells. Consistent with this possibility, expression of stereotyped BCRs characterized by broad autoreactivity has been associated with a greater risk for Richter transformation.[45,46]

One important feature of RS is the rapid and discordant growth of the malignant cells in localized lymph node or extranodal sites.[26] Interestingly, this feature was observed only with the TP53/CDKN2A/2B-ko tumors expressing the anti-Sm BCR but not with the tumors expressing an anti-PtC BCR. An important difference between these BCRs that was revealed in a previous study by our group is the stronger autonomous activity of the anti-Sm BCR.[11] Considering that integrin-mediated cell adhesion is regulated by BCR signals,[47,48] it is plausible to hypothesize that the more sustained nature of the BCR signal in the anti-Sm tumors may account for their greater local growth and retention. Studies are ongoing to further address this possibility and more precisely define the role of BCR-triggered integrin activation during Richter transformation.

Eμ-TCL1–transgenic mice have been used to establish several other RS models in recent years. In particular, Eμ-TCL1–transgenic mice overexpressing activated AKT,[49] activated NOTCH1,[49] or MYC[50] have been reported to develop aggressive lymphomas with diffuse large B-cell lymphoma morphology, although in the latter model the aggressive lymphomas were shown to be derived from B cells at an earlier maturation stage. In addition, aggressive lymphomas with RS features have been reported to develop in Eμ-TCL1 mice with B-cell–specific ablation of NFAT2 (typically characterized by downregulation of CDKN2A and TP53)[51] and rarely (<15% of cases) in Eμ-TCL1 mice with B-cell–specific TP53 deficiency.[52] Our model differs from these models in the simultaneous introduction of multiple RS-associated genetic lesions in already established leukemia cells, thus more accurately recapitulating the pattern of genetic evolution leading from CLL to RS and allowing evaluation of the combined vs individual role of these lesions during transformation. The model can be further improved by introducing the RS-associated lesions in murine leukemias with human CLL-specific genetic defects, and efforts toward that goal are ongoing in our laboratory.

Despite advances in CLL treatment, RS continues to be an area with urgent unmet clinical need.[53] RS patients typically have poor response to chemotherapy and poor overall survival, and this is particularly the case of patients with TP53 and CDKN2A/2B abnormalities.[25,54] The finding of this study that tumors with such abnormalities remain BCR dependent suggests that BCR inhibitors could be active in this subset of patients. In line with this possibility, clinical responses have been reported in chemotherapy-refractory RS patients treated with ibrutinib, idelalisib, or the more selective BTK inhibitor acalabrutinib, although typically of short duration.[55-57] Our data suggest that the activity of these drugs could be improved by combining them with a CDK4/6 inhibitor, such as palbociclib. Importantly, palbociclib has already been tested in combination with ibrutinib in a phase 1 clinical trial of relapsed/refractory mantle cell lymphoma, demonstrating good tolerability, a high response rate (67%; complete response, 37%) and durable responses (2-year response duration, 70%).[58] Together, these studies also provide the rationale to

explore this combination in patients with RS and possibly other B-cell malignancies with an activated BCR pathway and combined TP53/CDKN2A/2B abnormalities, such as de novo diffuse large B-cell lymphoma.[59]

Acknowledgments

This work was supported by the Associazione Italiana per la Ricerca sul Cancro (AIRC, Projects IG 2016, Id. 19236 and IG 2020, Id. 24566, P.I, Efremov Dimitar) and the Italian Ministry of Health (Progetto Ricerca Finalizzata PE-2016-02362756).

Authorship

Contribution: S.C. and D.G.E. designed the study and wrote the manuscript; S.C., C.M., F.P., I.F., A.B., M.D., and R.F. performed the experiments; B.S.Y. and S.P. performed the bioinformatic analysis; A.Z. performed the histopathological analysis; I.I., T.V., S.D., A.J.D., and L.L. provided vital reagents, patient specimens, and/or supervised certain experiments; and all authors analyzed data and reviewed and approved the final version of the manuscript.

Conflict-of-interest disclosure: The authors declare no competing financial interests.

ORCID profiles: C.M., 0000-0001-7136-7174; F.P., 0000-0002-6612-3068; A.B., 0000-0002-3634-6527; S.P., 0000-0002-7156-5434; B.S.Y., 0000-0002-3095-3369; S.D., 0000-0003-0632-5036; A.Z., 0000-0001-6203-7966; L.L., 0000-0002-8327-1396; D.G.E., 0000-0001-9081-5462.

Correspondence: Dimitar G. Efremov, Molecular Hematology Unit, International Center for Genetic Engineering and Biotechnology, Padriciano 99, 34149 Trieste, Italy; e-mail: efremov@icgeb.org.

Footnotes

Submitted 17 July 2020; accepted 6 March 2021; prepublished online on *Blood* First Edition 28 April 2021. DOI 10.1182/blood.2020008276.

Presented in abstract form at the 62nd American Society of Hematology (ASH) Annual Meeting and Exposition, Virtual, 7 December 2020.

The data reported in this article have been deposited in the Sequence Read Archive database (accession number PRJNA708156).

For original data, please contact efremov@icgeb.org.

The online version of this article contains a data supplement.

There is a *Blood* Commentary on this article in this issue.

The publication costs of this article were defrayed in part by page charge payment. Therefore, and solely to indicate this fact, this article is hereby marked "advertisement" in accordance with 18 USC section 1734

REFERENCES

1. Kipps TJ, Stevenson FK, Wu CJ, et al. Chronic lymphocytic leukaemia [published correction appears in *Nat Rev Dis Primers*. 2017;3:17008]. *Nat Rev Dis Primers*. 2017;3:16096.
2. Bosch F, Dalla-Favera R. Chronic lymphocytic leukaemia: from genetics to treatment. *Nat Rev Clin Oncol*. 2019;16(11):684-701.
3. Chiorazzi N, Efremov DG. Chronic lymphocytic leukemia: a tale of one or two signals? *Cell Res*. 2013;23(2):182-185.
4. Messmer BT, Albesiano E, Efremov DG, et al. Multiple distinct sets of stereotyped antigen receptors indicate a role for antigen in promoting chronic lymphocytic leukemia. *J Exp Med*. 2004;200(4):519-525.
5. Agathangelidis A, Darzentas N, Hadzidimitriou A, et al. Stereotyped B-cell receptors in one-third of chronic lymphocytic leukemia: a molecular classification with implications for targeted therapies. *Blood*. 2012;119(19):4467-4475.
6. Damle RN, Wasil T, Fais F, et al. Ig V gene mutation status and CD38 expression as novel prognostic indicators in chronic lymphocytic leukemia. *Blood*. 1999;94(6):1840-1847.
7. Hamblin TJ, Davis Z, Gardiner A, Oscier DG, Stevenson FK. Unmutated Ig V(H) genes are associated with a more aggressive form of chronic lymphocytic leukemia. *Blood*. 1999;94(6):1848-1854.
8. Herishanu Y, Pérez-Galán P, Liu D, et al. The lymph node microenvironment promotes B-cell receptor signaling, NF-kappaB activation, and tumor proliferation in chronic lymphocytic leukemia. *Blood*. 2011;117(2):563-574.
9. Efremov DG, Laurenti L. The Syk kinase as a therapeutic target in leukemia and lymphoma. *Expert Opin Investig Drugs*. 2011;20(5):623-636.
10. Burger JA, Wiestner A. Targeting B cell receptor signalling in cancer: preclinical and clinical advances. *Nat Rev Cancer*. 2018;18(3):148-167.
11. Iacovelli S, Hug E, Bennardo S, et al. Two types of BCR interactions are positively selected during leukemia development in the Eμ-TCL1 transgenic mouse model of CLL. *Blood*. 2015;125(10):1578-1588.
12. Jahrsdörfer B, Jox R, Mühlenhoff L, et al. Modulation of malignant B cell activation and apoptosis by bcl-2 antisense ODN and immunostimulatory CpG ODN. *J Leukoc Biol*. 2002;72(1):83-92.
13. Pascutti MF, Jak M, Tromp JM, et al. IL-21 and CD40L signals from autologous T cells can induce antigen-independent proliferation of CLL cells. *Blood*. 2013;122(17):3010-3019.
14. Schleiss C, Ilias W, Tahar O, et al. BCR-associated factors driving chronic lymphocytic leukemia cells proliferation ex vivo. *Sci Rep*. 2019;9(1):701.
15. Suljagic M, Longo PG, Bennardo S, et al. The Syk inhibitor fostamatinib disodium (R788) inhibits tumor growth in the Eμ-TCL1 transgenic mouse model of CLL by blocking antigen-dependent B-cell receptor signaling. *Blood*. 2010;116(23):4894-4905.
16. Herman SE, Barr PM, McAuley EM, Liu D, Wiestner A, Friedberg JW. Fostamatinib inhibits B-cell receptor signaling, cellular activation and tumor proliferation in patients with relapsed and refractory chronic lymphocytic leukemia. *Leukemia*. 2013;27(8):1769-1773.
17. Herman SE, Mustafa RZ, Gyamfi JA, et al. Ibrutinib inhibits BCR and NF-κB signaling and reduces tumor proliferation in tissue-resident cells of patients with CLL. *Blood*. 2014;123(21):3286-3295.
18. Chen SS, Chang BY, Chang S, et al. BTK inhibition results in impaired CXCR4 chemokine receptor surface expression, signaling and function in chronic lymphocytic leukemia. *Leukemia*. 2016;30(4):833-843.
19. Niemann CU, Mora-Jensen HI, Dadashian EL, et al. Combined BTK and PI3Kδ inhibition with acalabrutinib and ACP-319 improves survival and tumor control in CLL mouse model. *Clin Cancer Res*. 2017;23(19):5814-5823.
20. Burger JA, Li KW, Keating MJ, et al. Leukemia cell proliferation and death in chronic lymphocytic leukemia patients on therapy with the BTK inhibitor ibrutinib. *JCI Insight*. 2017;2(2):e89904.
21. Deglesne PA, Chevallier N, Letestu R, et al. Survival response to B-cell receptor ligation is restricted to progressive chronic lymphocytic leukemia cells irrespective of Zap70 expression. *Cancer Res*. 2006;66(14):7158-7166.
22. Guarini A, Chiaretti S, Tavolaro S, et al. BCR ligation induced by IgM stimulation results in gene expression and functional changes only in IgV H unmutated chronic lymphocytic leukemia (CLL) cells. *Blood*. 2008;112(3):782-792.
23. Krysov S, Dias S, Paterson A, et al. Surface IgM stimulation induces MEK1/2-dependent MYC expression in chronic lymphocytic leukemia cells. *Blood*. 2012;119(1):170-179.
24. Fabbri G, Khiabanian H, Holmes AB, et al. Genetic lesions associated with chronic lymphocytic leukemia transformation to Richter syndrome. *J Exp Med*. 2013;210(11):2273-2288.

25. Chigrinova E, Rinaldi A, Kwee I, et al. Two main genetic pathways lead to the transformation of chronic lymphocytic leukemia to Richter syndrome. *Blood.* 2013; 122(15):2673-2682.

26. Rossi D, Spina V, Gaidano G. Biology and treatment of Richter syndrome. *Blood.* 2018; 131(25):2761-2772.

27. Bojarczuk K, Sasi BK, Gobessi S, et al. BCR signaling inhibitors differ in their ability to overcome Mcl-1-mediated resistance of CLL B cells to ABT-199. *Blood.* 2016;127(25): 3192-3201.

28. Yang Z, Steentoft C, Hauge C, et al. Fast and sensitive detection of indels induced by precise gene targeting. *Nucleic Acids Res.* 2015;43(9):e59.

29. Ouyang Z, Wang S, Zeng M, et al. Therapeutic effect of palbociclib in chondrosarcoma: implication of cyclin-dependent kinase 4 as a potential target. *Cell Commun Signal.* 2019; 17(1):17.

30. Uras IZ, Walter GJ, Scheicher R, et al. Palbociclib treatment of FLT3-ITD+ AML cells uncovers a kinase-dependent transcriptional regulation of FLT3 and PIM1 by CDK6. *Blood.* 2016;127(23):2890-2902.

31. Sasi BK, Martines C, Xerxa E, et al. Inhibition of SYK or BTK augments venetoclax sensitivity in SHP1-negative/BCL-2-positive diffuse large B-cell lymphoma. *Leukemia.* 2019;33(10): 2416-2428.

32. Dal Bo M, D'Agaro T, Gobessi S, et al. The SIRT1/TP53 axis is activated upon B-cell receptor triggering via miR-132 up-regulation in chronic lymphocytic leukemia cells. *Oncotarget.* 2015;6(22):19102-19117.

33. Yan XJ, Albesiano E, Zanesi N, et al. B cell receptors in TCL1 transgenic mice resemble those of aggressive, treatment-resistant human chronic lymphocytic leukemia. *Proc Natl Acad Sci USA.* 2006;103(31):11713-11718.

34. Chen SS, Batliwalla F, Holodick NE, et al. Autoantigen can promote progression to a more aggressive TCL1 leukemia by selecting variants with enhanced B-cell receptor signaling. *Proc Natl Acad Sci USA.* 2013;110(16): E1500-E1507.

35. De Paoli L, Cerri M, Monti S, et al. MGA, a suppressor of MYC, is recurrently inactivated in high risk chronic lymphocytic leukemia. *Leuk Lymphoma.* 2013;54(5):1087-1090.

36. Edelmann J, Holzmann K, Tausch E, et al. Genomic alterations in high-risk chronic lymphocytic leukemia frequently affect cell cycle key regulators and NOTCH1-regulated transcription. *Haematologica.* 2020;105(5):1379-1390.

37. Vaisitti T, Braggio E, Allan JN, et al. Novel Richter syndrome xenograft models to study genetic architecture, biology, and therapy responses. *Cancer Res.* 2018;78(13):3413-3420.

38. Piatelli M, Tanguay D, Rothstein T, Chiles T. Cell cycle control mechanisms in B-1 and B-2 lymphoid subsets. *Immunol Res.* 2003;27(1): 31-52.

39. Qi CF, Martensson A, Mattioli M, Dalla-Favera R, Lobanenkov VV, Morse HC III. CTCF functions as a critical regulator of cell-cycle arrest and death after ligation of the B cell receptor on immature B cells. *Proc Natl Acad Sci USA.* 2003;100(2):633-638.

40. Lam EW, Glassford J, Banerji L, Thomas NS, Sicinski P, Klaus GG. Cyclin D3 compensates for loss of cyclin D2 in mouse B-lymphocytes activated via the antigen receptor and CD40. *J Biol Chem.* 2000;275(5):3479-3484.

41. Grdisa M. Influence of CD40 ligation on survival and apoptosis of B-CLL cells in vitro. *Leuk Res.* 2003;27(10):951-956.

42. Longo PG, Laurenti L, Gobessi S, et al. The Akt signaling pathway determines the different proliferative capacity of chronic lymphocytic leukemia B-cells from patients with progressive and stable disease. *Leukemia.* 2007;21(1):110-120.

43. Bomben R, Gobessi S, Dal Bo M, et al. The miR-17∼92 family regulates the response to Toll-like receptor 9 triggering of CLL cells with unmutated IGHV genes. *Leukemia.* 2012;26(7):1584-1593.

44. Leeksma AC, Baliakas P, Moysiadis T, et al. Genomic arrays identify high-risk chronic lymphocytic leukemia with genomic complexity: a multi-center study. *Haematologica.* 2021;106(1):87-97.

45. Rossi D, Spina V, Bomben R, et al. Association between molecular lesions and specific B-cell receptor subsets in chronic lymphocytic leukemia. *Blood.* 2013;121(24):4902-4905.

46. Gounari M, Ntoufa S, Apollonio B, et al. Excessive antigen reactivity may underlie the clinical aggressiveness of chronic lymphocytic leukemia stereotyped subset #8. *Blood.* 2015; 125(23):3580-3587.

47. Spaargaren M, Beuling EA, Rurup ML, et al. The B cell antigen receptor controls integrin activity through Btk and PLCgamma2. *J Exp Med.* 2003;198(10):1539-1550.

48. Tissino E, Benedetti D, Herman SEM, et al. Functional and clinical relevance of VLA-4 (CD49d/CD29) in ibrutinib-treated chronic lymphocytic leukemia. *J Exp Med.* 2018;215(2): 681-697.

49. Kohlhaas V, Blakemore SJ, Al-Maarri M, et al. Active AKT signaling triggers CLL towards Richter's transformation via over-activation of Notch1. *Blood.* 2021;137(5):646-660.

50. Lucas F, Rogers KA, Harrington BK, et al. Eμ-TCL1xMyc: a novel mouse model for concurrent CLL and B-cell Lymphoma. *Clin Cancer Res.* 2019;25(20):6260-6273.

51. Märklin M, Heitmann JS, Fuchs AR, et al. NFAT2 is a critical regulator of the anergic phenotype in chronic lymphocytic leukaemia. *Nat Commun.* 2017;8(1):755.

52. Knittel G, Rehkämper T, Korovkina D, et al. Two mouse models reveal an actionable PARP1 dependence in aggressive chronic lymphocytic leukemia. *Nat Commun.* 2017;8(1):153.

53. Ding W. Richter transformation in the era of novel agents. *Hematology Am Soc Hematol Educ Program.* 2018;2018:256-263.

54. Rossi D, Spina V, Deambrogi C, et al. The genetics of Richter syndrome reveals disease heterogeneity and predicts survival after transformation. *Blood.* 2011;117(12):3391-3401.

55. Tsang M, Shanafelt TD, Call TG, et al. The efficacy of ibrutinib in the treatment of Richter syndrome. *Blood.* 2015;125(10):1676-1678.

56. Visentin A, Imbergamo S, Scomazzon E, et al. BCR kinase inhibitors, idelalisib and ibrutinib, are active and effective in Richter syndrome. *Br J Haematol.* 2019;185(1):193-197.

57. Hillmen P, Schuh A, Eyre TA, et al. Acalabrutinib monotherapy in patients with Richter transformation from the phase 1/2 ACE-CL-001 clinical study [abstract]. *Blood.* 2016;128(22):60.

58. Martin P, Bartlett NL, Blum KA, et al. A phase 1 trial of ibrutinib plus palbociclib in previously treated mantle cell lymphoma [published correction appears in *Blood.* 2019;134(11):908]. *Blood.* 2019;133(11): 1201-1204.

59. Chapuy B, Stewart C, Dunford AJ, et al. Molecular subtypes of diffuse large B cell lymphoma are associated with distinct pathogenic mechanisms and outcomes [published corrections appear in *Nat Med.* 2018;24(8):1292 and *Nat Med.* 2018;24(8):1290–1291]. *Nat Med.* 2018;24(5): 679-690.

60. Magnuson VL, Ally DS, Nylund SJ, et al. Substrate nucleotide-determined non-templated addition of adenine by Taq DNA polymerase: implications for PCR-based genotyping and cloning. *Biotechniques.* 1996; 21(4):700-709.

61. Chou TC. Drug combination studies and their synergy quantification using the Chou-Talalay method. *Cancer Res.* 2010;70(2):440-446.

blood®
Regular Article

LYMPHOID NEOPLASIA

Macrophage- and BCR-derived but not TLR-derived signals support the growth of CLL and Richter syndrome murine models in vivo

Claudio Martines,[1] Supriya Chakraborty,[1] Marija Vujovikj,[2] Stefania Gobessi,[1] Tiziana Vaisitti,[3] Silvia Deaglio,[3] Luca Laurenti,[4] Aleksandar J. Dimovski,[2] and Dimitar G. Efremov[1]

[1]Molecular Hematology Unit, International Center for Genetic Engineering and Biotechnology, Trieste, Italy; [2]Research Center for Genetic Engineering and Biotechnology, Macedonian Academy of Sciences and Arts, Skopje, North Macedonia; [3]Functional Genomics Unit, Department of Medical Sciences, University of Turin, Turin, Italy; and [4]Department of Hematology, Catholic University of the Sacred Heart, Gemelli University Hospital, Rome, Italy

KEY POINTS

- Human Richter syndrome and murine CLL cells receive growth-promoting signals from B-cell receptor but not from Toll-like receptors in vivo.
- Depletion of macrophages results in reduced growth of murine CLL and human Richter syndrome cells in vivo.

A large amount of circumstantial evidence has accumulated suggesting that Toll-like receptor (TLR) signals are involved in driving chronic lymphocytic leukemia (CLL) cell proliferation, but direct in vivo evidence for this is still lacking. We have now further addressed this possibility by pharmacologically inhibiting or genetically inactivating the TLR pathway in murine CLL and human Richter syndrome (RS) patient-derived xenograft (PDX) cells. Surprisingly, we show that pharmacologic inhibition of TLR signaling by treatment with an IRAK1/4 inhibitor delays the growth of the transplanted malignant cells in recipient mice, but genetic inactivation of the same pathway by CRISPR/Cas9-mediated disruption of *IRAK4* or its proximal adaptor *MyD88* has no effect. We further show that treatment with the IRAK1/4 inhibitor results in depletion of macrophages and demonstrate that these cells can support the survival and enhance the proliferation of both murine Eμ-TCL1 leukemia and human RS cells. We also show that genetic disruption of the B-cell receptor (BCR) by CRISPR/Cas9 editing of the immunoglobulin M constant region gene inhibits the growth of human RS-PDX cells in vivo, consistent with our previous finding with murine Eμ-TCL1 leukemia cells. Finally, we show that genetic disruption of *IRAK4* does not result in negative selection of human CLL cell lines xenografted in immunodeficient mice. The obtained data suggest that TLR signals are unlikely to represent a major driver of CLL/RS cell proliferation and provide further evidence that signals from macrophages and the BCR promote the growth and survival of CLL and RS cells in vivo.

Introduction

B-cell receptor (BCR) signals generated by binding to external autoantigens or cell-autonomous BCR-BCR interactions play a major role in the pathogenesis of both human chronic lymphocytic leukemia (CLL) and murine models of the disease.[1-4] Such signals have been shown to provide a competitive advantage to the malignant B cells by increasing their apoptosis resistance and by promoting their homing to the lymph nodes, where they receive additional nourishing signals from the microenvironment.[5,6] However, BCR signals are unable to induce the proliferation of CLL cells on their own and require either costimulatory signals from the microenvironment or certain genetic lesions that result in loss of cell cycle control, such as inactivating genetic lesions in cell cycle inhibitors that frequently occur during Richter transformation.[7-9]

The microenvironmental signals that drive CLL cell proliferation have still not been fully characterized. In vitro, CLL cell proliferation can be induced efficiently by certain T cell– or Toll-like receptor (TLR)–derived signals, such as the combination of CD40L/IL-4/IL-21 or the TLR9 ligand CpG-DNA, respectively.[10-16] However, the extent to which such signals contribute to CLL cell proliferation in vivo is still unknown. Currently, there is substantial evidence that T cells play an important role, as CLL cells in lymph node proliferation centers are frequently seen in direct contact with CD4 T cells and display increased expression of genes that can be induced by T cell–derived stimuli.[12,17-19] Moreover, experiments in immunodeficient NOD/SCID/Il2Rγ^{null} (NSG) mice have shown that activated autologous CD4 T cells are required for the engraftment and expansion of xenografted human CLL cells, further suggesting that T cells provide proliferative signals in vivo.[20,21]

Evidence for a role of TLR signals in driving CLL cell proliferation is more scarce and mainly includes data from gene expression profiling studies showing enrichment of TLR9-target genes in the proliferating lymph node compartment.[22,23] Such enrichment is more prominent in CLL cells belonging to the IGHV-unmutated CLL (U-CLL) subset, which typically show a greater proliferative response upon stimulation with CpG-unmethylated DNA in vitro.[23-25] This CLL subset is also characterized by frequent reactivity of the leukemic BCRs with DNA or DNA-associated autoantigens, which could allow CLL cells to internalize DNA-containing complexes and activate the endosomally located TLR9.[26-28] Additional support for a possible role for TLR9 signaling in CLL pathogenesis is provided by recent studies showing that apoptotic cells and CpG-unmethylated cell–free DNA are commonly present in lymphoid tissues and plasma of patients with CLL and that cell-free plasma DNA levels positively correlate with a more aggressive clinical course.[29,30]

In addition to signals from the microenvironment, the TLR pathway can be activated in a small proportion of CLL cases (2%-4%) by an L265P mutation in the adaptor protein MyD88. This adaptor protein interacts with activated TLRs to form a signaling complex that recruits the kinases IRAK4 and IRAK1, which then activate several downstream effector pathways.[28] The MyD88 L265P mutation, which is also found in 95% of Waldenström macroglobulinemia (WM) and 30% of activated B-cell diffuse large B-cell lymphoma (ABC DLBCL) cases, increases the oligomerization propensity of the MyD88 TIR domain, resulting in TLR ligand–independent recruitment and activation of IRAK4.[31] The pathogenic role of this mutation in WM and ABC DLBCL has been further supported by studies showing that IRAK1/4 inhibitors suppress the growth of WM and ABC DLBCL cell lines that carry the mutation but have no effect on the growth of cells with wild-type MyD88.[32,33]

Two recent studies showed that IRAK4 inhibitors can also reduce the viability and proliferation of CpG-DNA–stimulated human CLL cells in vitro and delay the growth of murine Eμ-TCL1 CLL cells in vivo, further suggesting that the TLR pathway is involved in the pathogenesis of CLL and could represent a potential therapeutic target in this disease.[34,35] In addition, the BTK inhibitor ibrutinib has been shown to inhibit CpG-DNA–induced proliferation of CLL cells in vitro, indicating that part of the clinical activity of this drug could result from inhibition of TLR signaling.[23,36,37]

To further explore the relevance of the TLR pathway as a potential therapeutic target, we compared the effects of pharmacologic inhibition and genetic disruption of TLR signaling on the growth of murine Eμ-TCL1 CLL and patient-derived Richter syndrome (RS) cells transplanted in syngeneic or immunodeficient mice, respectively. Genetic disruption of the BCR was performed in parallel experiments in the human RS cells to compare the relevance of the 2 pathways in the same in vivo setting. We show that in contrast to genetic disruption of BCR signaling, disruption of TLR signaling does not negatively affect the expansion of the malignant cells. In addition, we show that IRAK4 inhibitor treatment in these in vivo models results in macrophage depletion with consequent deprivation of the malignant cells from macrophage-derived growth and survival signals, thus providing a potential explanation for the therapeutic activity of IRAK4 inhibitors in human and murine models of CLL and RS.

Materials and methods

CRISPR/Cas9 editing of murine CLL and human RS cells

Approval for the use of samples from CLL patients was obtained from the Institutional Review Board committee at the Catholic University Hospital (14563/15), whereas approval for the animal studies was obtained from the Italian Ministry of Health (no. 347/2017-PR).

CRISPR/Cas9-editing of murine Eμ-TCL1 leukemia cells was done as recently described.[9] Briefly, cells were thawed and cultured in RPMI-1640 supplemented with 10% heat-inactivated fetal bovine serum, 100 U/mL penicillin, 0.1 mg/mL streptomycin, 2 mM L-glutamine, 1 mM sodium pyruvate (Invitrogen), and 1 μM CpG-1668 (InvivoGen) at a concentration of 5×10^6 cells per mL for 20 hours prior to CRISPR/Cas9 editing with the Alt-R system (Integrated DNA Technologies). To generate the Cas9 ribonucleoprotein (RNP) complex that targets the *MyD88* gene, a predesigned *MyD88* cr-RNAs (1.5 μM) was combined with 1.5 μM ATTO 550-labeled tracr-RNA, 0.75 μM recombinant Cas9 protein, and 1.5 μM Alt-R Cas9 electroporation enhancer in 5 μL nuclease-free duplex buffer (all from Integrated DNA Technologies). The Cas9 RNP complex was then electroporated using the Amaxa Nucleofector II device and the Z-001 program into 6×10^6 leukemic cells resuspended in 100 μL mouse B cell Nucleofector solution (Lonza).

For CRISPR/Cas9 editing of the human RS–patient-derived xenograft (PDX) tumors, cells were thawed, cultured in the same medium as was used for the murine cells at a concentration of 5×10^6 cells per mL, and stimulated with 1 μM CpG-2006 and 25 ng/mL human IL-15 for 20 hours prior to transfection of the Cas9 RNPs using the NEPA21 Super Electroporator (Nepagene, Chiba, Japan) and the parameters from supplemental Table 1, available on the *Blood* website. Control cells were nucleofected with Cas9 RNPs without cr-RNA. Following transfection, cells were cultured for 3 days with 3T3-msCD40L fibroblasts and 25 ng/mL human IL-4 prior to injection in NSG mice. Editing efficiency was evaluated by amplicon capillary electrophoresis on a 3500 Genetic Analyzer (Applied Biosystems) of polymerase chain reaction fragments spanning the region of genomic DNA around the targeted site, as described in more detail elsewhere.[9] Cr-RNA and polymerase chain reaction primer sequences are provided in supplemental Tables 2 and 3.

In vivo experiments with murine models

All animal procedures were performed under a protocol approved by the Italian Ministry of Health (no. 347/2017-PR). CRISPR/Cas9-edited Eμ-TCL1 leukemia cells were transferred by intraperitoneal injection of 3×10^7 cells in 2- to 3-month-old NSG or C57BL/6 mice. The human RS-PDX cells were inoculated intraperitoneally (2×10^6 cells) and subcutaneously in the right flank of NSG mice (1.2×10^7 cells in 0.2 mL of a 50:50 mixture of cells and Matrigel Matrix). For the in vivo treatment experiments, C57BL/6 mice or NSG mice were fed with standard diet containing vehicle control or medicated chow containing 0.25 g/kg R221 (kindly provided by Rigel

Pharmaceuticals, Inc). Additional information is provided in the supplemental Materials and Methods.

Results

Treatment with an IRAK1/4 inhibitor delays leukemia progression in Eμ-TCL1 adoptive transfer model

To further understand the role of TLR signaling in CLL cell growth and expansion, we first tested the capacity of R191, a dual inhibitor of the kinases IRAK4 and IRAK1, to inhibit TLR signaling in murine Eμ-TCL1–derived CLL cells and human RS-PDX cells. Experiments performed with primary leukemic cells isolated from 4 different Eμ-TCL1 mice showed that R191 completely inhibited proliferation induced by the TLR ligands CpG or LPS (Figure 1A-B). Treatment with R191 also inhibited the proliferation of human RS-PDX cells induced by stimulation with CpG while having only a modest effect on proliferation induced by CD40L/IL-4/IL-21 stimulation (supplemental Figure 1). R191 was also modestly cytotoxic against unstimulated TCL1 and RS-PDX cells, whereas it was not toxic for unstimulated human CLL cells. However, CpG-stimulated or CD40L/IL-4/IL-21–stimulated human CLL cells underwent apoptosis in the presence of R191 (supplemental Figure 2).

Next, to investigate the effects of inhibition of TLR signaling with this drug in vivo, we inoculated C57BL/6 mice with primary leukemic cells isolated from 2 different Eμ-TCL1 mice (TCL1-355 and TCL1-333) and treated them with the R191 prodrug R221 or vehicle control. Analysis of leukemia cell counts showed no differences until day 20 of treatment, but a significant reduction was observed in R221-treated mice after day 35 (Figure 1C). Consistent with the delayed leukemia progression, mice treated with R221 also exhibited a significantly longer survival compared with the control mice (Figure 1D).

Genetic disruption of MyD88 does not affect the growth of adoptively transferred Eμ-TCL1 leukemia cells

In addition to inhibiting its primary targets IRAK1 and IRAK4 (IC50 of 3 nmol/L), R191 has been reported to inhibit the kinase activity of 13 other kinases by >80% at concentrations ranging from 50 nmol/L to 250 nmol/L.[38] Therefore, to determine whether the effect of R221 treatment was caused by inhibition of TLR signaling, we targeted the *MyD88* gene in the Eμ-TCL1 leukemias TCL1-355 and TCL1-333 by CRISPR/Cas9 editing (Figure 2A). Targeting of the *MyD88* gene was done by nucleofection-mediated delivery of a ribonucleoprotein complex containing recombinant Cas9 and a guide RNA against *MyD88*, resulting in an editing efficiency of 60% to >90% and a strong reduction of MyD88 protein expression (Figure 2B-C). Leukemic cells with >90% *MyD88* knockout were resistant to TLR stimulation, as evidenced by the lack of an increase in BrdU incorporation or phosphorylation of the NF-kB subunit p65 following stimulation with CpG (supplemental Figure 3).

The edited cells were injected in the peritoneal cavity of recipient mice and recovered 5 weeks later for analysis of the proportion of mutant and wild type alleles. Surprisingly, no negative selection of *MyD88*-mutant alleles was observed, suggesting that cells with a disrupted TLR signaling pathway do not have a growth disadvantage in vivo (Figure 2B). To extend these findings and exclude possible off-target effects, a separate set of experiments using another *MyD88* guide RNA and leukemia cells derived from 6 other Eμ-TCL1 transgenic mice was performed (Figure 2D). In addition, to investigate whether there is a difference in the behavior of cells from the CLL and RS phase of the disease, we included 2 recently established Eμ-TCL1–derived RS models (TCL1-355 TKO and TCL1-699 TKO).[9] The results of 17 independent experiments with the 8 Eμ-TCL1–derived CLL and 2 Eμ-TCL1–derived RS lines are summarized in Figure 2E. Comparison of the mutant allele frequency of the injected and recovered cells again showed no negative selection of cells with *MyD88*-mutant alleles in any of the 3 investigated compartments (peritoneal cavity, spleen, and peripheral blood).

Different effects of pharmacologic inhibition and genetic disruption of IRAK4 on the growth of xenografted human RS cells

The results of the previous experiments confirmed reported findings that treatment with an IRAK1/4 inhibitor delays leukemia progression in the Eμ-TCL1 model[35] but also suggested that this effect is not caused by disruption of TLR signaling in the malignant cells themselves. To validate these findings in a human setting, we repeated these experiments using 4 recently established RS-PDX models.[39,40] These RS-PDX models cannot be propagated in vitro because of spontaneous apoptosis but grow efficiently in immunodeficient NSG mice, suggesting that they receive and are responsive to microenvironmental growth and/or survival signals in vivo.

To investigate whether TLR signals are required for the growth of these cells in vivo, we first tested the activity of R221 against the xenografted RS-PDX models RS9737 and RS1316. Because the malignant cells at different anatomic sites may receive different microenvironmental signals, these cells were transplanted both intraperitoneally and subcutaneously in each mouse. After 27 days of treatment, the total number of malignant B cells was evaluated in the subcutaneous tumor, peritoneal cavity, and spleen of vehicle and R221-treated mice. Interestingly, in both experiments a significant reduction in the number of malignant B cells was observed in the subcutaneous tumor and spleen but not in the peritoneal cavity of R221-treated mice, suggesting that IRAK1/4 inhibitor treatment differently affects the growth of the malignant cells in different anatomic compartments (Figure 3A).

To determine whether these effects are caused by disruption of IRAK1/4 signaling in the malignant B cells, we targeted exon 4 of the human *IRAK4* gene by CRISPR/Cas9 and inoculated the malignant cells intraperitoneally and subcutaneously in each mouse (Figure 3B, and 3C top panels). Consistent with the previous experiments using murine Eμ-TCL1 leukemia cells, no negative selection of *IRAK4*-mutant alleles was observed in cells isolated from any of the 3 investigated anatomic compartments. A repeated experiment with 2 additional RS-PDX models (IP867/17 and RS1050) yielded identical results (Figure 3C bottom panels). Figure 3D summarizes the results of 11 independent experiments with the 4 RS-PDX models, showing no reduction in the MAF of injected cells versus those isolated from the PC, spleen, or subcutaneous tumor 4 to 5 weeks later.

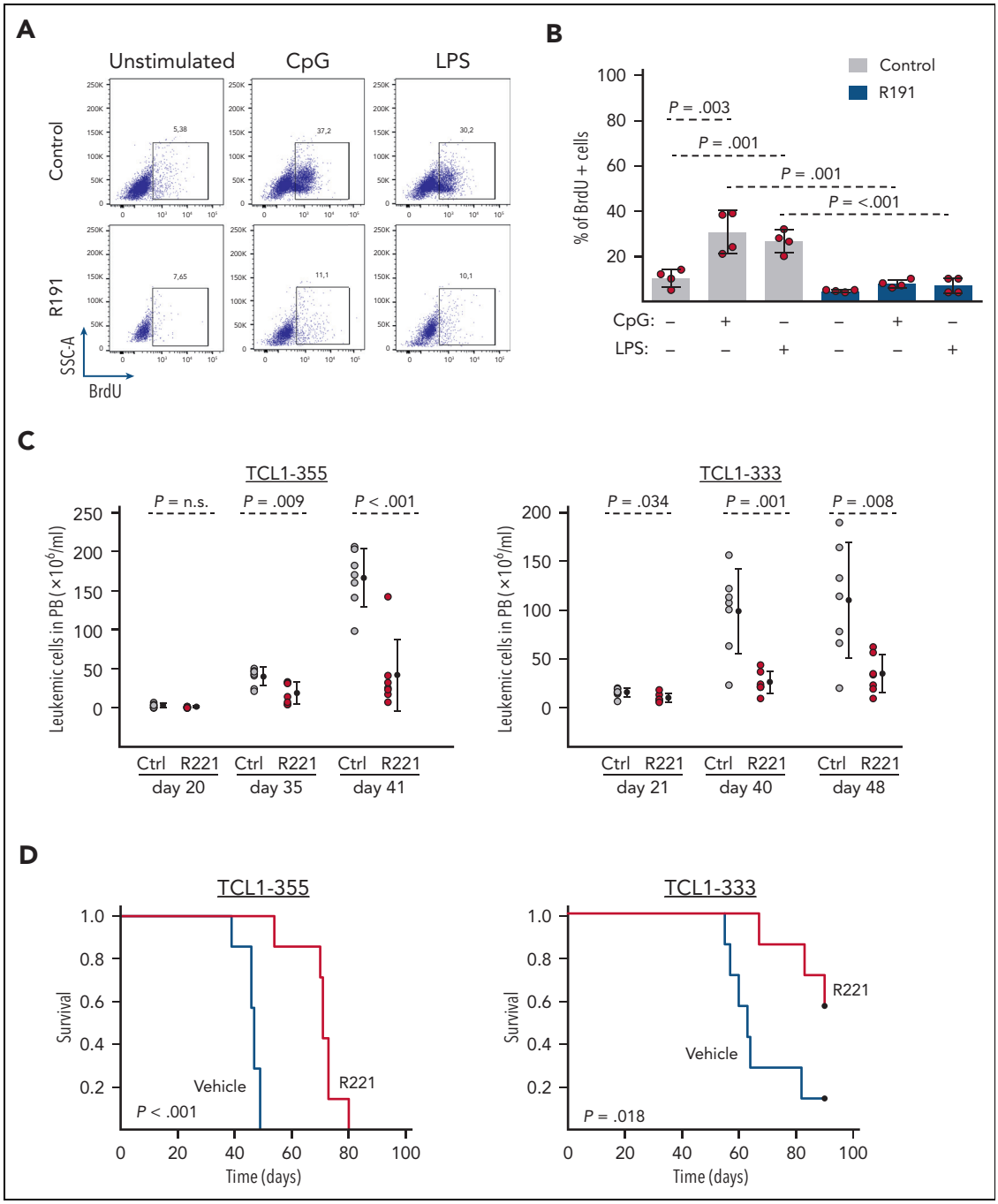

Figure 1. The IRAK1/4 inhibitor R191/R221 inhibits TLR signaling and delays the growth of murine Eμ-TCL1 CLL cells in vivo. (A-B) Effect of R191 on proliferation of TLR-stimulated Eμ-TCL1 CLL cells. The percentage of proliferating cells was determined by analysis of 5-bromo-2′-deoxyuridine (BrdU) incorporation in viable Eμ-TCL1 leukemia cells that were cultured for 28 hours in the presence or absence of CpG-1668 (1 μM), LPS (5 μg/mL), and R191 (1 μM) and then for additional 20 hours in the presence of BrdU (10 μM). One representative experiment with TCL1-333 cells is shown in panel A, and a summary of 4 experiments with CLL cells derived from 4 different Eμ-TCL1 transgenic mice is shown in panel B. Statistical analysis was done using 1-way repeated measures analysis of variance (ANOVA) with Tukey test for multiple comparisons. (C) Analysis of leukemia cell counts ($CD5^+/CD19^+$) in peripheral blood of mice inoculated with TCL1-355 or TCL1-333 leukemia cells and treated with R221 or vehicle control (n = 7 per group). Statistical analysis was done using the *t* test or Mann-Whitney test, as appropriate. (D) Survival analysis of mice treated with R221 or vehicle control. Treatment was started 3 days after tumor transfer. X-axis indicates days from tumor transfer. Survival curves were estimated using the Kaplan-Meier method, and curve differences were assessed using the log-rank test.

To further validate our experimental approach, we targeted the human immunoglobulin M (IgM) constant region gene (*IGHM*) in RS9737, RS1316, IP867/17, and RS1050 cells and investigated changes in MAF following in vivo propagation. In contrast with the *IRAK4*-knockout experiments, we observed a significant reduction in the proportion of mutant *IGHM* alleles in all 3 investigated compartments, which was accompanied with selective loss of leukemic cells lacking surface IgM expression (Figure 4). A separate set of experiments using another *IGHM* guide RNA yielded identical results, providing further evidence that RS cells depend on BCR signals for their growth and/or survival (supplemental Figure 4).

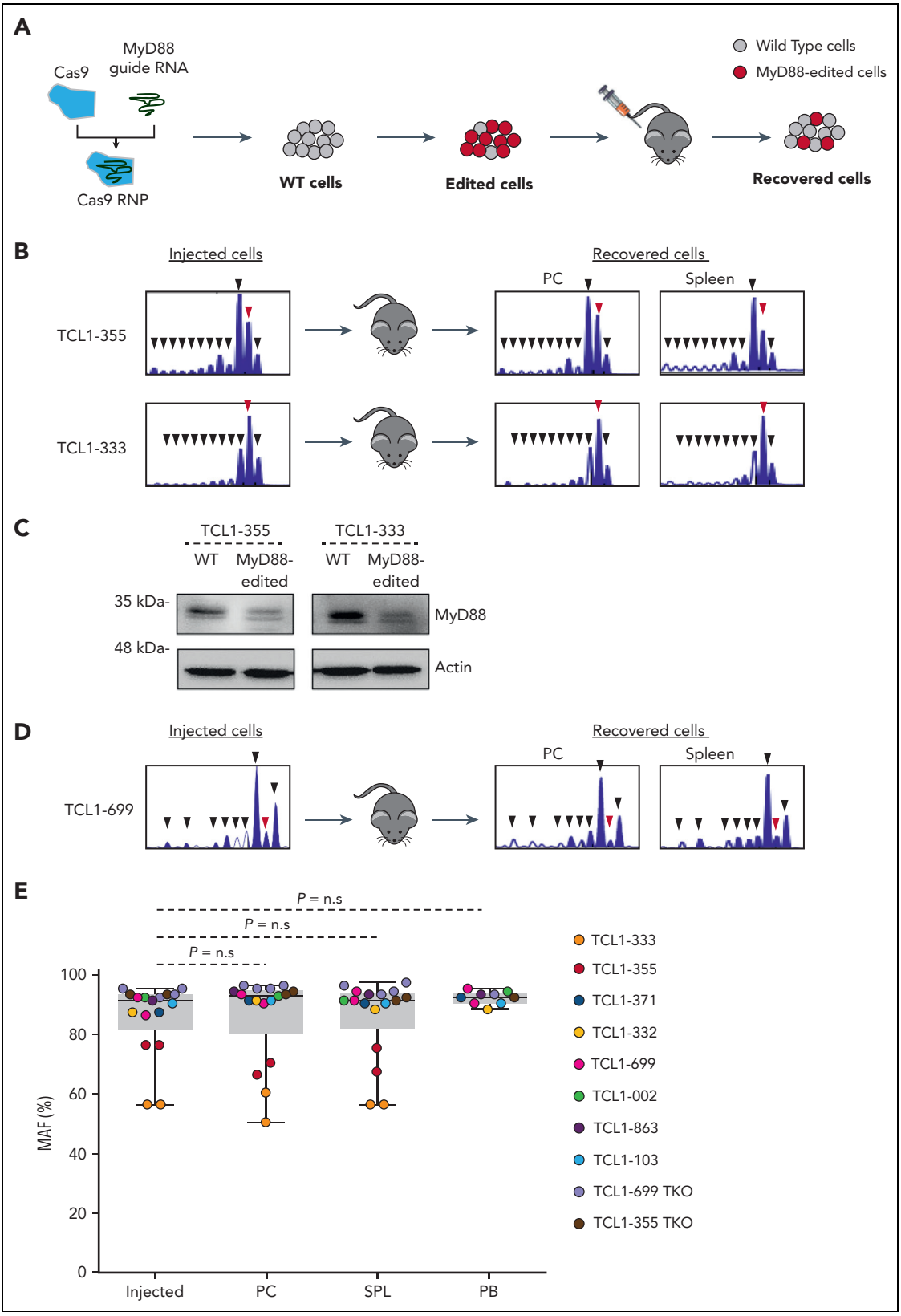

Figure 2. Murine CLL cells with disrupted MyD88 are not negatively selected in vivo. (A) Schematic representation of the procedure to investigate the impact of CRISPR/Cas9-mediated disruption of the *MyD88* gene on the growth of adoptively transferred Eμ-TCL1 CLL cells. The scheme illustrates expected outcome in case TLR signals are required for leukemia growth in vivo. (B) Indel analysis by amplicon capillary electrophoresis of the targeted region of *MyD88* in TCL1-355– and TCL1-333–injected and recovered leukemia cells isolated from peritoneal cavity (PC) and spleen. The wild type allele is indicated by a red arrow, and mutant alleles are indicated by black arrows. (C) Immunoblotting analysis of wild type (WT) and *MyD88*-edited TCL1-355 and TCL1-333 leukemia cells. (D) Amplicon capillary electrophoresis of the targeted region of *MyD88* in TCL1-699–injected and recovered leukemia cells isolated from PC and spleen. Experiment was performed with the second *MyD88* guide RNA. (E) *MyD88* mutant allele frequency (MAF) in injected leukemia cells and cells isolated from the PC and spleen of mice 21 to 35 days after adoptive transfer. Seventeen independent experiments were performed with the 8 TCL1-derived CLL and the 2 TCL1-derived RS lines. MAF was calculated by dividing the area of the mutated alleles with the total area of all amplified alleles (mutant + WT) detected in the amplicon capillary electrophoresis. Statistical analysis was done using 1-way repeated measures ANOVA.

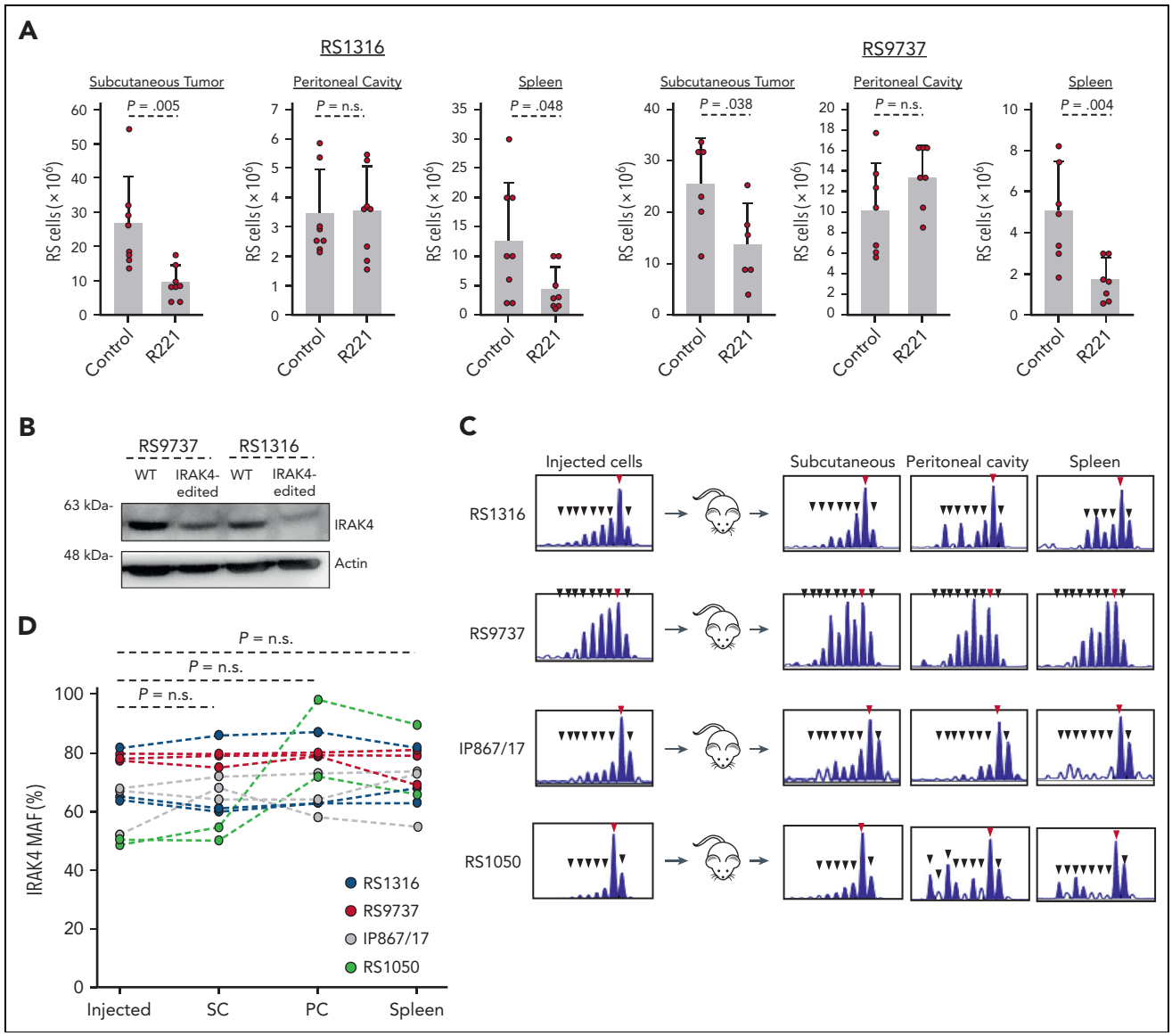

Figure 3. R221 treatment and *IRAK4* knockdown differently affect the growth of xenografted human RS cells. (A) Treatment with R221 results in reduced growth of RS1316 and RS9737 cells in subcutaneous tumor and spleen but not in PC of xenografted NSG mice. Graphs show absolute number of leukemic cells at each site. Statistical analysis was done using the *t* test or Mann-Whitney test, as appropriate. (B) Immunoblotting analysis of IRAK4 expression in WT and *IRAK4*-edited RS9737 and RS1316 cells. (C) Indel analysis by amplicon capillary electrophoresis of the targeted region of *IRAK4* in injected and recovered leukemia cells isolated from subcutaneous tumor, PC, and spleen. The WT allele is indicated by a red arrow, and mutant alleles are indicated by black arrows. (D) *IRAK4* MAF in injected leukemia cells and cells isolated from subcutaneous tumors, PCs, and spleens of NSG mice. The tumor cells were recovered between 27 and 34 days after transplantation. Eleven independent experiments were performed, 3 each with RS1316, RS9737, and IP867/17 and 2 with RS1050 cells. Statistical analysis was done using 1-way repeated measures ANOVA.

To determine whether the findings from the human RS models are applicable to human CLL cells, we investigated the impact of *IRAK4* and *IGHM* knockout in the human CLL cell lines MEC1, C1, and HG3 (Figure 5). The experiments with the CLL cell lines showed no negative selection of *IRAK4*-knockout cells following propagation in vivo but also did not show negative selection of *IGHM*-knockout cells, presumably because all CLL cell lines express the Epstein-Barr virus LMP2A protein, which is a BCR mimic that can substitute for the BCR.[41]

IRAK4 inhibitor treatment depletes macrophages in NSG and wild-type mice

The previous experiments showed that treatment with R221 reduces the growth of the malignant B cells in vivo but also that this effect is not caused by disruption of TLR signaling in the malignant B cells themselves. Considering that the reduction in tumor growth occurred only after prolonged R221 treatment, we investigated whether it could be related to an effect on some other cellular subset present in the tumor microenvironment. We focused in particular on monocytes and macrophages, which rely for their activity on TLR-mediated signals and have been shown to support CLL cell survival in vitro and in vivo.[42-46] A significant reduction in the absolute number of granulocytes ($CD11b^{+}F4/80^{-}$) and monocytes ($CD11b^{+}F4/80^{int}$) and almost complete disappearance of macrophages ($CD11b^{low}F4/80^{hi}$) was observed in the spleens of NSG mice xenografted with RS9737 cells that had been treated for 18 days with R221 (Figure 6A). A separate experiment with

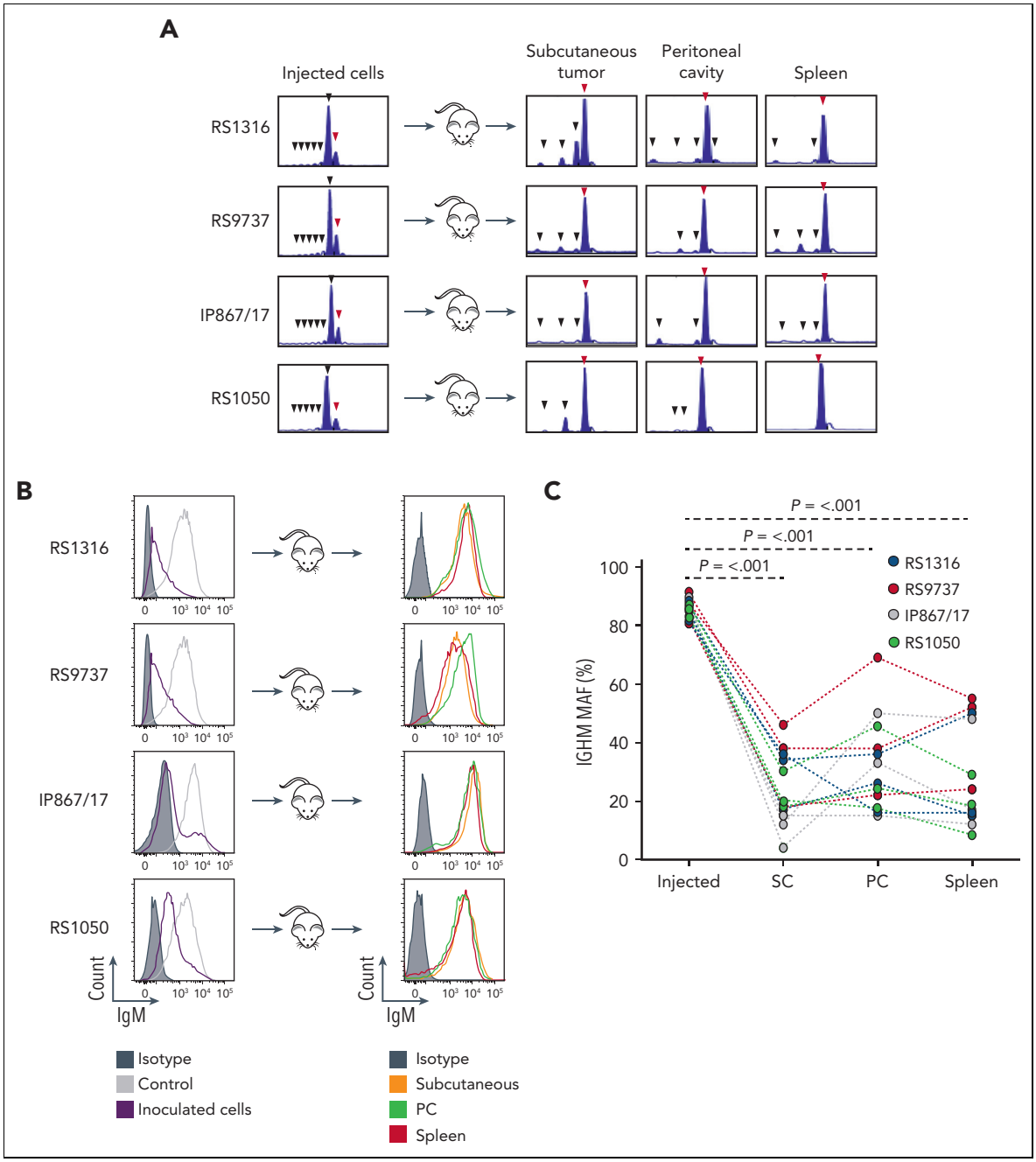

Figure 4. RS-PDX cells with CRISPR/Cas9-disrupted *IGHM* gene are negatively selected in vivo. (A) Indel analysis of the targeted region of the *IGHM* gene in injected and recovered leukemia cells isolated from subcutaneous tumor, PC, and spleen of xenografted NSG mice. The wild type allele is indicated by a red arrow, and mutant alleles are indicated by black arrows. (B) Flow cytometry analysis of surface IgM expression in *IGHM*-edited tumor cells before injection and after recovery from subcutaneous tumor, PC, and spleen of xenografted NSG mice. Control refers to mock-transfected cells. (C) *IGHM* MAF in injected leukemia cells and cells isolated from subcutaneous tumors, PCs, and spleens of NSG mice. The tumor cells were recovered 30 to 31 days after transplantation. Twelve independent experiments were performed, 3 each with RS1316, RS9737, IP867/17, and RS1050 cells. Statistical analysis was done with 1-way repeated measures ANOVA with Tukey test for multiple comparisons.

wild-type C57BL/6 mice that had not been inoculated with leukemia cells also showed depletion of macrophages and a significant reduction in the number of granulocytes in the spleen of R221-treated mice (Figure 6B and supplemental Figure 5). In contrast, treatment with R221 induced no change in the number or percentage of macrophages in the peritoneal cavity, where no effect on the growth of the malignant B cells had been observed (Figure 6C and supplemental Figure 6). In vitro experiments showed that both peritoneal cavity– and bone marrow–derived macrophages are susceptible to 1.0 μM R191, suggesting that the lack of an effect in vivo against peritoneal cavity macrophages is not because of different sensitivity to the drug (supplemental Figure 7).

Macrophages sustain the survival of murine TCL1 and human RS leukemia cells

To determine the capacity of murine macrophages to support the survival of human RS cells, we cocultured RS1316 and

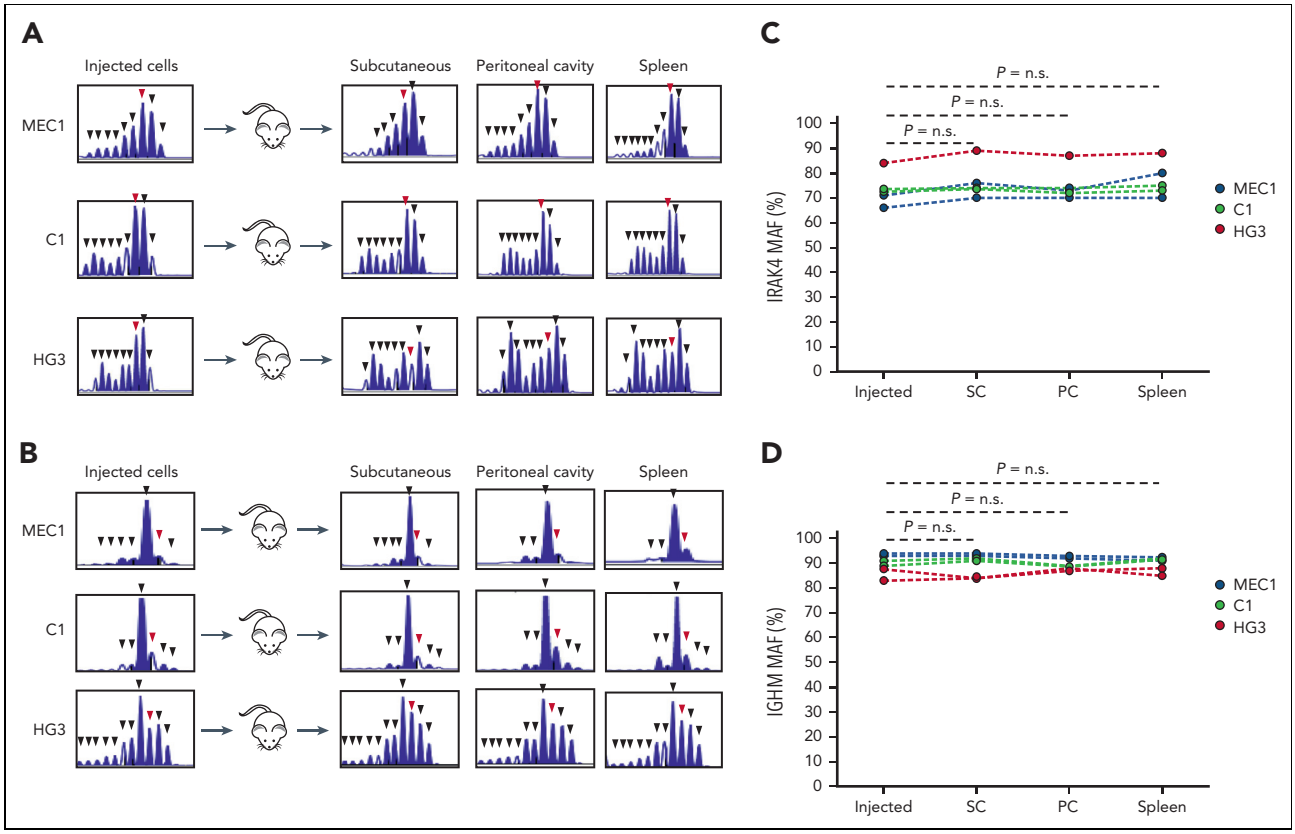

Figure 5. Analysis of changes in *IGHM* or *IRAK4* MAF following in vivo propagation of human CLL cell lines MEC1, C1, and HG3. (A) Indel analysis of the targeted region of the *IRAK4* gene or (B) *IGHM* gene in injected and recovered leukemia cells isolated from subcutaneous tumor, PC, and spleen of xenografted NSG mice. The wild type allele is indicated by a red arrow, and mutant alleles are indicated by black arrows. (C-D) *IRAK4* and *IGHM* MAF in injected leukemia cells and cells isolated from subcutaneous tumors, PCs, and spleens of NSG mice. The tumor cells were recovered 24 to 37 days after transplantation. Each circle represents an independent experiment. Statistical analysis was done with 1-way repeated measures ANOVA with Tukey test for multiple comparisons.

RS9737 cells with peritoneal cavity– or bone marrow–derived macrophages from NSG mice (Figure 7A-B). In both sets of experiments, coculture with macrophages significantly protected the malignant B cells from spontaneous apoptosis. Moreover, an independent experiment with the RS-PDX lines RS9737, RS1316, and IP867/17 and peritoneal cavity macrophages, which were used because of the ease of isolation, showed that the malignant B cells can be induced to proliferate and can be maintained in culture for extended periods (>10 days) if supplemented every 3 to 4 days with viable macrophages (supplemental Figure 8). The effects on survival were abrogated when the cells were cocultured with macrophages that had been pretreated with R191 (Figure 7C). Coculture experiments with peritoneal cavity macrophages from C57BL/6 mice and the murine leukemias TCL1-355 and TCL1-863 also showed a significant increase in the percentage of viable and proliferating CLL cells (supplemental Figure 9). The supportive effect of macrophages was primarily contact-dependent, as it was largely lost when RS-PDX cells were separated from the macrophages with well inserts to prevent them from directly interacting (supplemental Figure 10). However, a small increase in viability was observed when RS-PDX cells were cultured with recombinant BAFF and IL-15 but not with other soluble macrophage-derived factors that have been reported to support the survival of CLL cells in vitro, such as Wnt5a and CXCL12 (supplemental Figure 11).

Collectively, the previous data suggested that the antileukemic activity of R221 may be primarily caused by deprivation of the malignant B cells from macrophage-derived growth and survival signals rather than a direct effect on the malignant B cells. To further evaluate this possibility, we repeated the experiment described in Figure 1C, except that this time we included an additional group of mice in which macrophages were depleted by R221 pretreatment for 14 days prior to injection of TCL1-355 leukemia cells. Treatment was continued thereafter in both groups for 21 days, when mice were euthanized for analysis of tumor burden. In contrast to mice that had not received pretreatment, a significant reduction in the number of leukemic cells was observed in the peripheral blood and spleen of the R221-pretreated mice in comparison to the untreated mice (Figure 7D). Consistent with the lack of an effect on peritoneal cavity macrophages, no reduction in the number of leukemic cells at this site was observed.

Discussion

Over the past decades, numerous microenvironmental signals have been identified that can increase the survival or induce the proliferation of CLL cells in vitro, but the relevance of these signals in promoting the growth and survival of the leukemic cells in vivo has still not been fully established. In this article, we performed in vivo pharmacologic inhibition and CRISPR/Cas9

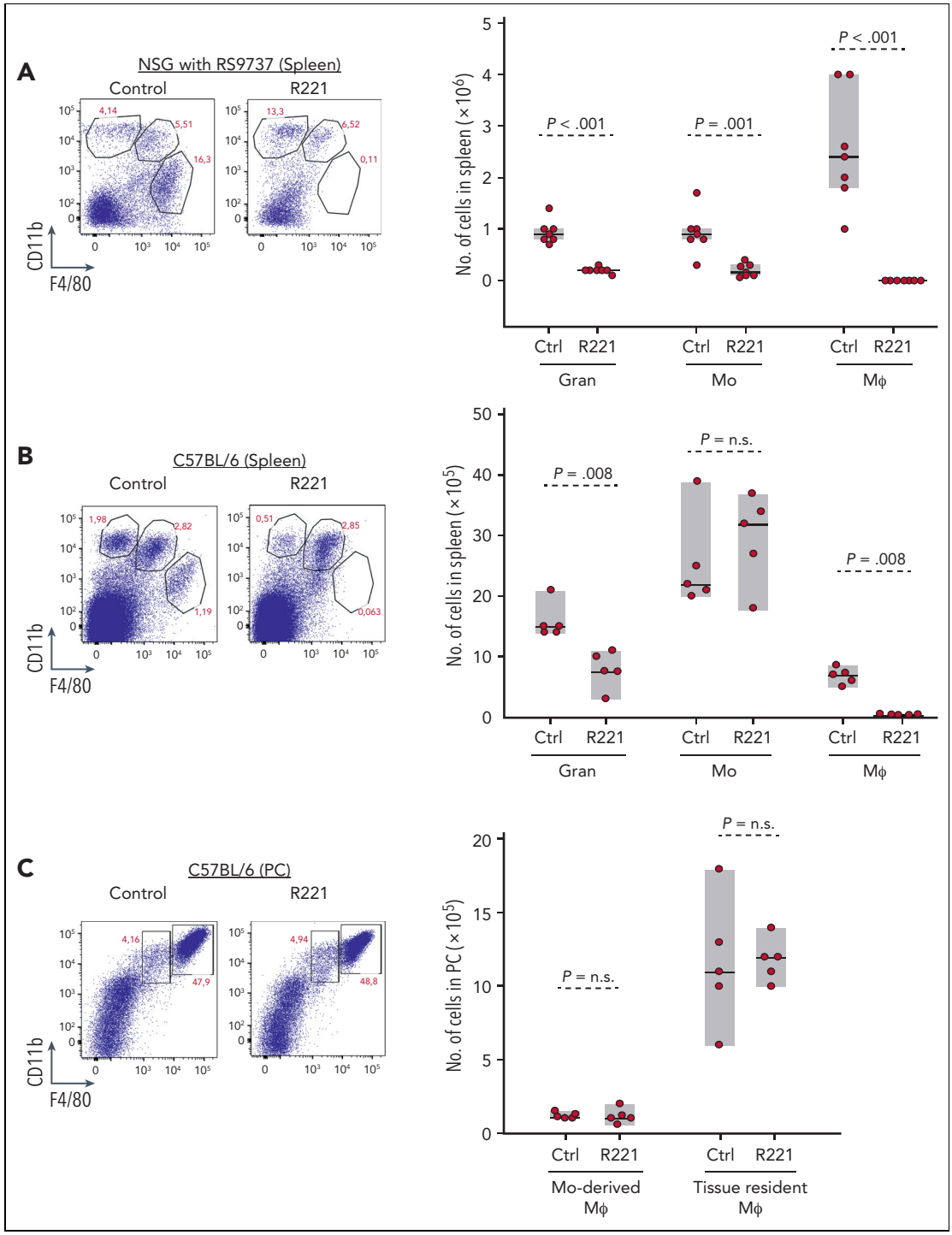

Figure 6. Effects of R221 treatment on monocyte/macrophage populations in NSG and C57BL/6 mice. (A) Representative flow cytometry analysis showing the percentage of granulocytes (CD11b^{+}F4/80^{-}), monocytes (CD11b^{+}F4/80^{int}), and monocyte-derived macrophages (CD11b^{low}F4/80^{hi}) gated on viable CD45^{+} cells isolated from the spleen of R221- or vehicle control–treated NSG mice (n = 7 per group) xenografted with RS9737 cells. The box plot shows the absolute number of granulocytes (Gran), monocytes (Mo), and macrophages (Mϕ) in the spleen of vehicle control– and R221-treated NSG mice. (B) Flow cytometry dot plots and box plot showing the percentage (left) and the absolute number (right) of Gran, Mo, and Mϕ in the spleen of R221- or vehicle control–treated C57/BL6 mice. (C) Flow cytometry dot plots and box plot showing the percentage (left) and the absolute number (right) of monocyte-derived Mϕ (CD11b^{+}F4/80^{int}) and tissue-resident Mϕ (CD11b^{+}F4/80^{hi}) in the PC of R221 and vehicle control C57/BL6 mice. Cell populations were defined as described in Hanna et al[44] Statistical analysis was done using the *t* test or Mann-Whitney test, as appropriate.

gene editing of murine and human PDX models to interrogate the role of the TLR pathway in the pathogenesis of CLL and RS. In contrast to our initial expectations, we find no evidence that TLR signals influence the growth of the malignant cells in any of the investigated in vivo models. Instead, our data provide additional genetic evidence for a major dependence of the

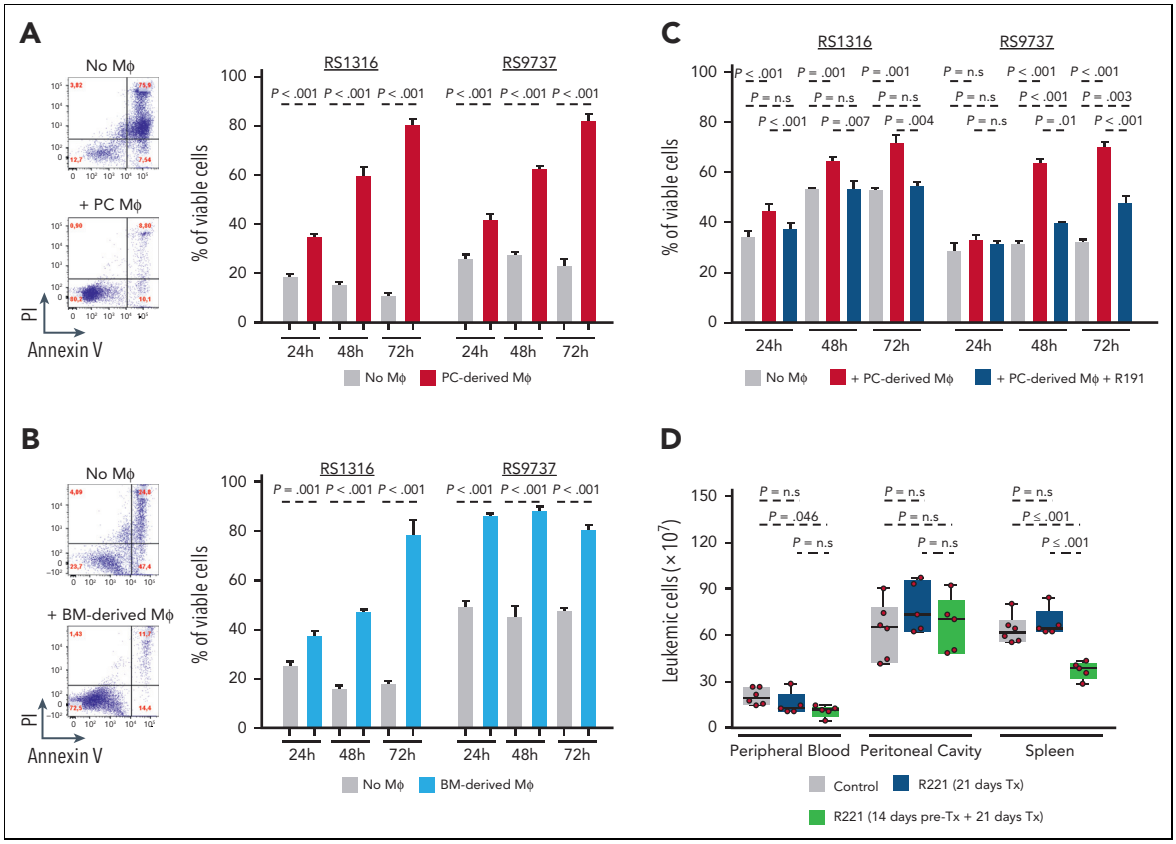

Figure 7. Macrophages prolong the survival of PDX-RS cells in vitro, and their depletion delays the expansion of adoptively transferred TCL1 leukemia cells in vivo. (A) Representative annexin V/propidium iodide (PI) analysis of RS1316 cells cultured for 72 hours in the presence or absence of PC-isolated Mϕ (left); summary of 3 independent experiments using RS1316 and RS9737 cells (right). (B) Representative annexin V/PI analysis of RS1316 cells cultured for 72 hours in the presence or absence of bone marrow (BM)-derived Mϕ generated by differentiating BM mononuclear cells for 4 days in culture with M-CSF (left); summary of 3 independent experiments using RS1316 and RS9737 cells (right). (C) Percentage of viable RS1316 or RS9737 cells following coculture with peritoneal cavity–derived macrophages that had previously been exposed to 1μM R191 for 24 hours. Macrophages were washed to remove R191 prior to coculture with the RS-PDX cells. Viability was assessed by annexin V/PI staining. Graph represents summary of 3 independent experiments. (D) Analysis of leukemia cell counts ($CD5^+/CD19^+$) in peripheral blood, peritoneal cavity, and spleen of mice treated with vehicle control (n = 6), mice treated for 21 days with R221 (n = 5), or mice pretreated for 14 days with R221 prior to tumor transfer and then treated for additional 21 days (n = 5). Statistical analysis was done using 1-way ANOVA with Tukey test for multiple comparisons.

malignant cells on BCR signals and further emphasize an important role for macrophages in supporting the growth and survival of CLL and RS cells.

The negative findings of our study cannot completely exclude the possibility for a less essential role of TLR signals in CLL pathogenesis or progression. In particular, considering that both the murine TCL1 and the human RS models are characterized by rapid tumor growth, a more subtle effect of TLR pathway disruption may have remained undetected. For example, a recent study by Kennedy et al suggested that mitochondrial DNA, which is present at higher levels in the plasma of CLL patients compared with healthy controls, increases by two-fold the propensity of the leukemic cells to migrate towards CXCL12.[30] Such an effect is unlikely to have a major impact on the growth of rapidly proliferating tumors and would likely be missed in our experimental models. However, using the same experimental approach, we readily demonstrated strong negative selection of human *IGHM*-knockout RS-PDX cells, thus demonstrating that our experimental system is robust enough to identify signals that are essential for the growth of the malignant cells.

Another limitation of our study is that it cannot exclude the possibility that TLR9 signaling is involved in the pathogenesis of a subset of CLL cases that were not represented by our models. Such a possibility is supported by data from 2 recent studies that reported the presence of activated TLR9 complexes in lymph node CLL cells from only 2 of 14 biopsies investigated with the proximity ligation assay.[23,47] In addition, it is worth noting that TLR9 activation depends on the availability of a BCR capable of recognizing and transporting DNA-containing complexes to the endosomal compartment where TLR9 is located, and such reactivity has been detected in only a fraction of cases.[27] Future experiments with primary CLL xenografts, which were not possible in the current study because of insufficient editing efficiency, will be required to address this possibility.

Another unexpected finding of our study was the compartment-restricted effect of R191/R221 treatment on the growth of the transplanted malignant B cells. One possible explanation for this phenomenon is lower bioavailability of R191 in the peritoneal cavity and an off-target cytotoxic effect of the drug. R191 has been reported to downregulate MYC, CDK4, and CDK6

and induce cell cycle arrest and apoptosis in WM cell lines, suggesting that it could be selectively toxic for cycling cells.[38] In line with this possibility, we observed that R191 reduces the viability of RS, TCL1, and CpG- or CD40L/IL-4/IL-21–stimulated human CLL samples, which all contain a substantial proportion of cycling cells, but has no impact on the viability on unstimulated, resting CLL cells. However, considering that the difference in tumor growth in vivo was seen only after prolonged R221 treatment and coincided with a reduction in the number of macrophages, another nonmutually exclusive possibility is that the effect of treatment was a consequence of reduced availability of macrophage-derived growth and survival signals. This possibility was additionally supported by our in vitro coculture experiments and by the study of Giménez et al, who, using another IRAK4 inhibitor, also observed a concomitant reduction in the number of monocytes, macrophages, and adoptively transferred murine TCL1 leukemia cells in the spleens of treated mice.[35]

The mechanism causing macrophage depletion in IRAK4 inhibitor–treated mice is currently unknown. In the study of Giménez et al,[35] IRAK4 inhibitor treatment was associated with reduced monocyte expression of the chemokine receptor CCR2, which is essential for the CCL-2–mediated recruitment of monocytes by CLL cells.[48] However, in our study the effect of IRAK4 inhibitor treatment was more direct, resulting in selective killing of monocytes and macrophages but not B and T cells present in the same compartment. Whether the cytotoxic effect of R191 against macrophages is a consequence of inhibition of TLR signals, which are required for the differentiation of blood monocytes into macrophages,[49-51] or an unrelated pathway remains to be determined.

The capacity of macrophages to support CLL cell survival has been well established in numerous in vitro studies with primary CLL cells and has been further validated in in vivo studies with Eμ-TCL1–derived murine CLL cells or the human CLL cell line MEC1.[43-46,52-55] The novelty of our findings in this respect is that the same effect was seen with nonimmortalized human RS-PDX cells, suggesting that therapeutic strategies based on interfering with macrophage-tumor cell interactions could provide a therapeutic benefit in this condition. In addition, coculture experiments showed enhanced ex vivo proliferation of the human RS-PDX cells in the presence of macrophages, whereas no proliferation was detected with nontransformed human CLL cells (supplemental Figure 8). This finding, together with previous observations that human RS cells, unlike human CLL cells, can be grown efficiently in the absence of T cells in immunodeficient mice,[20,21,39,40] suggests that macrophage-derived signals, in combination with certain genetic lesions in cell cycle regulators,[9] may substitute for T cell–derived signals in driving the proliferation of RS cells.

Acknowledgment

This research was supported by a grant from the Fondazione AIRC per la Ricerca sul Cancro (AIRC project IG 2020, ID no. 24566 [D.G.E.]).

Authorship

Contribution: C.M. and D.G.E. designed the study. C.M., S.C., M.V., and S.G. performed the experiments. T.V., S.D., L.L., and A.J.D. provided vital reagents and/or supervised certain experiments. C.M. and D.G.E. wrote the manuscript. All authors analyzed data and reviewed and approved the final version of the manuscript.

Conflict-of-interest disclosure: The authors declare no competing financial interests.

ORCID profiles: C.M., 0000-0001-7136-7174; S.D., 0000-0003-0632-5036; L.L., 0000-0002-8327-1396; D.G.E., 0000-0001-9081-5462.

Correspondence: Dimitar G. Efremov, Molecular Hematology Unit, ICGEB, Padriciano 99, 34149 Trieste, Italy; email: efremov@icgeb.org.

Footnotes

Submitted 10 March 2022; accepted 1 September 2022; prepublished online on *Blood* First Edition 9 September 2022. https://doi.org/10.1182/blood.2022016272.

Data are available from the corresponding author, Dimitar G. Efremov (efremov@icgeb.org).

The online version of this article contains a data supplement.

The publication costs of this article were defrayed in part by page charge payment. Therefore, and solely to indicate this fact, this article is hereby marked "advertisement" in accordance with 18 USC section 1734.

REFERENCES

1. Chiorazzi N, Efremov DG. Chronic lymphocytic leukemia: a tale of one or two signals? *Cell Res*. 2013;23(2):182-185.
2. Stevenson FK, Forconi F, Kipps TJ. Exploring the pathways to chronic lymphocytic leukemia. *Blood*. 2021 Sep 9;138(10):827-835.
3. Dühren-von Minden M, Übelhart R, Schneider D, et al. Chronic lymphocytic leukaemia is driven by antigen-independent cell-autonomous signalling. *Nature*. 2012;489(7415):309-312.
4. Iacovelli S, Hug E, Bennardo S, et al. Two types of BCR interactions are positively selected during leukemia development in the Eμ-TCL1 transgenic mouse model of CLL. *Blood*. 2015;125(10):1578-1588.
5. Dal-Bo M, Bertoni F, Forconi F, et al. Intrinsic and extrinsic factors influencing the clinical course of B-cell chronic lymphocytic leukemia: prognostic markers with pathogenetic relevance. *J Transl Med*. 2009;7:76.
6. Ten Hacken E, Burger JA. Microenvironment interactions and B-cell receptor signaling in chronic lymphocytic leukemia: implications for disease pathogenesis and treatment. *Biochim Biophys Acta*. 2016;1863(3):401-413.
7. Schleiss C, Ilias W, Tahar O, et al. BCR-associated factors driving chronic lymphocytic leukemia cells proliferation ex vivo. *Sci Rep*. 2019;9(1):701.
8. Haselager MV, Kater AP, Eldering E. Proliferative signals in chronic lymphocytic leukemia; what are we missing? *Front Oncol*. 2020;10:592205.
9. Chakraborty S, Martines C, Porro F, et al. B-cell receptor signaling and genetic lesions in TP53 and CDKN2A/CDKN2B cooperate in Richter transformation. *Blood*. 2021;138(12):1053-1066.
10. Tretter T, Schuler M, Schneller F, et al. Direct cellular interaction with activated CD4(+) T cells overcomes hyporesponsiveness of B-cell chronic lymphocytic leukemia in vitro. *Cell Immunol*. 1998;189(1):41-50.
11. Os A, Bürgler S, Ribes AP, et al. Chronic lymphocytic leukemia cells are activated and proliferate in response to specific T helper cells. *Cell Rep*. 2013;4(3):566-577.
12. Pascutti MF, Jak M, Tromp JM, et al. IL-21 and CD40L signals from autologous T cells can induce antigen-independent

proliferation of CLL cells. *Blood*. 2013;122:3010-3019.

13. Decker T, Schneller F, Kronschnabl M, et al. Immunostimulatory CpG-oligonucleotides induce functional high affinity IL-2 receptors on B-CLL cells: costimulation with IL-2 results in a highly immunogenic phenotype. *Exp Hematol*. 2000;28(5):558-568.

14. Decker T, Hipp S, Ringshausen I, et al. Rapamycin-induced G1 arrest in cycling B-CLL cells is associated with reduced expression of cyclin D3, cyclin E, cyclin A, and survivin. *Blood*. 2003;101(1):278-285.

15. Dicker F, Schnittger S, Haferlach T, Kern W, Schoch C. Immunostimulatory oligonucleotide-induced metaphase cytogenetics detect chromosomal aberrations in 80% of CLL patients: a study of 132 CLL cases with correlation to FISH, IgVH status, and CD38 expression. *Blood*. 2006;108(9):3152-3160.

16. Wagner M, Oelsner M, Moore A, et al. Integration of innate into adaptive immune responses in ZAP-70-positive chronic lymphocytic leukemia. *Blood*. 2016;127(4):436-448.

17. Ghia P, Strola G, Granziero L, et al. Chronic lymphocytic leukemia B cells are endowed with the capacity to attract $CD4^+$, $CD40L^+$ T cells by producing CCL22. *Eur J Immunol*. 2002;32(5):1403-1413.

18. Ruiz-Lafuente N, Alcaraz-García MJ, Sebastián-Ruiz S, et al. The gene expression response of chronic lymphocytic leukemia cells to IL-4 is specific, depends on ZAP-70 status and is differentially affected by an NFκB inhibitor. *PLoS One*. 2014;9(10):e109533.

19. Aguilar-Hernandez MM, Blunt MD, Dobson R, et al. IL-4 enhances expression and function of surface IgM in CLL cells. *Blood*. 2016;127(24):3015-3025.

20. Bagnara D, Kaufman MS, Calissano C, et al. A novel adoptive transfer model of chronic lymphocytic leukemia suggests a key role for T lymphocytes in the disease. *Blood*. 2011;117(20):5463-5472.

21. Patten PEM, Ferrer G, Chen SS, et al. A detailed analysis of parameters supporting the engraftment and growth of chronic lymphocytic leukemia cells in immune-deficient mice. *Front Immunol*. 2021;12:627020.

22. Herishanu Y, Pérez-Galán P, Liu D, et al. The lymph node microenvironment promotes B-cell receptor signaling, NF-kappaB activation, and tumor proliferation in chronic lymphocytic leukemia. *Blood*. 2011;117(2):563-574.

23. Dadashian EL, McAuley EM, Liu D, et al. TLR signaling is activated in lymph node-resident CLL cells and is only partially inhibited by ibrutinib. *Cancer Res*. 2019;79(2):360-371.

24. Longo PG, Laurenti L, Gobessi S, et al. The Akt signaling pathway determines the different proliferative capacity of chronic lymphocytic leukemia B-cells from patients with progressive and stable disease. *Leukemia*. 2007;21(1):110-120.

25. Tarnani M, Laurenti L, Longo PG, et al. The proliferative response to CpG-ODN stimulation predicts PFS, TTT and OS in patients with chronic lymphocytic leukemia. *Leuk Res*. 2010;34(9):1189-1194.

26. Lanemo Myhrinder A, Hellqvist E, Sidorova E, et al. A new perspective: molecular motifs on oxidized LDL, apoptotic cells, and bacteria are targets for chronic lymphocytic leukemia antibodies. *Blood*. 2008;111(7):3838.

27. Catera R, Silverman GJ, Hatzi K, et al. Chronic lymphocytic leukemia cells recognize conserved epitopes associated with apoptosis and oxidation. *Mol Med*. 2008;14(11-12):665-674.

28. Efremov DG, Bomben R, Gobessi S, Gattei V. TLR9 signaling defines distinct prognostic subsets in CLL. *Front Biosci (Landmark Ed)*. 2013;18(1):371-386.

29. Mongini PK, Gupta R, Boyle E, et al. TLR-9 and IL-15 synergy promotes the in vitro clonal expansion of chronic lymphocytic leukemia B cells. *J Immunol*. 2015;195(3):901-923.

30. Kennedy E, Coulter E, Halliwell E, et al. TLR9 expression in chronic lymphocytic leukemia identifies a promigratory subpopulation and novel therapeutic target. *Blood*. 2021;137(22):3064-3078.

31. Ngo VN, Young RM, Schmitz R, et al. Oncogenically active MYD88 mutations in human lymphoma. *Nature*. 2011;470(7332):115-119.

32. Kelly PN, Romero DL, Yang Y, et al. Selective interleukin-1 receptor-associated kinase 4 inhibitors for the treatment of autoimmune disorders and lymphoid malignancy. *J Exp Med*. 2015;212(13):2189-2201.

33. Yang G, Zhou Y, Liu X, et al. A mutation in MYD88 (L265P) supports the survival of lymphoplasmacytic cells by activation of Bruton tyrosine kinase in Waldenström macroglobulinemia. *Blood*. 2013;122(7):1222-1232.

34. Delvecchio VS, Sana I, Mantione ME, et al. Interleukin-1 receptor-associated kinase 4 inhibitor interrupts toll-like receptor signalling and sensitizes chronic lymphocytic leukaemia cells to apoptosis. *Br J Haematol*. 2020;189(3):475-488.

35. Giménez N, Schulz R, Higashi M, et al. Targeting IRAK4 disrupts inflammatory pathways and delays tumor development in chronic lymphocytic leukemia. *Leukemia*. 2020;34(1):100-114.

36. Slinger E, Thijssen R, Kater AP, Eldering E. Targeting antigen-independent proliferation in chronic lymphocytic leukemia through differential kinase inhibition. *Leukemia*. 2017;31(12):2601-2607.

37. Gounari M, Ntoufa S, Gerousi M, et al. Dichotomous Toll-like receptor responses in chronic lymphocytic leukemia patients under ibrutinib treatment. *Leukemia*. 2019;33(4):1030-1051.

38. Ni H, Shirazi F, Baladandayuthapani V, et al. Targeting myddosome signaling in Waldenstrom's macroglobulinemia with the interleukin-1 receptor-associated kinase 1/4 inhibitor R191. *Clin Cancer Res*. 2018;24(24):6408-6420.

39. Vaisitti T, Braggio E, Allan JN, et al. Novel Richter syndrome xenograft models to study genetic architecture, biology, and therapy responses. *Cancer Res*. 2018;78(13):3413-3420.

40. Vaisitti T, Arruga F, Vitale N, et al. ROR1 targeting with the antibody-drug conjugate VLS-101 is effective in Richter syndrome patient-derived xenograft mouse models. *Blood*. 2021;137(24):3365-3377.

41. Mancao C, Hammerschmidt W. Epstein-Barr virus latent membrane protein 2A is a B-cell receptor mimic and essential for B-cell survival. *Blood*. 2007;110(10):3715-3721.

42. Murphy M, Pattabiraman G, Manavalan TT, Medvedev AE. Deficiency in IRAK4 activity attenuates manifestations of murine lupus. *Eur J Immunol*. 2017;47(5):880-891.

43. Reinart N, Nguyen PH, Boucas J, et al. Delayed development of chronic lymphocytic leukemia in the absence of macrophage migration inhibitory factor. *Blood*. 2013;121(5):812-821.

44. Hanna BS, McClanahan F, Yazdanparast H, et al. Depletion of CLL-associated patrolling monocytes and macrophages controls disease development and repairs immune dysfunction in vivo. *Leukemia*. 2016;30(3):570-579.

45. Galletti G, Scielzo C, Barbaglio F, et al. Targeting macrophages sensitizes chronic lymphocytic leukemia to apoptosis and inhibits disease progression. *Cell Rep*. 2016;14(7):1748-1760.

46. Nguyen PH, Fedorchenko O, Rosen N, et al. LYN kinase in the tumor microenvironment is essential for the progression of chronic lymphocytic leukemia. *Cancer Cell*. 2016;30(4):610-622.

47. Phelan JD, Young RM, Webster DE, et al. A multiprotein supercomplex controlling oncogenic signalling in lymphoma. *Nature*. 2018;560(7718):387-391.

48. van Attekum MHA, van Bruggen JAC, Slinger E, et al. CD40 signaling instructs chronic lymphocytic leukemia cells to attract monocytes via the CCR2 axis. *Haematologica*. 2017;102(12):2069-2076.

49. Jia L, Clear A, Liu FT, et al. Extracellular HMGB1 promotes differentiation of nurse-like cells in chronic lymphocytic leukemia. *Blood*. 2014;123(11):1709-1719.

50. Audrito V, Serra S, Brusa D, et al. Extracellular nicotinamide phosphoribosyltransferase (NAMPT) promotes M2 macrophage polarization in chronic lymphocytic leukemia. *Blood*. 2015;125(1):111-123.

51. Managò A, Audrito V, Mazzola F, et al. Extracellular nicotinate phosphoribosyltransferase binds Toll like receptor 4 and mediates inflammation. *Nat Commun*. 2019;10(1):4116.

52. Polk A, Lu Y, Wang T, et al. Colony-stimulating factor-1 receptor is required for nurse-like cell survival in chronic lymphocytic leukemia. *Clin Cancer Res*. 2016;22(24):6118-6128.

53. Edwards VDK, Sweeney DT, Ho H, et al. Targeting of colony-stimulating factor 1 receptor (CSF1R) in the CLL microenvironment yields antineoplastic activity in primary patient samples. *Oncotarget*. 2018;9(37):24576-24589.

54. Burger JA, Tsukada N, Burger M, Zvaifler NJ, Dell'Aquila M, Kipps TJ. Blood-derived nurse-like cells protect chronic lymphocytic leukemia B cells from spontaneous apoptosis through stromal cell-derived factor-1. *Blood*. 2000;96(8):2655-2663.

55. Nishio M, Endo T, Tsukada N, et al. Nurselike cells express BAFF and APRIL, which can promote survival of chronic lymphocytic leukemia cells via a paracrine pathway distinct from that of SDF-1alpha. *Blood*. 2005;106(3):1012-1020.